Master Thesis

Czech
Technical
University
in Prague

F3

Faculty of Electrical Engineering
Department of Control Engineering

Brake-by-Wire System Development

Bc. Tomáš Veselý

Supervisor: doc. Ing. Tomáš Haniš, PhD.
Field of study: Cybernetics and Robotics
May 2022

MASTER'S THESIS ASSIGNMENT

I. Personal and study details

Student's name: **Veselý Tomáš** Personal ID number: **474780**

Faculty / Institute: **Faculty of Electrical Engineering**

Department / Institute: **Department of Control Engineering**

Study program: **Cybernetics and Robotics**

Branch of study: **Cybernetics and Robotics**

II. Master's thesis details

Master's thesis title in English:

Brake-by-wire system development

Master's thesis title in Czech:

Vývoj brake-by-wire systémů vozu

Guidelines:

The goal of the thesis is to design the hardware and software implementation of the Brake-by-wire system, which can be deployed on the full-scale vehicle demonstrator. The thesis will be addressed in following points:
1) Review of existing Brake-by-Wire solutions. Analysis of possible approaches, which are applicable in real vehicles.
2) Hardware implementation of Brake-by-Wire unit – actuators and control electronic
3) Software development of Brake-by-wire system – baseline control laws design for Brake-by-wire unit
4) Implementation of braking system strategies on vehicle level
5) Validation of developed solutions

Bibliography / sources:

[1] Limebeer, David J. N. Massaro, Matteo. (2018). Dynamics and Optimal Control of Road Vehicles. Oxford University Press.
[2] Rajamani, R., 2011. Vehicle dynamics and control. Springer Science & Business Media.
[3] Dieter Schramm, Manfred Hiller, Roberto Bardini – Vehicle Dynamics – Duisburg 2014
[4] Robert Bosch GmbH - Bosch automotive handbook - Plochingen, Germany : Robet Bosch GmbH ; Cambridge, Mass. : Bentley Publishers

Name and workplace of master's thesis supervisor:

doc. Ing. Tomáš Haniš, Ph.D. Department of Control Engineering FEE

Name and workplace of second master's thesis supervisor or consultant:

Date of master's thesis assignment: **28.01.2022** Deadline for master's thesis submission: **20.05.2022**

Assignment valid until:
by the end of summer semester 2022/2023

doc. Ing. Tomáš Haniš, Ph.D.	prof. Ing. Michael Šebek, DrSc.	prof. Mgr. Petr Páta, Ph.D.
Supervisor's signature	Head of department's signature	Dean's signature

III. Assignment receipt

The student acknowledges that the master's thesis is an individual work. The student must produce his thesis without the assistance of others, with the exception of provided consultations. Within the master's thesis, the author must state the names of consultants and include a list of references.

.

Date of assignment receipt Student's signature

Acknowledgements

I would like to express my gratitude to my supervisor doc. Ing. Tomáš Haniš, PhD. for his friendly attitude, excellent advice and his time. Also, I want to thank Ing. David Vošahlík for selflessly answering all of my questions.

I would also like to thank my girlfriend for her support and help with proofreading.

Last but not least, I would like to thank my colleagues and friends from the Smart Driving Solutions research group for having a great time during my studies.

Declaration

I hereby declare that this master thesis was developed independently and that I have cited all used sources of information in accordance with the methodical instructions for observing the ethical principles in the preparation of a university thesis.

In Prague, May 20, 2022

....

Abstract

This thesis deals with designing and implementing an innovative Brake-by-Wire solution for the currently emerging SDS prototype vehicle project. The main goal of this work is to deliver hardware and software implementation of the Brake-by-Wire unit that can be used to deploy, validate, and verify the developed control algorithms on a real prototype vehicle.

The first part of the thesis is dedicated to a comprehensive overview of the available state-of-the-art brake system solutions. The second part is dedicated to the construction and software implementation of the designed Brake-by-Wire unit.

Finally, high-level control laws for maintaining the vehicle's longitudinal and lateral stability are implemented. A hardware-in-the-loop simulation setup is developed to test the designed high-level control laws on the real Brake-by-Wire hardware. Performed tests show the functionality and benefits of the proposed brake system solution, such as fast and precise system response, high reliability, and maintaining longitudinal vehicle stability under various adverse road conditions.

Keywords: Brake-by-Wire, automotive brake system design, electro-hydraulic brake, vehicle stability control algorithms, HIL simulation

Supervisor: doc. Ing. Tomáš Haniš, PhD.
Czech Technical University in Prague
Faculty of Electrical Engineering
Department of Control Engineering - K13135
Karlovo náměstí 13
12135 Praha 2

Abstrakt

Tato diplomová práce se zabývá návrhem a implementací inovativního Brake-by-Wire brzdného systému pro potřeby vznikajícího prototypu vozidla v rámci projektu výzkumné skupiny SDS. Hlavním cílem této práce je hardwarová a softwarová implementace Brake-by-Wire jednotky, která může být instalována do prototypu vozidla a která umožní otestování navržených řídících algoritmů.

První část práce obsahuje ucelený přehled současně dostupných řešení brzdných systémů. Druhá část práce se zabývá vlastní mechanickou konstrukcí a softwarou implementací navrženého Brake-by-Wire řešení.

Na závěr jsou navrženy řídící algoritmy pro udržovaní podélné a příčné stability vozu. Pro otestování funkčnosti navržených řídících algoritmů, které zajišťují stabilitu vozu, na skutečném hardwaru Brake-by-Wire jednotky je zkonstruován hardware-in-the-loop simulátor. Všechny provedené testy prokázály, že navržené řešení je plně funkční a nabízí výhody, jako je rychlá a přesná odezva systému, vysoká spolehlivost a zajištění podélné stability vozu i za nepřiznivých jízdních podmínek.

Klíčová slova: Brake-by-Wire, návrh brzdných systémů automobilu, elektrohydraulické brzdy, stabilizační programy vozu, HIL simulace

Překlad názvu: Vývoj brake-by-wire systému vozu

Contents

Figures

Tables

List of Abbreviations

SDS . . . . . Smart Driving Solutions research group
DBW . . . . . Drive-by-Wire
BBW . . . . . Brake-by-Wire
TBW . . . . . Throttle-by-Wire
FWD . . . . . Front wheel drive
RWD . . . . . Rear wheel drive
AWD . . . . . All wheel drive
ABS . . . . . Anti-lock brake system
EHA . . . . . Electro-hydraulic actuator
EHB . . . . . Electro-hydraulic brake
EMB . . . . . Electro-mechanical brake
MRB . . . . . Magneto-Rheological brake
EWB . . . . . Electronic wedge brake
HV . . . . . High voltage
LV . . . . . Low voltage
MV . . . . . Middle voltage
CAN . . . . . Controller Area Network
ECU . . . . . Electronic control unit
VCU . . . . . Vehicle control unit
NO . . . . . Normally open
NC . . . . . Normally closed
CoG . . . . . center of gravity
PWM . . . . . Pulse width modulation
CPU . . . . . Central processing unit
ADC . . . . . Analog-to-digital converter
DAC . . . . . Digital-to-analog converter
SPI . . . . . Serial peripheral interface
I2C . . . . . Inter-integrated circuit
eCAP . . . . . Capture mode pin
USB . . . . . Universal serial bus
LLC . . . . . Logic level converter
PCB . . . . . Printed circuit board
TP . . . . . Timer period
HIL . . . . . Hardware-in-the-loop

Chapter 1

Introduction

Autonomous or so-called highly automated self-driving vehicles are a topic that has resonated with the general public during the last few years. From the statements of various automotive promoters, businessmen, visionaries, and even some car manufacturers, one can easily think that the future is here, and the autonomous vehicle era has already begun. However, this is not completely true yet. There are plenty of electronic assistants in modern cars, such as line assist, collision avoidance system, or autonomous emergency braking system, which nobody thought of 20 years ago. Nevertheless, there is still no fully autonomous vehicle on the market these days. I believe that the reason for that is quite simple. Fully autonomous driving is an extraordinarily complex and challenging task, where many technical, legislative, and even ethical issues need to be addressed in order to bring fully autonomous vehicles to the streets.

In order to develop the autonomous vehicle, three main challenges need to be tackled. Firstly, all mechanical coupling between the vehicle and the human driver needs to be removed and replaced by an electric coupling. The mechanical decoupling allows the actuators such as motors, brakes, or steering servos to be controlled by electric signals without the need for any input force generated by the human driver. Mechanical decoupling is a crucial step to autonomous driving because it enables the possibility of easily replacing the human driver with an autonomous driving program. Without the mechanical decoupling, the replacement of the driver with the autonomous driving program would be overly complex, thus expensive and unfeasible. Secondly, the longitudinal and lateral vehicle stability and maneuverability need to be ensured all the time. The stability control reduces and suppresses phenomena such as tire slipping and skidding or wheel spinning and locking. Moreover, it increases the overall stability of the vehicle under various maneuvers and road conditions in order to maximize passenger safety and comfort. The problems of mechanical decoupling and vehicle stability control are often addressed together and can be found under the name Drive-by-Wire approach or Drive-by-Wire architecture. Finally, the last challenge which needs to be tackled is the autonomous driving program. The program should interact with the vehicle's surroundings, such as pedestrians, other vehicles, or traffic lights, in order to safely transport the passengers from point A to point B. Simply put, the autonomous driving program should be able to fully replace the driver, thus transforming the driver into just another passenger.

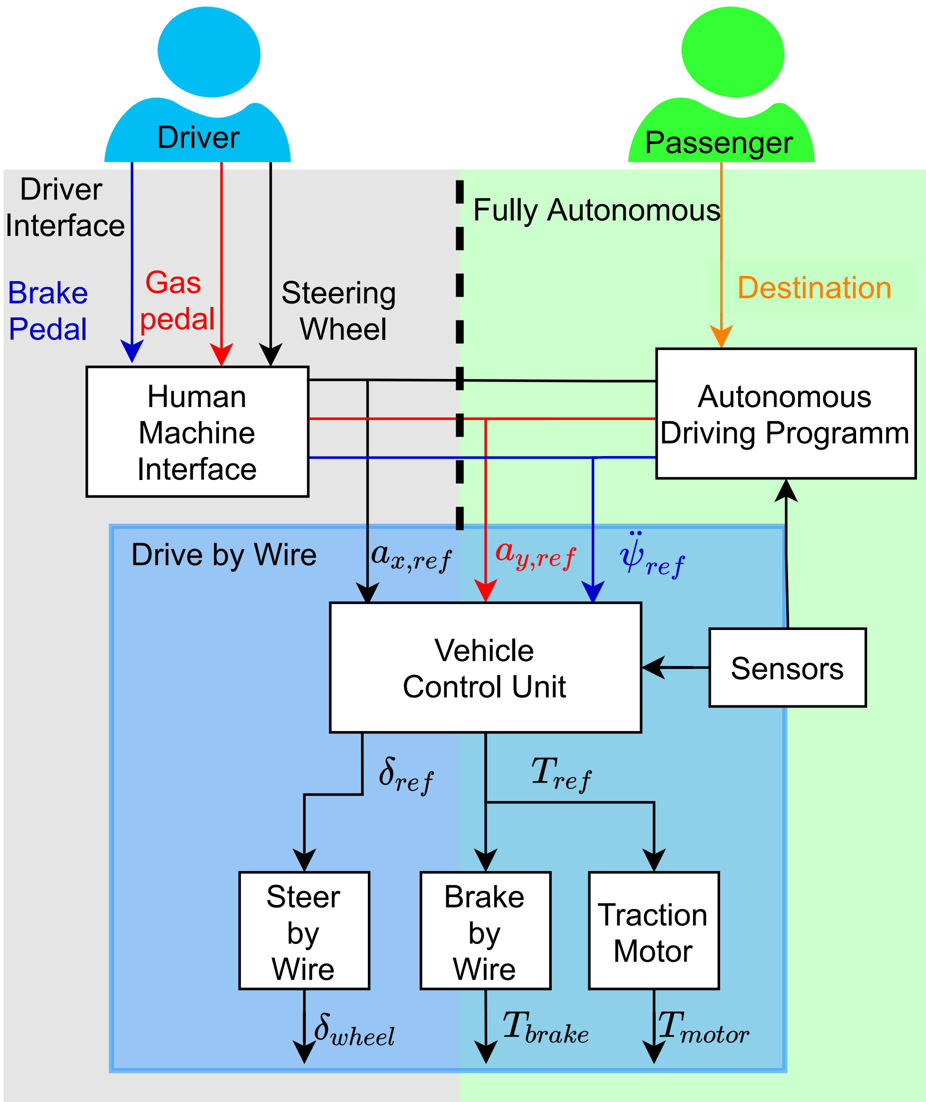

Figure 1.1: Decomposition of autonomous vehicle's control systems.

The decomposition of the autonomous driving problem described above is depicted in figure 1.1. As always in engineering practice, it makes sense to start from the bottom and then proceed all the way up to the fully autonomous driving program. Therefore, the best approach is to start with the development of the X-by-Wire units, followed by integrating the units with stability control algorithms. This then results in the full Drive-by-

Wire functionality. Finally, the autonomous driving program can be built on top of it. Surprisingly, many developers and manufacturers (e.g., Tesla) had not followed this decomposition scheme for many years. Instead, they struggled with the effort to develop and deliver the whole autonomous driving functionality at once. However, the situation in the industry has begun to change recently as some of the leading automotive suppliers, such as Brembo or Schaeffler, started releasing their X-by-Wire solutions on the market.

1.1 Project Background

As a member of the Smart Driving Solutions (SDS) research group at the Czech Technical University in Prague, I contribute to the currently emerging Drive-by-Wire demonstrator platform vehicle project. This project aims to design and construct a real-size, full Drive-by-Wire prototype vehicle with an electric powertrain. The purpose of the prototype vehicle is to deploy and verify the control algorithms that were developed by our group on a real-size vehicle. Also, the aim of this project is to show the benefits and possibilities of the Drive-by-Wire architecture, which has been demonstrated in the simulation environment.

The simplified scheme of the prototype vehicle platform is depicted in figure 1.3, the Drive-by-Wire architecture scheme is depicted in figure 1.2.

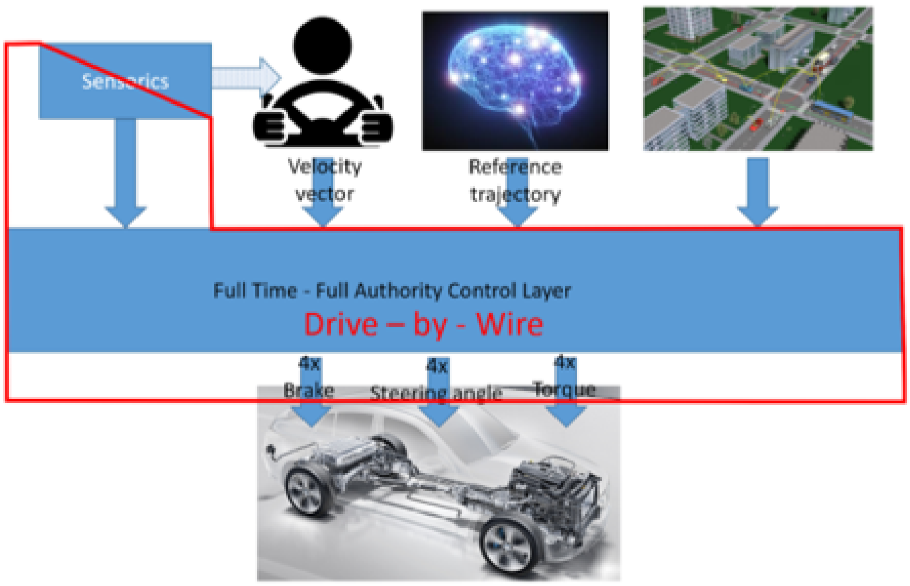

Figure 1.2: Proposed Drive-by-Wire control architecture. Adopted from [Han].

The proposed prototype vehicle consists of the main parts listed below.

- 4x independently driven high-performance traction electric motors
- 1x highvoltage LiPo battery pack
- 4x independently electronically controllable brakes
- 4x independently electronically controllable steering servos
- 4x independently electronically controllable camber angle actuators
- 1x GPS and IMU unit
- 1x real-time Linux based Vehicle Control Unit (VCU)

Because of the independntly driven, braked, and steered wheels, the prototype platform is also referred to as 4x4x4.

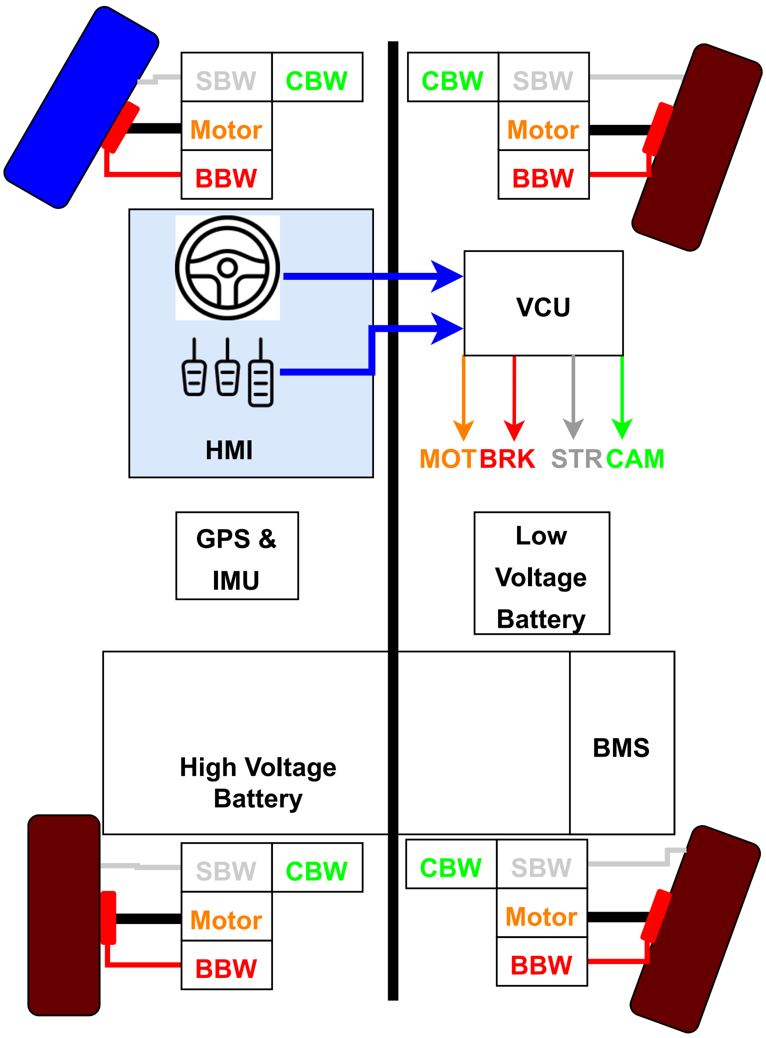

Figure 1.3: Simplified scheme of the Drive-by-wire prototype.

The prototype is intentionally designed as an over-actuated vehicle. The over-actuation simply means that there are multiple possibilities as how to execute one maneuver. For example, when the driver wants to decelerate the vehicle, it can be done using either the frictional brakes or the traction motors. On the one hand, the over-actuated vehicle brings several benefits, such as

- simple vehicle reconfiguration - from AWD to FWD or RWD; from steered front axle to all steered axles and so on, only by simple software changes
- the possibility of design and development of various X-by-Wire systems, such as Brake-by-Wire, Steer-by-Wire, Throttle-by-Wire, ...
- a design inherited redundancy - when brake system malfunction occurs, the vehicle can slow down using the traction motors or even steering; when steering system malfunction occurs, the vehicle can be steered using the torque vectoring and so on.

On the other hand, the control of the over-actuated platform is quite a challenging and complex task that needs to be addressed. The control of the over-actuated platforms is also known as the control allocation problem, which is the current field of study in control engineering.

1.2 Project Outline

The objective of this thesis is to develop the Brake-by-Wire actuator and its control system for the vehicle demonstrator platform. The thesis will be addressed in the following points

- review of the currently existing brake system solutions
- selection and mechanical design of the Brake-by-Wire unit
- hardware implementation of the Brake-by-Wire unit
- software implementation of low-level control laws for the Brake-by-Wire unit
- deployment and validation of the developed vehicle level control strategies

Chapter 2

Review of Currently Existing Brake System Solutions

This chapter reviews state-of-the-art solutions and trends in automotive brake systems. Firstly, to get an insight into the basic working principle of hydraulic brake systems, the conventional hydraulic brake systems deployed in the majority of today's passenger vehicles will be briefly described. This description grasps only the essential foundation of the hydraulic brake problematic. For those who are interested in a deeper explanation of the brake systems' working principles, please refer to [Meu18], [vHNK14] or [Ves20]. For a more detailed description of the main components of the hydraulic brake systems, please refer to [Maj15] and [Pro19]. Secondly, the currently emerging Brake-by-Wire solutions and current trends in the automotive research and industry will be summarized. For a more detailed summary, please refer to [Li19], [Hu22], [Ber09], [Meu18] or [AG19]. Namely [Li19] provides a comprehensive overview of the brake system problematic.

2.1 Convetional Hydraulic Brake Systems

Two types of hydraulic brake systems can be found in contemporary vehicles. The first type is a purely hydraulic brake system, where the braking force is controlled only by the driver. The second type is an extension of the purely hydraulic system, where the ABS unit has been integrated. After the 1st of July 2006, the ABS unit became an obligatory part of the brake systems in passenger vehicles sold in Europe [Pec18]; therefore, the majority of cars on the streets are equipped with this brake system.

2.1.1 Purely Hydraulic Brake System

The conventional hydraulic brake system has been used for over 100 years.

Although many improvements have been made, the main working principle remains the same. The driver depresses the brake pedal, which pushes the rod that is connected with pistons inside the master cylinder. The movement of the pistons seals the hydraulic circuit, which creates a closed hydraulic system. After that, hydraulic pressure is built. The pressure then acts on the piston inside the wheel caliper, which pushes the brake pads against the brake disc, generating brake torque. To fulfill the safety requirements, two independent brake circuits are typically used to preserve the brake functionality even when one of the circuits malfunctions.

The advantages of this brake system architecture are high system reliability and safety, excellent price-to-performance ratio, high efficiency, and low complexity [Ves20]. The disadvantages of this architecture are the overall weight of the system, the need for regular maintenance, usage of the toxic brake fluid, and finally, the absence of the possibility to modify the driver-generated brake pressure in order to prevent the wheel lock. A simplified scheme of the purely hydraulic brake system is depicted in figure 2.1.

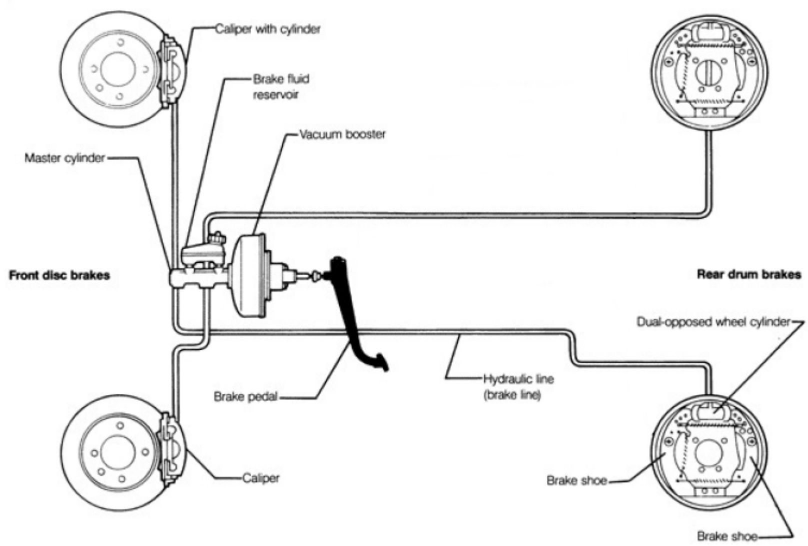

Figure 2.1: Simplified scheme of the hydraulic brake system. Adopted from [vHNK14].

2.1.2 Hydraulic Brake System With ABS Unit

This architecture is based on the purely hydraulic brake system augmented by the ABS unit. The ABS unit consists of several solenoid valves, and a small displacement pump [vHNK14]. The ABS unit allows the modification of the built pressure to prevent the wheels from locking. For a more detailed description of the ABS unit working principles, please refer to [Meu18] or [Gmb14]. Because the hydraulic brake system with the ABS unit is based on the purely hydraulic one, the advantages and disadvantages of both systems are very similar. The only difference is introduced by the ABS unit. On the one hand, it allows the modification of the brake pressure generated by the driver. On the other hand, the ABS unit dramatically increases the complexity and cost of the whole system. The scheme of the brake system with the ABS unit is depicted in figure 2.2.

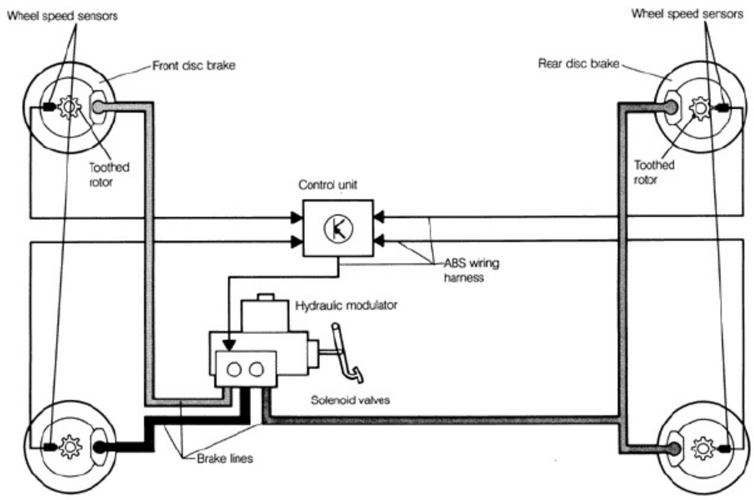

Figure 2.2: Simplified scheme of the hydraulic brake system with the ABS unit. Adopted from [vHNK14].

The main limitation of both described brake systems is the pressure generation process. The force needs to be applied on the brake pedal to generate the brake pressure. Afterward, generated pressure can be slightly adjusted by the displacement pump. However, due to its size, the pump is not able to generate sufficient pressure on its own without the force being applied on the pedal. Because of that, the functionality of the brakes is limited. Therefore, some advanced control systems, such as collision-avoidance system or emergency brake system, cannot be deployed on vehicles equipped with these kinds of brakes.

2.2 Brake-by-Wire Systems

As mentioned in the introduction, the so-called X-by-Wire systems combine two main functionalities. The first one is the mechanical decoupling of the driver interface and the actuators. The second one is the implementation of advanced vehicle stability control programs. The Drive-by-Wire approach was adopted from the aerospace industry, where the Fly-by-Wire architecture has been successfully applied both in the military and civil aircraft since the 1980s [Air]. The Fly-by-Wire concepts were adopted by the automotive industry quite fast. In 1988, BMW released their Throttle-by-Wire (TBW) system, which removed the mechanical coupling between the accelerator pedal and the throttle body [Jer18]. For many years, the Throttle-by-Wire was the only X-by-Wire system used in automotive. The change came with the introduction of the electric and hybrid drives as the need for mechanical decoupling of the brake pedal and the brake system emerged.

The hybrid and electric drives allow to decelerate the vehicle using the electric motor and store some of the vehicle's kinetic energy in the traction battery, which leads to better fuel economy and driving range extension. However, the brake torque produced by the regenerative brakes is limited by many factors so far. Therefore, the regenerative brakes have to be combined with the conventional friction-based brake system. This raises the issue of how to change the driver interface to allow the usage of the regenerative and friction-based brakes at the same time. Currently, two approaches can be found in the industry. The first one, called One-pedal driving (used by, e.g., Tesla), remaps the accelerator pedal profile in such a way that both positive and negative torque references can be generated [Tes07]. This allows the control of the regenerative brakes by the accelerator pedal. The friction-based brakes are controlled by the brake pedal in the same way as in vehicles with an internal combustion engine. Therefore, it is not necessary to decouple the brake pedal from the brake system itself at all. The second approach is based on the mechanical decoupling of the brake pedal and the brake actuators (used by, e.g., Toyota, Mercedes-Benz, or Bosch). The working principle of this approach is the following. When the brake pedal is depressed, an electronic signal is sent to the vehicle control unit, where the brake torque demand is computed and distributed between the regenerative and the friction brakes. Then, the brake torque demand is sent to the electronic brake actuators, which generate the demanded brake torque.

The deployment of the Brake-by-Wire based systems in vehicles offers benefits such as system customization. It enables changing the response and the settings of the brake system with only a simple software change. Therefore, the same brake system can be used in a city car as well as in a racing vehicle. Moreover, the X-by-Wire systems allow the elimination of mechanical elements such as a brake pedal rod or a steering column. This results in an increase in passive safety in case of an accident. Last but not least, the overall system weight and complexity are dramatically reduced. On the other side, issues such as the loss of driver's feedback, fault detection, and fault tolerance mechanisms need to be addressed.

2.2.1 Electro-hydraulic Brake

The Electro-Hydraulic Brake (EHB) systems can be divided into centralized and decentralized. Both of them adopt the conventional hydraulic brake system components and working principles and augment them with several electro-hydraulic actuator (EHA) units. For a more detailed description of

EHB systems, please refer to [vHNK14] or [Ber09].

Centralized Approach

The centralized EHB systems typically consist of one hydraulic pump and one high-pressure reservoir, which form the EHA unit for pressure generation. To prevent the wheel lock, the generated pressure needs to be modified by the wheel EHA units, which are typically formed by the inlet and outlet solenoid valves. These units allow holding, releasing, and increasing the pressure acting on the wheel calipers. The working principle is the following. The Vehicle Control Unit (VCU) reads and processes a signal generated by the brake pedal depression and calculates the brake pressure demand for each wheel. Then, the desired pressure is applied by the EHA units. The scheme of the centralized EHB system is depicted in figure 2.3. As it can be seen, the master cylinder is still preserved in the design and is still connected to the brake pedal for safety reasons. Under normal operation conditions, the isolating valves disconnect the master cylinder from the hydraulic circuit, and the pressure is built by the hydraulic pump. If the failure of the hydraulic pump or the wheel EHA unit occurs, the isolating valves connect the master cylinder to the hydraulic circuit and allow the driver to brake the vehicle conventionally.

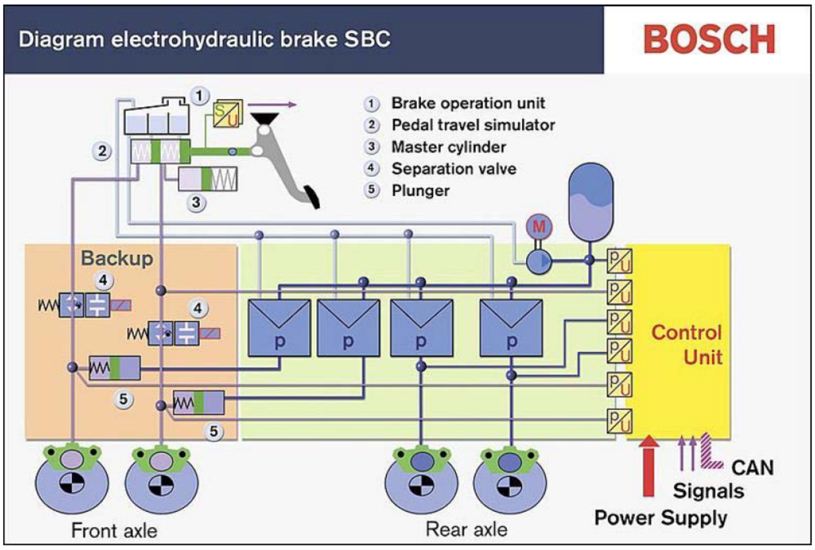

Figure 2.3: Scheme of the centralized Electro-hydraulic Brake system architecture. Adopted from [Ber09].

The advantages of the centralized EHB solution are its high reliability and safety due to mechanical backup. Furthermore, conventional brake components such as brake calipers and brake lines can still be used. Moreover, the wheel unsprung mass is dramatically reduced compared to the decentralized approach because only the brake caliper is attached to the wheel suspension. Finally, the usage of the high-pressure reservoir allows faster pressure rise in the brake system and serves as the backup system for the hydraulic pump. Typically, the hydraulic reservoir is designed to store enough pressure for several full-stop braking.

The disadvantages of the centralized architecture are the overall system complexity, weight, and space requirements. Moreover, every wheel's EHA unit is connected to the hydraulic pump and reservoir only by a single brake line, which introduces the single point of failure. Finally, the overall costs of the system are quite high. Therefore, it can be typically found in high-class vehicles. On today's market, the centralized EHB system can be found under the names *SBC* used by Mercedes-Benz, *EHB* used by Toyota, or *IBooster* used by Bosch.

Decentralized Approach

The decentralized EHB system works with the idea of creating a fully independent brake circuit for each wheel. The decentralized system only consists of the wheel EHA units, the Electronic Control Unit (ECU), and the brake pedal. The wheel EHA units are typically integrated directly into the brake calipers or brake cylinders. The working principle is quite straightforward; the ECU reads the electric signal from the brake pedal and computes the brake pressure for each wheel, which is then generated by the wheel EHA units. The scheme of the decentralized brake system solution developed by Brembo is depicted in figure 2.4.

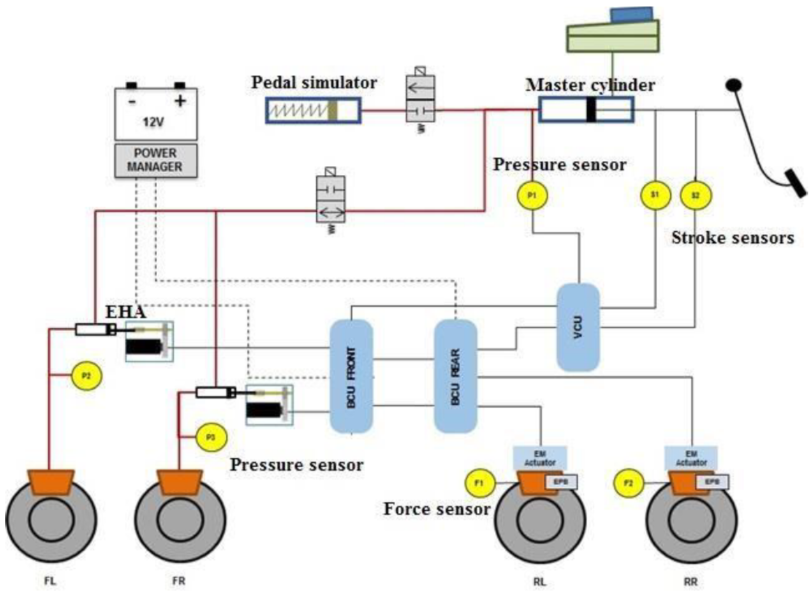

Figure 2.4: Scheme of the Brembo Brake-by-Wire system for EVC-1000 project. Adopted from [AG19].

As it can be seen from figure 2.4, the overall complexity and space requirements of the Brembo brake system solution are dramatically reduced. Also, the integration of the EHA with the brake cylinder results in a significant reduction of the brake pipe length. Therefore, the hydraulic transport delay is eliminated. For safety reasons, the front brake calipers are still connected to the master cylinder by the isolation valves, similarily to the centralized approach. Finally, note that the rear wheel brakes are realized by the Electro-Mechanical Brake (EMB), which will be described in more detail in the next section. The Brembo developed EHA, which integrates the electric motor with the brake cylinder, is depicted in figure 2.5.

Figure 2.5: Brembo Electro-hydraulic Actuator with brake cylinder integration. Adopted from [AG19].

The decentralized approach offers many advantages, such as reducing the system complexity and space requirements, reducing the overall system weight, or eliminating the hydraulic transport delay. Moreover, the preservation of the hydraulic mechanism allows easy connection of front calipers to the master cylinder to get a necessary level of redundancy to satisfy the safety requirements. On the other hand, as mentioned above, the unsprung mass of the vehicle increases significantly by the weight of the electro-hydraulic actuator. Therefore, special effort needs to be devoted to the actuator selection in order to minimize the increase of the unsprung mass.

The Brembo solution described above was originally developed as part of the EVC-1000 research project; for more details, refer to [AG19]. A few months ago, the Brembo Brake-by-Wire solution was released on the market under the name *Sensify*. Another interesting decentralized EHB concept comes from the Stockholm KTH Royal Institute of Technology. The diploma thesis *Investigation of a new e-caliper concept with a mechanical backup system* by [Meu18] proposes an interesting design of the brake caliper with an integrated input piston actuated by the electric motor, see figures 2.6 and 2.7. To satisfy the safety requirements, the second input piston, which is mechanically actuated, is added to the design. Under normal operating conditions, the desired brake pressure is created by the electric motor. When a malfunction of the electric motor or electricity supply occurs, the brake pressure can be generated by the second input piston connected to the brake pedal by a cable. The main benefit of this solution is the elimination of all hydraulic lines; therefore, it becomes even more compact than the Brembo solution.

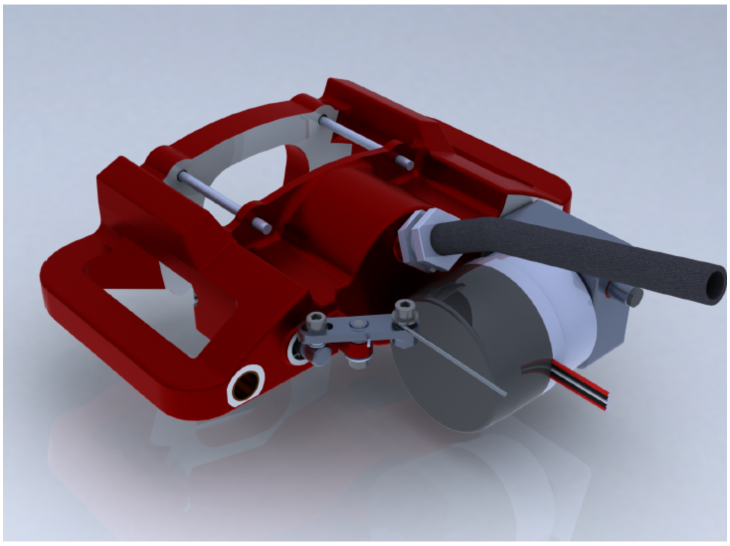

Figure 2.6: E-caliper assembly, rear view. Adopted from [Meu18].

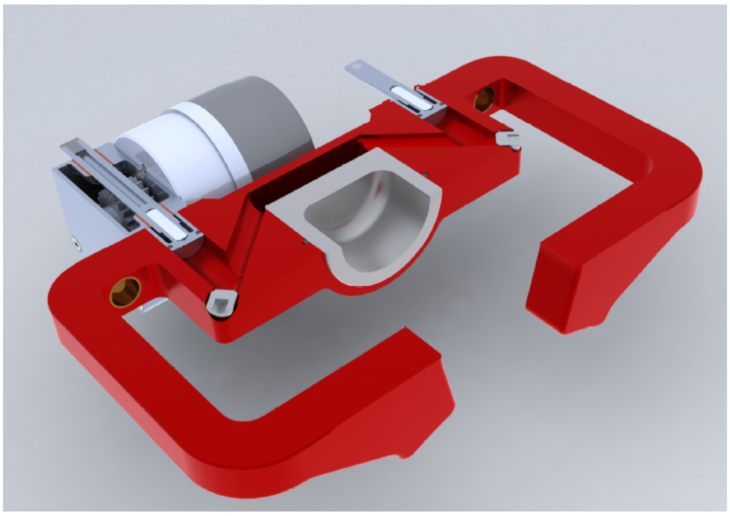

Figure 2.7: Cross-section of the e-caliper. Adopted from [Meu18].

The SpeedE vehicle platform from Aachen University should be mentioned to make the list of the state-of-the-art electro-hydraulic brake solutions complete. The SpeedE project developed the EHB actuator for each wheel. The actuator consists of the hydraulic piston, which is actuated by an electric motor. The picture of the constructed actuator is depicted in figure 2.8. For a more detailed description, please refer to [SFE15].

Figure 2.8: Electro-hydraulic brake actuator developed at the Aachen University. Adopted from [SFE15].

2.2.2 Electro-mechanical Brake

The electro-mechanical brake (EMB) system eliminates all hydraulic components and consists only of the mechanical and electrical ones [Ves20]. The EMB consists of the brake pedal, the ECU, and the wheel brake unit. The wheel brake unit is formed by the EMB brake caliper. The EMB caliper is typically formed by the electric motor with a linear gearbox mechanically connected to the brake piston, which actuates the brake pads. An example of the construction of the EMB caliper is depicted in figure 2.9. The working principle is similar to the decentralized EHB system. The only difference is that the force generated by the electric motor acts directly on the brake pads, and no hydraulic force amplification is used.

The advantage of the EMB solution is the elimination of the hydraulic part of the system, which results in an even simpler design. Moreover, it eliminates the toxic brake fluid; therefore, it is an environment-friendly solution. However, the elimination of the hydraulic parts increases the magnitude of the force which has to be generated by the motor. This increases the size of the motor itself, so it is able to generate the same force as the EHB-based system.

Furthermore, the linear gearbox should be non-self-locking in order to satisfy the safety requirements for brake systems. Finally, the vehicle's unsprung mass is increased, and a new mechanically actuated caliper needs to be designed. Because of that, the EMB brakes are suitable only for rear-wheel brakes, while the force needed for braking rear wheels is significantly smaller. On today's market, the EMB system can be found in Brembo's *Sensify* solution, where the EMB is used on rear wheels.

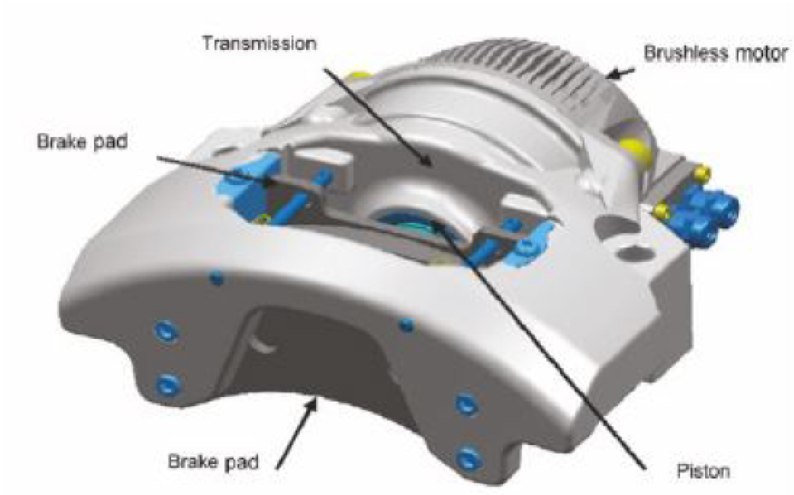

Figure 2.9: Electro-mechanical brake caliper. Adoted from [ST10].

2.2.3 Other Brake Concepts

Finally, the Magneto-Rheological brake (MRB) and the electronic wedge brake (EWB) should be mentioned to make the literature overview complete. The MRB system is currently a hot topic in the automotive brake research, as many research teams are trying to develop their own MRB systems for vehicles [Li19]. The MRB is a fluid operated device where the demanded brake torque is generated by the shear force of the magneto-rheological fluid [AEEGE17]. The MRB offers many advantages, such as fast response time and a simple mechanism [Li19]. However, the MRB system suffers from excessive overheating or limited magnitude of the generated torque, which need to be overcome before its deployment. For more details about the working concept of the MRB, please refer to [Li19] or [AEEGE17].

The latter brake system is the EWB, also called eBrake. It was developed in the German Aerospace Center in 2002. The designed actuator is an electric friction brake with high self-reinforcement capability [HSPG02]. For further details, please refer to [HSPG02] and [HRHG06].

Chapter 3

Sizing of the Brake-by-Wire System for the Project Vehicle

This chapter deals with selecting and designing the most appropriate Brake-by-Wire solution for the SDS prototype vehicle project. Firstly, the requirements and limitations which need to be considered during the brake system design are listed. Secondly, the forces acting on the vehicle and brake system components during the deceleration will be studied so the forces that need to be generated by the brake actuators can be computed. Thirdly, all considered brake actuators with their advantages and disadvantages are studied in order to select the best possible solution for our project. Finally, the sizing of the selected actuator is discussed.

3.1 Brake System Design Requirements

3.1.1 Project Requirements

Thanks to the fact that the design of the prototype vehicle is tailored directly for the needs of the SDS project, the number of design constraints is relatively small. There are only three major requirements for the system design. The selected solution has to allow easy deployment of the control algorithms developed by the SDS research group. This requirement disqualifies all of the industrial automotive brake systems mentioned in chapter 2, because they are supplied as closed black-box solutions, which cannot be easily modified or customised. Typically, to modify the original control algorithms supplied by the manufacturer, the reverse engineering of the whole system needs to be done, which is quite a demanding and ethically questionable task. Moreover, industrial automotive brake systems can hardly be obtained by an end-user. Because of that, our own implementation of the Brake-by-Wire system needs to be designed.

The second requirement is connected to the brake system design. Simply put, the main goal of this thesis is to design the brake system in the simplest way possible and with the maximal use of existing components. The concern of this work is to prepare a hardware platform for the deployment and validation of developed advanced control algorithms, not to design and construct a brake system from scratch. Moreover, as a Control Engineering student, I am not even capable of designing the brake system components. Finally, to meet the requirement for the Brake-by-Wire nature of the system, the designed brake system has to be fully electrically operated.

Mechanical Limitations

The designed brake system has to bring the vehicle to a stop safely and in a reasonable amount of time. As discussed in Chapter 2, the currently existing non-friction-based brake systems cannot deliver the desired brake torque. Therefore, the proposed brake system needs to be friction-based. Moreover, the friction-based approach allows the use of the standard automotive brake components such as brake discs or brake pads.

As the brake system is a safety-critical one, the prototype vehicle should still be equipped with the conventional hydraulic brakes to maximize the safety during the testing. At least the front brakes should be connected to this backup brake system, which will be, also for safety reasons, operated by the same pedal as the Brake-by-Wire system.

A conventional hydraulic brake caliper will be used to simplify the design. Several reasons justify the selection of the hydraulic caliper. The first reason is a significant amplification of the input force. Without using the hydraulic mechanism, the demand on the force magnitude generated by the electric actuator would be quite high since the force acting on the brake pads is relatively high during the braking. Therefore, as mentioned in chapter 2, the purely electro-mechanical caliper is not suitable for this application. Moreover, the preservation of the conventional hydraulic brake caliper in the design significantly reduces the unsprung mass of the vehicle because the brake actuator can be installed into the vehicle body and connected to the brake caliper by a conventional hydraulic line. Furthermore, the space requirements on the brake actuator are greatly reduced because the installation space in the vehicle is significantly less limited compared to the installation space in the wheel hub. The second reason is a self-compensation of the brake pad wear; therefore, the caliper piston stroke remains the same no matter the condition of the brake pads [Meu18]. Furthermore, the use of the hydraulic caliper allows connecting the backup brake system to the same caliper. Finally, the hydraulic caliper is a cheap standardized automotive component that can be easily purchased. On the other side, the preservation of the hydraulic fluid in the design raises issues such as the possibility of brake fluid leakage or its toxicity. However, I still believe that the listed pros outbalance the cons.

Electrical Limitations

In the current vehicle design, three different electric circuits are considered; the 170V high-voltage (HV) circuit for powering the traction motors, the 12V low-voltage (LV) circuit, and the 24V middle-voltage (MV) circuit. The simplified scheme of the vehicle electric circuits is depicted in 3.2. For the power supply of the friction brake actuators, both 12V and 24V power supplies can be used. The HV supply cannot be used because the brakes have to function even when the traction battery is discharged, damaged, or disconnected from the circuit. The usage of the 12V or 24V circuits is preferable; however, the 48V supply can be added if needed.

Controller Area Network (CAN) is used as the main communication interface. Therefore, the designed Brake-by-Wire unit and all other units in the vehicle have to implement the CAN communication interface.

3.1.2 Legislative Requirements

Because the developed prototype vehicle is not intended for deployment in real traffic, there is no need for a detailed study and fulfillment of the legislative requirements. However, when these requirements are followed, the functional safety of the designed system is improved. Moreover, if the brake system design is in accordance with the legislative, it significantly simplifies the eventual certification of the system and allows the deployment of the developed solution in the streets. Therefore, it is a good practise to design in such a way that as many of those requirements as possible are be met.

In Europe, the design of the automotive brake systems is subject to regulation EHK-R13 [EHK10], which was issued by the United Nations Economic Commission for Europe. Among others, the legislative framework defines the following regulations

- minimal braking distance
- minimal mean deceleration value under normal operation of $6.43\,\mathrm{ms}^{-2}$
- requirement for the service and the emergency brake
- requirement for braking system redundancy
- maintenance of the lateral stability during the braking
- deployment of the assistance systems such as ABS

and many others. The items listed above are the most critical ones; therefore, the designed brake system should include at least these features.

3.1.3 Computation of Desired Brake Force

In the following section, the maximal forces acting on the vehicle and the brake components during the braking will be computed. The computation of the maximal force is crucial for the correct sizing of the selected brake system components and actuators. Because the majority of the brake force is delivered by the front brakes in most vehicles, the forces acting on the front brakes will be considered for sizing. The used equations are a simplification of the vehicle longitudinal dynamics, where phenomena such as the tire roll resistance, the aerodynamical resistance, or the tire dynamics, which is modeled by the Pacejka model, are neglected. The visualization of the forces acting on the wheel and brake components is depicted in figure 3.1.

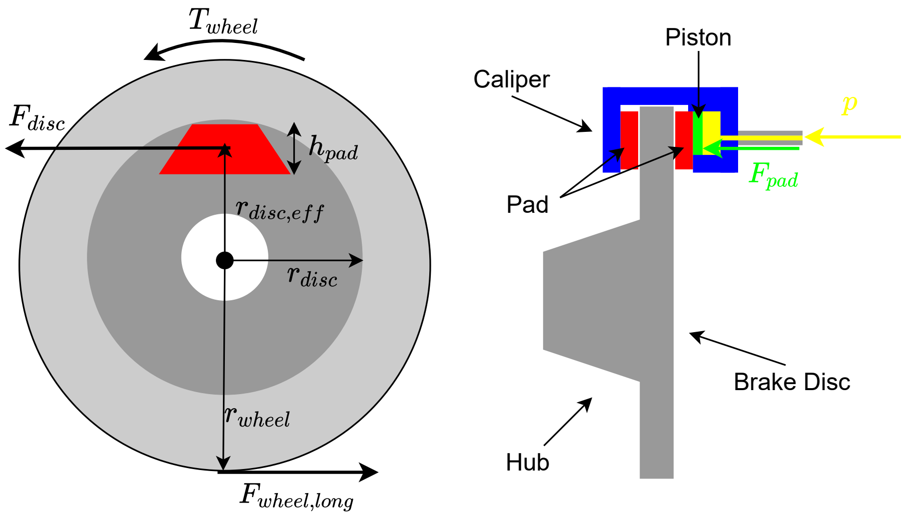

Figure 3.1: Visualization of the forces acting on the brake components.

The maximal braking force acting on the vehicle in the longitudinal direction can be described using Newton's second law

$$F_{long} = ma_{max}, \tag{3.1}$$

where m is the total mass of the vehicle and a_{max} is the maximal considered deceleration of the vehicle. The longitudinal braking force acting on one wheel can be computed using the equation

$$F_{wheel,long} = \frac{F_{long} dist_{ratio}}{2}, \tag{3.2}$$

where the $dist_{ratio}$ represents the distribution coefficient of the braking force between the front and the rear axle. The brake torque can be computed from the equation

$$T_{wheel} = F_{wheel,long} r_{wheel}, \tag{3.3}$$

where the r_{wheel} is the effective radius of the wheel. The longitudinal force acting on the brake disc is given by the equation

$$F_{disc} = \frac{T_{wheel}}{r_{disc,eff}}, \tag{3.4}$$

where the $r_{disc,eff}$ is the effective radius of the brake disc, which can be computed using the equation

$$r_{disc,eff} = r_{disc} - \frac{h_{pad}}{2}, \tag{3.5}$$

where r_{disc} is the radius of the brake disc and the h_{pad} is the height of the brake pad. The force pushing the brake pads against the brake disc is given by the equation

$$F_{pad} = \frac{F_{disc}}{2\mu_{pads}}, \tag{3.6}$$

where μ_{pads} is the friction coefficients between brake disc and brake pads and the constant 2 represents the fact that the brake pads are pushed against the brake disc from both sides. Finally, the hydraulic pressure acting on the caliper piston is given by the equation

$$p = \frac{F_{pad}}{S_{cp}}, \tag{3.7}$$

where S_{cp} is the area of the caliper piston, which can be computed from the caliper piston diameter d_{cp} using the equation

$$S_{cp} = \pi \left(\frac{d_{cp}}{2}\right)^2. \tag{3.8}$$

Several vehicle parameters need to be fixed to get numeric values of the forces and the pressures acting on the brake pads. First of all, the total mass of the vehicle and the brake force distribution between front and rear brakes need to be determined. The prototype vehicle will be constructed on the Škoda Fabia I chassis. The traction battery will be located in the center of the vehicle floor, and the traction motors will be located near the front or the rear axle, see figure 3.2. This leads to a skateboard-like vehicle platform with neutral weight distribution and a low center of gravity (CoG). The estimated total mass of the vehicle, including the passengers, is about 1.5 tons. The geometry of the vehicle chassis and the position of the CoG needs to be known to determine the brake force distribution. However, none of those parameters is known at this moment, while the vehicle is not constructed yet. Therefore, the exact distribution cannot be computed and has to be estimated instead. The typical value of the brake force distribution is set to 0.6-0.7 for front brakes, and 0.3-0.4 for rear brakes [ST10]. The distribution coefficient is set to 0.65 for front and 0.35 for rear brakes for design purposes.

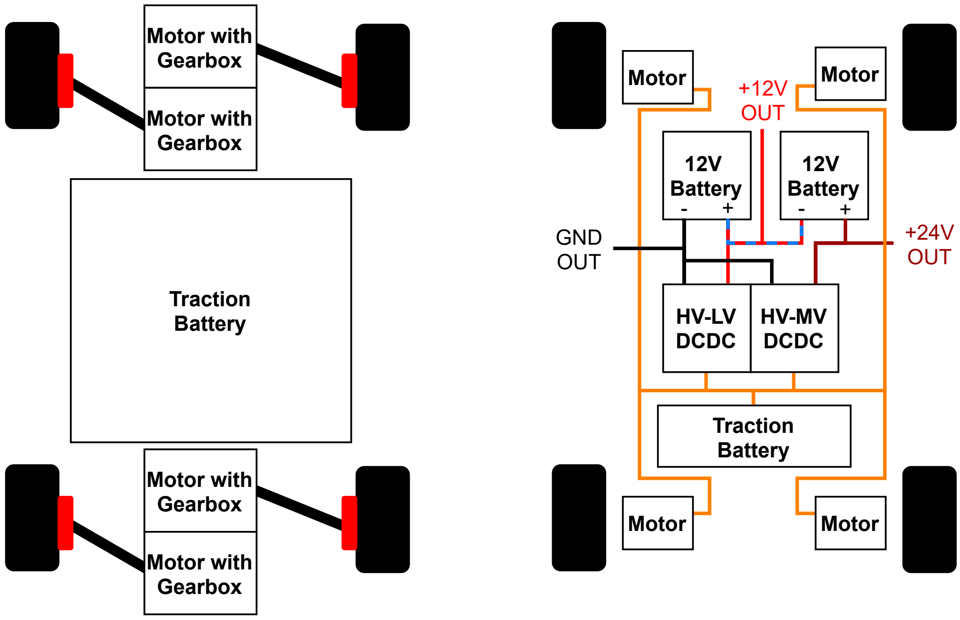

Figure 3.2: Simplified mechanical and electrical scheme of the prototype vehicle.

Another parameter that needs to be fixed is the maximal vehicle deceleration. The vehicle deceleration is highly dependent on the friction coefficient between tires and the road. Let us assume that the vehicle is driving on a straight road with zero road incline. Then the following equation needs to be satisfied

$$ma_{max} = mg\mu_{road}, \tag{3.9}$$

where m is the total mass of the vehicle, g is the gravitational constant, and μ_{road} is the friction coefficient between the tire and the road surface. The maximal deceleration value can be obtained from 3.9 as the following

$$a_{max} = g\mu_{road}. \tag{3.10}$$

The biggest deceleration is achieved on the dry-asphalt surface, where the $\mu_{road} \approx 1$ for the conventional tires. Therefore, the maximal vehicle deceleration is $a_{max} \approx g$. For simplification, the maximal vehicle deceleration of $10\,\mathrm{ms^{-2}}$ will be considered.

Then, the parameters such as tire size, brake disc radius, the height of the brake pads, or friction coefficients between disc and pads need to be determined. The radiuses of the used wheels and brake discs are set to be as large as possible to decrease the magnitude of the force acting on the pads. Therefore, after the consultation with the mechanic, who is responsible for the prototype construction, the wheels and discs from the Škoda Octavia III were selected because they are bigger than the original ones installed on the Fabia, but they still fit in the Fabia's chassis. Similarly, the brake caliper with the largest possible piston was selected to decrease the magnitude of the pressure which needs to be generated. Finally, the performance brake pads, which have a significantly higher friction coefficient than the normal ones, will be used [Mot20] or [Dix].

Finally, the maximal mechanical power needs to be computed. The maximal power is given by the equation

$$P = \frac{W}{t} = \frac{F_{pad} s_{pad}}{t}, \tag{3.11}$$

where s_{pad} is the travel distance of the brake pad, also known as the brake pad clearance and t is the actuation time. After consulting the mechanic, the brake pad clearance was set to 0.5 mm. The value of $t = 0.1\,\mathrm{s}$ is selected as a reasonable actuation time. Moreover, the selected time constant is in accordance with the ABS system frequency, which is in range of 5 Hz to 10 Hz.

The parameters used for the brake pad force calculation can be found in table 3.1. The magnitudes of the calculated normal force, pressure acting on the pads and mechanical power are

$$F_{pads} = 14\,205\,\mathrm{N} \tag{3.12}$$
$$p = 50.24\,\mathrm{Bar} \tag{3.13}$$
$$P = 71\,\mathrm{W}. \tag{3.14}$$

parameter	parameter value	description
m	1500 kg	total mass of vehicle
a_{max}	$10\,\mathrm{ms}^{-2}$	maximal vehicle deceleration
$dist_{ratio}$	0.65	brake force distribution ratio; front brakes
r_{wheel}	0.321 m	wheel radius; used wheel type R18 205/45
r_{disc}	0.17 m	brake disc radius
h_{pad}	0.0646 m	height of the used brake pad
μ_{pad}	0.4	brake disc-pad friction coefficient
d_{cp}	0.06 m	caliper piston diameter
s_{pad}	0.5 mm	brake pad clearance
t	0.1 s	actuation time

Table 3.1: Parameters used for the brake system calculation.

3.2 Considered Brake Actuators

As discussed above, the preservation of the conventional hydraulic brake caliper in the brake system design brings more advantages than disadvantages. Therefore, the conventional hydraulic brake caliper is used in the proposed Brake-by-Wire system. This means that the proposed Brake-by-Wire system is electro-hydraulic. Because of that, a suitable actuator for hydraulic pressure generation needs to be selected. Firstly, it has to be decided whether the proposed Brake-by-Wire system will be centralized or decentralized. As discussed in the previous chapter, the decentralized approach offers benefits such as reducing overall system complexity and weight or reducing the hydraulic transport delay. Moreover, the system redundancy increases because each wheel has its own pressure generation unit. Therefore, the decentralized approach is selected as the most suitable for the proposed Brake-by-Wire system. The actuator itself will be located in the vehicle body to reduce the unsprung mass of the vehicle and lower the requirements on the installation space. It will be connected to the brake caliper using the conventional hydraulic line. A brief description of the brake actuator solutions that are considered follows, and their advantages and disadvantages will be discussed as well.

3.2.1 Hydraulic Pump

The simplest way of generating pressure is the use of a hydraulic pump. The hydraulic pump is a device that pressurizes hydraulic fluid flowing through it. It is typically powered by an electric motor. However, the hydraulic pump is not able to control the amount of the generated pressure precisely and on its own. For precise and fast control of the pressure, several components need to be added to the actuator design, namely the proportional valve, the three-way valve, the pressure limiter, and the high-pressure reservoir. This increases the complexity and leads to a non-trivial hydraulic system design. Therefore, the idea of the custom design and construction of the electro-hydraulic actuator based on the hydraulic pump is abandoned, and a commercial solution is looked for instead.

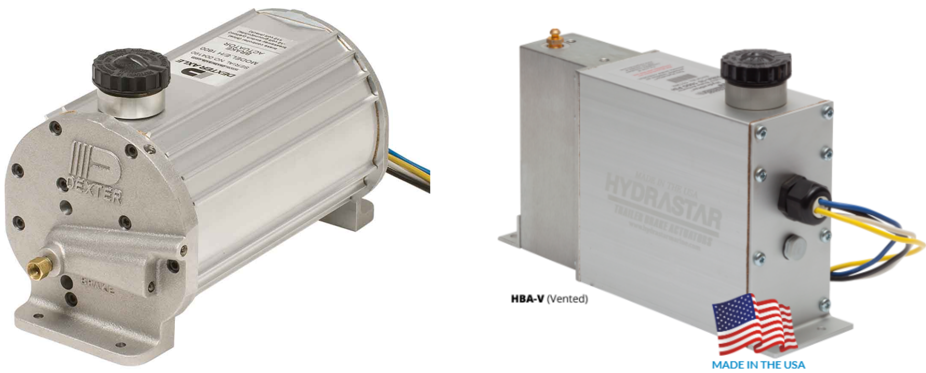

(a) : EHA by Dexter

(b) : EHA by Hydrastar

Figure 3.3: Examples of the commercially available EHAs. Adopted from [Dex] and [Hyd].

Several implementations of the electro-hydraulic actuators based on the hydraulic pump are available on the market. Moreover, some of them, for example *Electric/Hydraulic Brake Actuator* by Dexter company depicted in 3.3a or *Hydraulic Trailer Brake Actuator* by Hydrastar company depicted in 3.3b are even certified for the automotive application in the USA. As the name suggests, the primal use of those actuators is to brake heavy trailers towed by passenger vehicles. Both vendors offer several variants. All of the variants can generate pressure up to nearly 70 Bar, which is sufficient for our application. Furthermore, the generated pressure is proportional to the input electric signal; therefore, it can be easily controlled and modified. Both solutions offer advantages such as easy pressure control, compact size, integration of all components in the aluminum casing, easy installation, and high reliability. On the other side, both actuators are available only in the USA, significantly prolonging shipping time and costs. Moreover, the price of these actuators is relatively high; Dexter charges $1,600 per unit. Therefore, commercial hydraulic pump-based solution is abandoned mainly due to its unavailability on the European market and relatively high price.

3.2.2 Master Cylinder

Another way to generate pressure is to use the conventional brake master cylinder. The master cylinder transforms applied force into fluid pressure; therefore, the combination of the master cylinder with some force-generating device (e.g., an electric motor) forms a unit that is capable of generating the demanded pressure. The following force needs to be applied to the master cylinder rod to generate the desired brake pressure

$$F_{master} = pS_{mp} + F_{spring}, \tag{3.15}$$

where F_{spring} is the force needed for compression of the spring inside the master cylinder, p is the desired pressure, and S_{mp} is the area of the master piston, which is given by the equation

$$S_{mp} = \pi \left(\frac{d_{mp}}{2}\right)^2, \tag{3.16}$$

where d_{mp} is the diameter of the master piston. The stroke of the master piston, which is needed to cover the brake pad clearance, is given by the equation

$$s_{master} = \frac{S_{cp}}{S_{mp}} s_{pad} + s_{cut}, \tag{3.17}$$

where the first term on the right side corresponds to the brake pad stroke, and the second term on the right side represents the stroke that needs to be performed to seal the hydraulic circuit so that the pressure can be generated.

Because each brake will be actuated by its own actuator, the single outlet master cylinder will be used. To minimize the magnitude of the force acting on the master cylinder rod, a master cylinder with a small piston diameter will be used, so the hydraulic amplification ratio is maximized. The performance single outlet master cylinder by Wilwood was selected because it fits all these demands the best. The selected master cylinder is depicted in figure 3.4. The parameters of the selected master cylinder are displayed in table 3.2.

(a) : Wilwood GS Compact master cylinder.

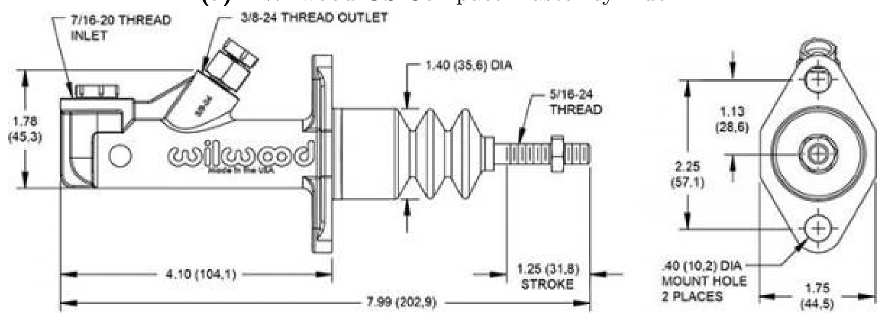

(b) : Scheme of the Wilwood GS Compact.

Figure 3.4: Selected master cylinder. Adopted from [Wil].

parameter	parameter value	description
d_{mp}	12.7 mm	master piston diameter
F_{spring}	150 N	inner spring compression force; measured experimentally
s_{cut}	2 mm	stroke needed for sealing the hydraulic circuit; measured experimentally

Table 3.2: Parameters of the selected master cylinder.

The master piston stroke and force can be computed using the equations above. The computed numerical values are the following

$$F_{master} = 786\,\mathrm{N} \tag{3.18}$$
$$s_{master} = 13.16\,\mathrm{mm}. \tag{3.19}$$

Mechanical transmission, such as a lever, can be used to decrease the force, which needs to be applied to the master cylinder rod. However, the decrease in the force magnitude results in an increase of the stroke. Therefore, the decision of whether to use an additional mechanical transmission will be made after the selection of the electric actuator and fixing its parameters. More about it can be found in chapter 4.

Linear Solenoid

The first actuator considered is the linear solenoid. The linear solenoid consists of the winding and magnetic core connected to the plunger, which will be connected to the master cylinder rod. When an electric current flows through the winding, a magnetic field is generated. Generated magnetic field interacts with the magnetic field of the solenoid core and results in the movement of the core.

The solenoid force is easily controllable by the magnitude of the input current; therefore, it seems to be the perfect actuator for our application. Unfortunately, all solutions available on the market, which satisfy the force and stroke requirements, are entirely out of our budget; the cost of the suitable solenoids ranges from $3,000 to $25,000. Moreover, the weight of these actuators is about 18 kg, which is a lot. Because of that, there was an attempt to design my own implementation of the linear solenoid. A brief description of the proposed actuator design follows.

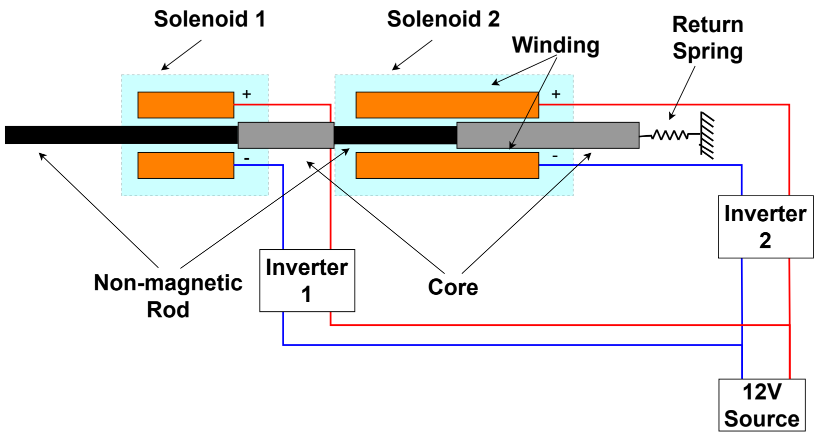

Figure 3.5: Scheme of the proposed linear solenoid actuator.

The proposed linear actuator should consist of two serially connected solenoids with a common plunger, as depicted in figure 3.5. The first solenoid should generate the actual brake force with only minimal movement. The second solenoid should deliver a high stroke but a relatively small force just to overcome the force generated by the return spring of the master cylinder and other resistances. The intended working principle is the following. When no braking force needs to be generated, none of the solenoids is energized, and they remain in position 0, see figure 3.6a. When the driver lifts his foot from the accelerator pedal, the high-stroke solenoid will be energized, which results in the movement of the plunger. The movement of the plunger causes that the core of the first solenoid gets into the operational position and that the brake pads will be slightly squeezed against the brake disc, generating a negligible amount of brake force, see figure 3.6b. Finally, when the driver pushes the brake pedal, the second solenoid will be energized, and the desired brake force will be generated, see figure 3.6c.

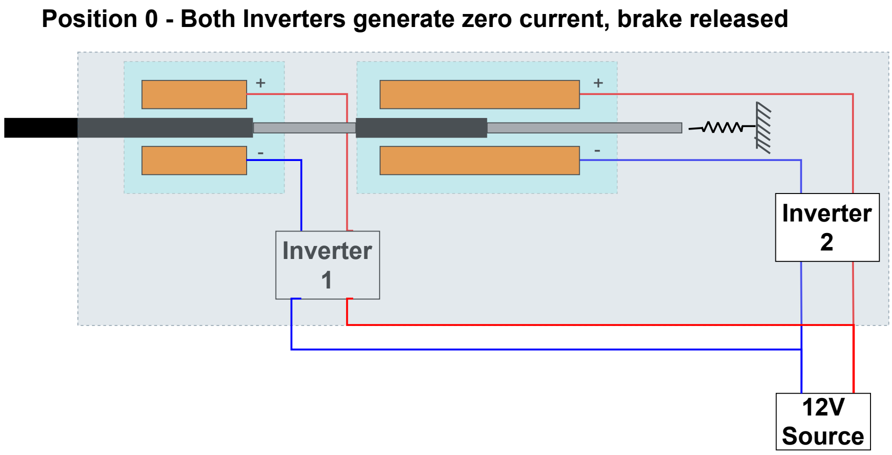

(a) : Position 0 - brake released

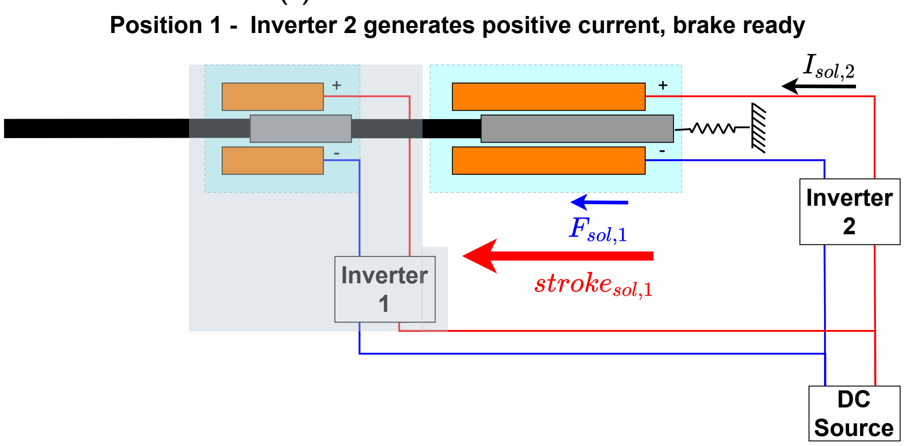

(b) : Position 1 - brake ready

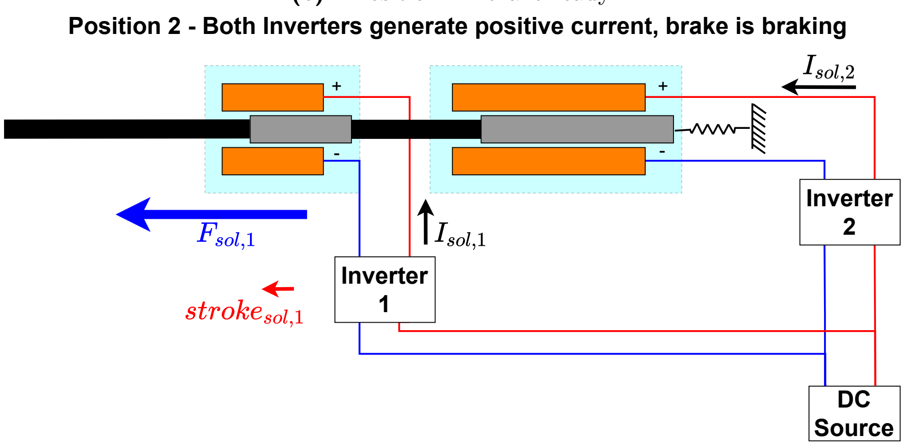

(c) : Position 2 - brake braking

Figure 3.6: The working principle of the proposed actuator.

The design and computation of the parameters of the proposed solenoid actuator were based on the Biot-Savart law and on the approach adopted from paper [SL15], which deals with the design of small solenoid actuator for miniaturized robot applications. Unfortunately, all design attempts lead to either a too heavy coil (the designed solution was even heavier than the commercially available one) or too high inner resistance of the coil. Because of that, both commercial and own designed solenoid solutions are unsuitable for the brake system actuation, and therefore, another, more suitable actuator needs to be selected.

Linear Motor

The second considered linear actuator is the electric motor. Only the motors with integrated linear drive were considered, so there is no need to design and select the linear transmission. The following two types of the linear motor were studied; the DC motor with integrated linear transmission and the linear stepper motor. Moreover, for an easy installation and linear actuator's connection to the master cylinder rod, the output rod of the linear motor should perform only a linear, not a rotary movement. Examples of the described linear motors can be seen in figure 3.7

The DC motor with integrated linear transmission typically consists of a rotary electrical motor and a lead screw linear transmission. This actuator offers high output force, high stroke, and relatively high actuation speed. Moreover, plenty of vendors and variants are available on the market for reasonable prices. On the other side, the size and weight of the actuator are quite large, and the position control of the motor is less precise compared to the stepper motor. Furthermore, the lead screw transmission is typically self-locking, which can easily cause jamming of the brake when a malfunction of the electric motor occurs.

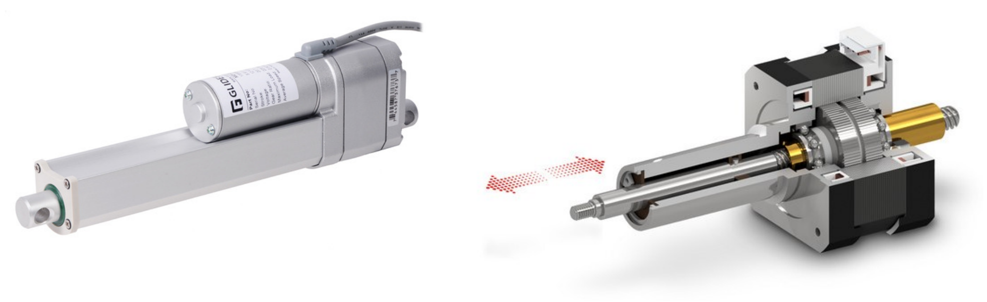

(a) : DC motor with linear drive by Pololu.

(b) : Linear captive stepper motor by Nanotec.

Figure 3.7: Examples of linear electric motors. Adopted from [Pol] and [Nanb].

The linear stepper motor allows easy and precise control of the motor position. This motor consists of a rotary stepper motor and a lead screw mechanism that converts rotary motion into linear. Compared to the DC motor with a linear drive, available stepper motors offer smaller output force and stroke. An additional transmission (e.g., lever mechanism) needs to be used to compensate for the smaller force output. On the other hand, the actuation speed is typically higher, the position control of the motor is more straightforward and precise, the motor casing is more compact and significantly lighter, and the purchase price is a little bit lower.

3.3 Selected Actuator

Finally, the most suitable solutions will be selected from the solutions mentioned above. As discussed, the single outlet master cylinder from Wilwood will be used. To actuate the master cylinder, both the stepper and the DC motor are suitable. In the end, the linear stepper motor is selected because of its more compact and lighter sizing and faster actuation speed. Finally, the delivery time of the selected stepper motor was significantly shorter than the delivery time of the considered DC motor, which also influenced the final decision, while the time for the project completion is limiting.

parameter	parameter value
maximal force	476.7 N
maximal stroke	38.1 mm
maximal speed	$100\,\mathrm{mm s^{-1}}$
nominal voltage	24 V
maximal current per phase	2 A
electrical power	48 W
step resolution	0.03 mm/step
number of steps per resolution	200
weight	0.75 kg
motor type	bipolar

Table 3.3: Parameters of the selected linear stepper motor.

The selected linear stepper motor is the *LGA561S20-A-TSGA-038* from Nanotec. The technical drawing of the motor and the list of the motor parameters are attached in appendix B. The selected variant of the motor is a captive one, which means that the linear guide is attached to the front of the lead screw, which prevents the lead from rotating. Moreover, the selected motor is bipolar, which means that it has a single winding per phase. The most important parameters are listed in table 3.3 above. The maximal force of the motor is smaller than the desired one, see 3.18. Therefore, an additional transmission in form of a lever will be used. More about the transmission design can be found in the next chapter 4, where the mechanical and hardware implementation of the designed Brake-by-Wire unit is described in greater detail.

The selected motor is depicted in figure 3.8. The force-velocity curve of the motor can be seen in figure 3.9. As it can be seen in figure 3.9, the maximal speed of the actuator is limited by the magnitude of the generated force. This is caused by the fact that the ideal stepper motor is the constant output power transducer. Because power is defined as force multiplied by linear speed, it is evident that maximal speed is dependent on momentary force to keep constant power. To achieve maximal actuation speed and thus minimize the time needed for brake pressure build-up, the motor speed needs to be controlled dynamically according to the magnitude of the generated force. For more about the motor speed control and Brake-by-Wire unit control, please refer to chapter 5.

Figure 3.8: Selected linear captive stepper motor. Adopted from [Nana]

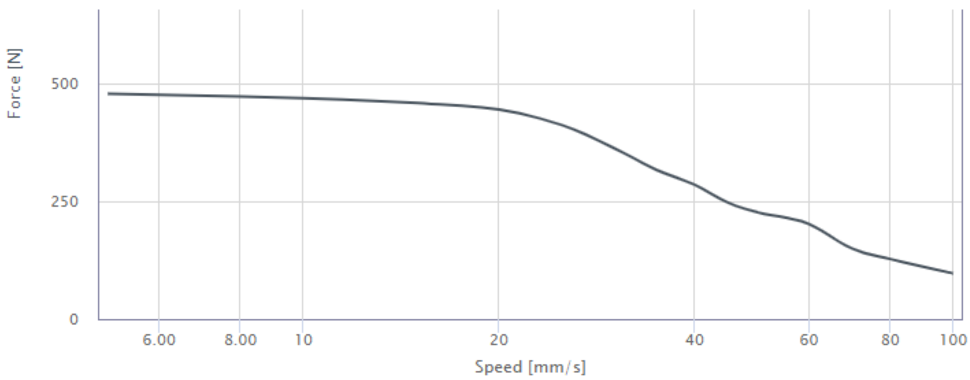

Figure 3.9: Force-velocity curve of the selected motor. Adopted from [Nana]. Please excuse the poor readability of the graph; the supplier did not provide any better graph.

As the attentive reader surely noticed, the value of the actuator power computed in the equation 3.14 is greater than the power of the selected actuator, refer to table 3.3. While the force generated by the actuator is sufficient, as discussed in chapter 4, the smaller value of the actuator power will result in a lower actuation speed than intended. On the one hand, this is limiting, because the lower actuation speed prolongs the time needed for the pressure build-up, which prolongs the brake response and the braking distance of the vehicle. On the other hand, the selected linear stepper motor is the best compromise of the actuator price, weight, size, performance and most importantly, the delivery time. Moreover, the resulting 'limited' performance is still sufficient to demonstrate the concept.

Finally, I believe that at this moment, it is essential to develop some solution, even a slower one, that can be deployed and tested in the real vehicle. The deployment and testing in the real vehicle will give us valuable feedback and data, which can help improve the proposed solution design. If the data collected during the testing show that the actuation speed of the selected solution is insufficient, the designed solution can be improved in order to address this issue by adding a second actuator to the design or by replacing the currently selected actuator with a more powerful one.

Chapter 4

Hardware Implementation of the Brake-by-Wire Unit

This chapter will describe the mechanical construction of the Brake-by-Wire unit itself and the hardware selection. The selected sensorics and the control electronics will be briefly described. Then, the casing box for the control electronics will be created to protect it from dust, dirt, and water. Moreover, the casing box facilitates the unit's installation in the vehicle. Because the selection of the linear stepper motor and its parameters and limitations were discussed in great detail in the previous chapter 3, the description of the motor will be omitted in this chapter.

4.1 Mechanical Construction

As discussed in the previous chapter, the combination of the master cylinder and linear stepper motor will be used as a pressure generation unit. While the maximal force delivered by the motor is smaller than the maximal force needed for the master cylinder actuation, see 3.18 and 3.3, generated motor force needs to be amplified. This can be easily done by the single lever mechanism depicted in figure 4.1. The equation describing the single lever mechanism is the following

$$F_{master} l_1 = F_{motor} l_2, \tag{4.1}$$

where the meaning of the variables is self explanatory from figure 4.1. From 4.1, the force amplification ratio can be computed using the equation

$$\frac{l_2}{l_1} = \frac{F_{master}}{F_{motor}} = \frac{786}{476} \approx 1.65. \tag{4.2}$$

To ensure that the required force on the master cylinder is generated even in the presence of friction and other resistances that have been neglected during the design and to ensure safety margin, the coefficient is increased to

1.8. Therefore, the length of the lever's l_2 section can be computed using the equation

$$l_2 = 1.8 \cdot l_1. \tag{4.3}$$

To save weight and size of the lever, the lever should be short. Due to the dimensions of the master cylinder and the linear stepper motor, the minimal distance between the master piston rod and the motor shaft, which is equal to $l_2 - l_1$, is 64 mm. Now, it is possible to compute the values of lever's l_1 and l_2 sectors,

$$l_1 = 80\,\mathrm{mm} \tag{4.4}$$

$$l_2 = 144\,\mathrm{mm}. \tag{4.5}$$

Finally, using the following equation, the value of the motor stroke can be computed. The meaning of the used variables can be seen in figure 4.1

$$s_{motor} = \frac{l_2}{l_1} s_{master} = \frac{144}{80} \cdot 13.16 = 23.69\,\mathrm{mm}. \tag{4.6}$$

The computed value of the motor stroke is smaller than the maximal value of the stroke, which can be generated by the motor. Therefore, the designed mechanical lever solution is feasible.

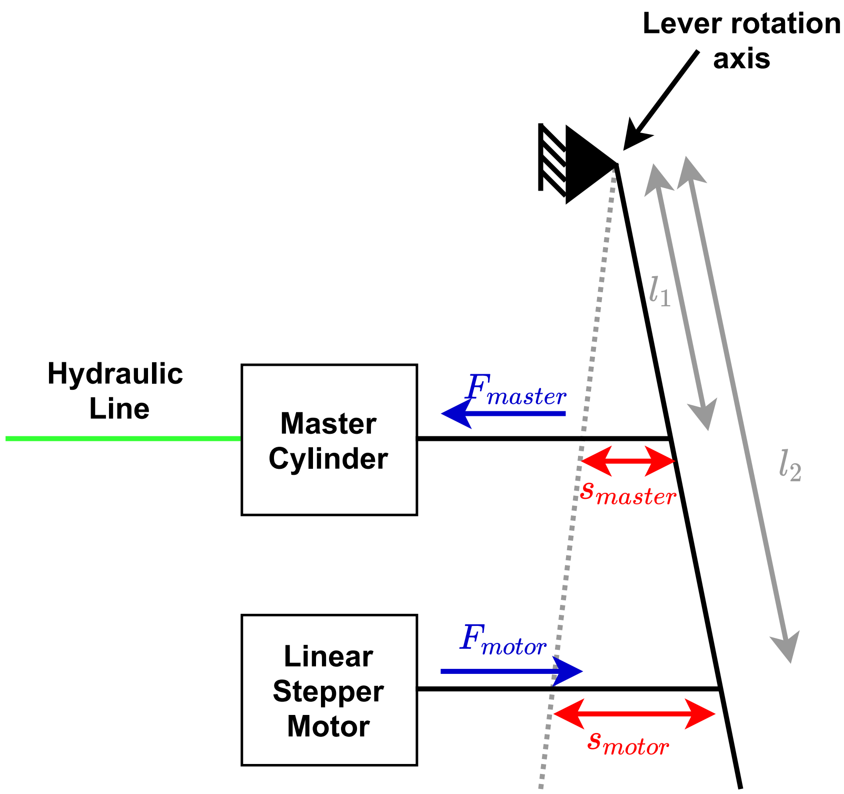

Figure 4.1: Scheme of the single-lever mechanism.

Now, when the lever is designed and the dimensions are fixed, the mechanical realization of the lever mechanism and the actuator mounting will be done. As my experience with mechanical design and the number of available tools are limited, a mechanical solution that is easily manufacturable even with limited resources will be selected.

The core of the Brake-by-Wire unit will be a hollow iron cube with a size of 250 mm, formed by iron profiles (30x20x2 mm) welded together, see figure 4.2. On the left side of the cube, two additional beams for mounting the master cylinder and the motor are welded. On the rear side, one beam that serves as the lever's mounting point is welded. Finally, one beam for the lever support and the limit switch installation is welded on the front side. On the bottom side, four 8.5 mm mounting holes for easy installation into the testing vehicle are drilled. Moreover, the chipboard platform is attached to the base of the cube. The chipboard platform will be used for mounting the control electronic casing box, so all mechanical and electrical components of the designed Brake-by-Wire unit can be packed in one compact box.

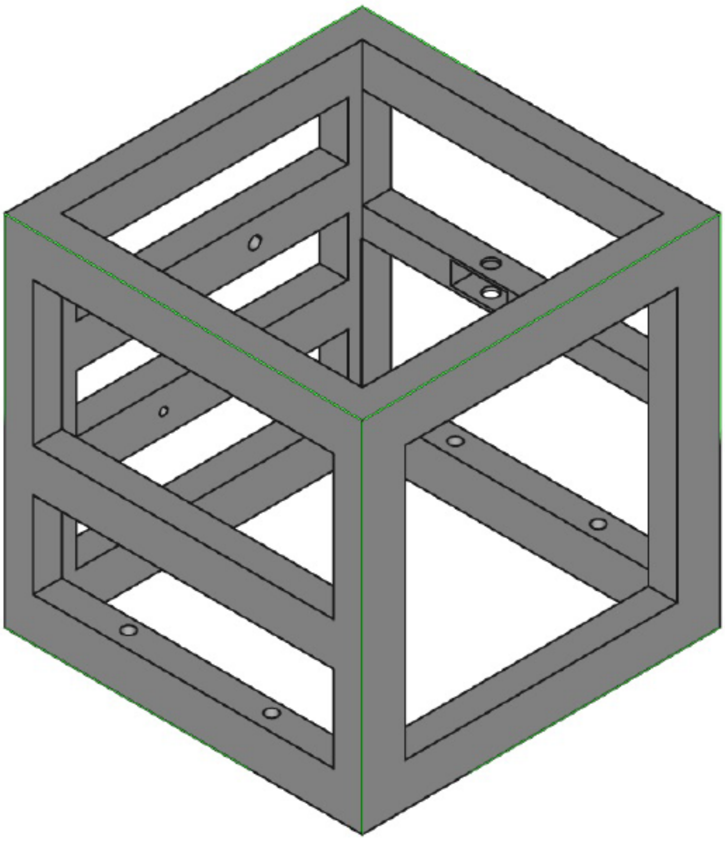

Figure 4.2: 3D visualization of the mechanical construction of the Brake-by-Wire unit.

Obviously, the designed mechanical solution of the Brake-by-Wire unit is not the best or optimal one, mainly due to its size and weight. Nevertheless, the designed solution serves well for testing purposes and as a proof of concept. Moreover, the designed mechanical solution offers great flexibility in the sensors and actuators placement, which is beneficial for unit development. Finally, when testing shows that this solution is applicable and fulfills all the requirements, a new and more compact design tailored directly for the testing vehicle will be created.

The lever itself is made of one iron profile and one M10 uniball bearing connected together, see figure 4.3. A conventional M10 screw fixed into the beam on the rear side is used as a lever rotation axis. As it can be seen in figure 4.2, a uniball bearing has been mounted directly into the iron profile in order to increase the strength of the mount. Moreover, the vertical movement of the lever is limited by this kind of mounting. Two more holes for mounting the master cylinder and the motor rods are drilled in the lever body. Because of the circular motion of the lever, the master cylinder rod and the motor rod also need to be connected to the lever body by the uniball bearings. Those uniball bearings introduce the required degree of freedom, which is needed for flawless operation because a direct connection of the rods and the lever can result in a mechanical deformation or even a damage of the components. For the same reasons as mentioned above, the uniball bearings are mounted inside the lever, so the structural strength of the connection is increased.

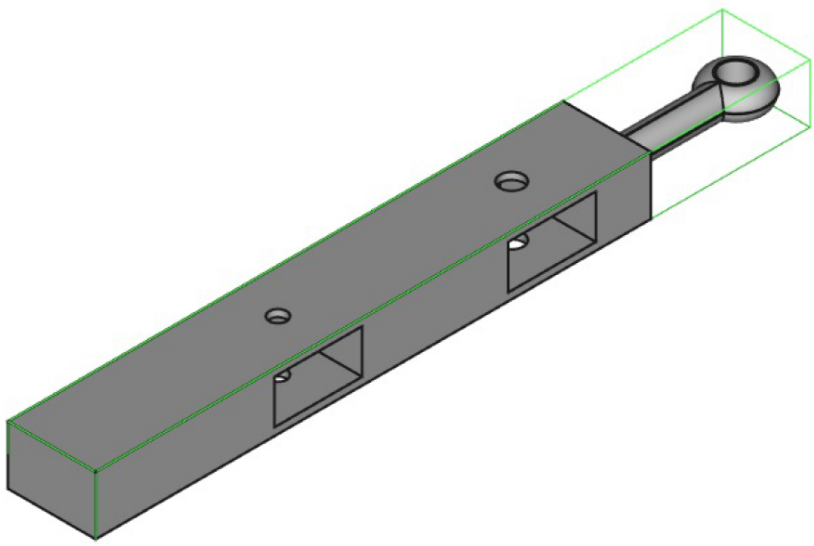

Figure 4.3: 3D visualization of the designed lever.

In figures 4.4 and 4.5, the 3D visualization of the designed Brake-by-Wire unit fitted with the master cylinder, the linear stepper motor, and the proposed lever mechanism can be seen. The photos of the real-life construction of the Brake-by-Wire unit can be seen in section 4.3 in figures 4.16 - 4.19.

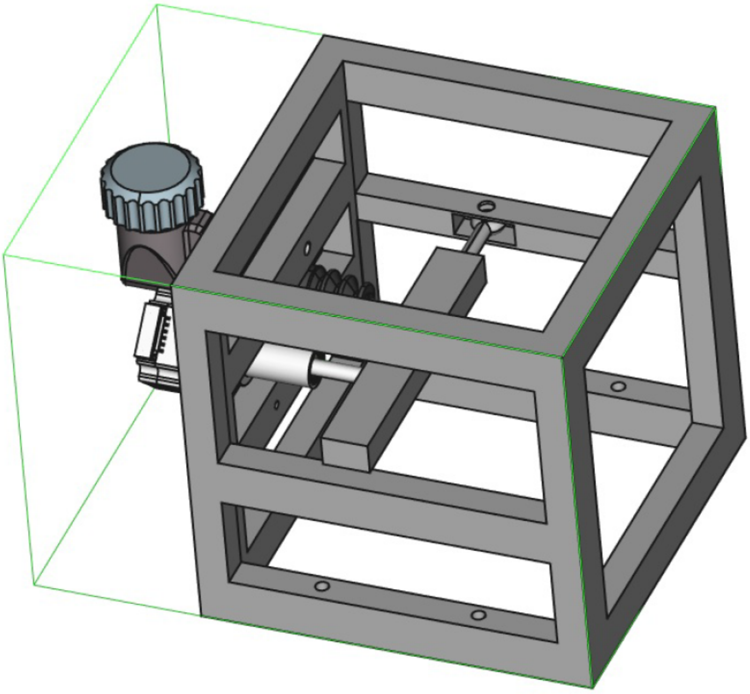

Figure 4.4: 3D visualization of the designed unit. The 3D model of the stepper motor is adopted from [Nana]. The 3D model of the master cylinder is adopted from [Hod18].

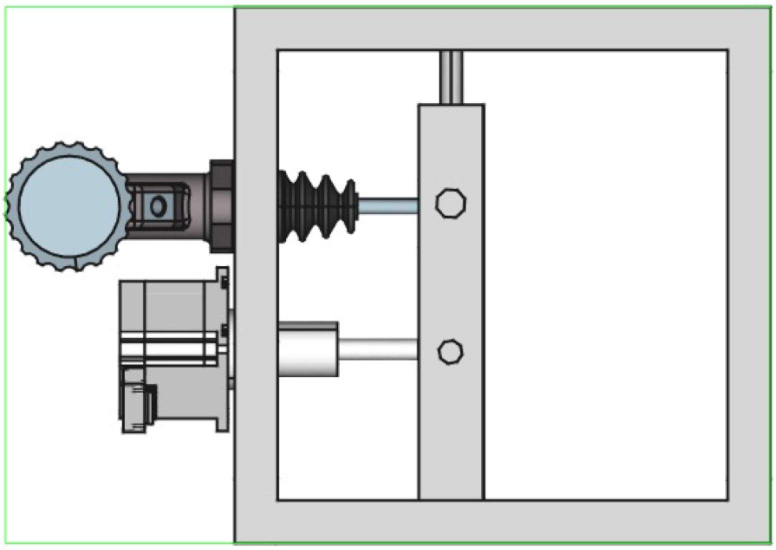

Figure 4.5: Top view of the designed unit. The 3D model of the stepper motor is adopted from [Nana]. The 3D model of the master cylinder is adopted from [Hod18].

4.2 Control Electronics

4.2.1 Main Computational Unit

The *TI LAUNCHXL-F28379D development board* from the Texas Instruments was selected as the main computational unit for the Brake-by-Wire unit. There are two main reasons. Firstly, the TI Launchpad allows writing the code in the Simulink environment, which is then automatically translated into the C language by the built-in code generation tool; the model-based approach can be used, which speeds up the programming of the board. Moreover, Matlab & Simulink are used as the main programming language of the SDS project, so it is beneficial to use it for programming the BBW unit as well. Secondly, the TI launchpad board has a built-in CAN interface so that the board can be easily connected to the vehicle communication buses without the need for any external boards implementing the CAN interface. The selected board is depicted in figure 4.6. The list of the selected hardware features follows; for all hardware features and a more detailed description of the TI board, please refer to Texas Instruments' website [TI].

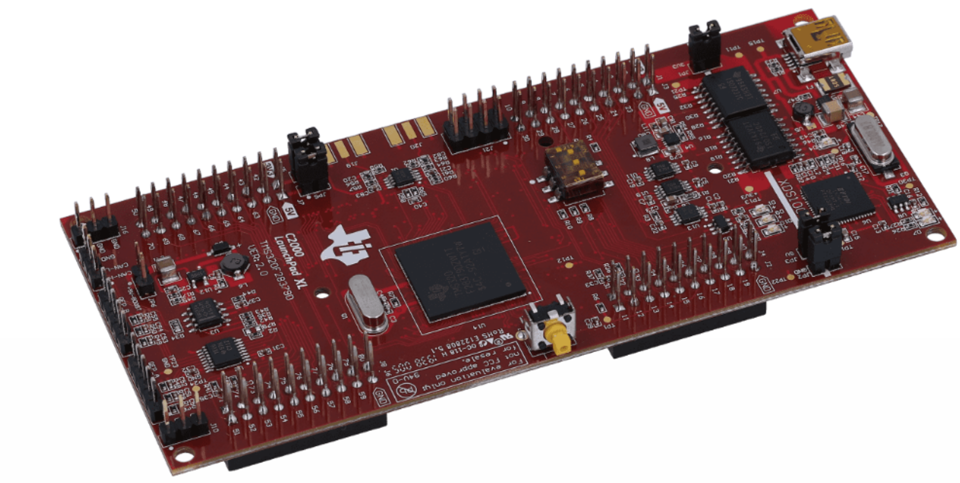

Figure 4.6: Picture of the selected board. Adopted from [TI].

- programmable buttons and LEDs
- 200 MHz dual C28x CPU
- 1 MB flash memory
- 12x 12-bit ADCs and 4x DAC
- 2x CAN interface
- 3.3V digital outputs and inputs

- 3.3V and 5V power supply inputs
- I2C, SPI interface
- ePWM, eCAP pins
- programmable via USB cable
- powered either by USB cable or power pins

As mentioned above, the TI launchpad board will be used as the main computational unit of the BBW unit. All sensors, motor drivers, and communication buses will be connected to the TI board. The main purpose of the TI board is to read the information from the sensors and CAN bus, evaluate this information, and compute the control commands for the motor driver to deliver the desired brake force. Moreover, the TI board sends all measured data back to the vehicle control unit via the CAN bus.

4.2.2 Motor Driver

Originally, the motor driver *C5-01* supplied by the manufacturer of the linear stepper motor Nanotec was supposed to be used, see figure 4.7a. However, after the motor and the driver had been ordered, the supplier changed the delivery time of the driver from originally the beginning of March to the middle of April. Because of that, a different motor driver was purchased. As a workaround solution, the *DM542* stepper motor driver was selected; see figure 4.7b. The DM542 is the open-loop stepper motor controller, which can be used for controlling most of the bipolar stepper motors on the market, and it is supplied in a compact metal casing.

(a) : Stepper motor driver by Nanotec.

(b) : DM542 stepper motor driver.

Figure 4.7: The considered and selected stepper motor drivers. Adopted from [Nana] and [DM].

Compared to the Nanotec motor driver, the DM542 is not programmable and offers fewer features. On the other hand, the DM542 is significantly cheaper, the delivery time was only two days, and most importantly, it is sufficient for our application. The main features of the DM542 driver are listed below.

- supply voltage range 24 - 50 V
- maximal output current 3 A
- configurable overcurrent protection
- microstepping up to 25600 steps per revolution
- control supply range 4.5 - 28 V; signal low level 0 - 0.5 V; signal high level 4.5 - 28 V
- maximal input frequency of PUL input 200 kHz

The power inputs are connected to the 24 V power supply, and the power outputs of the driver are connected directly to the motor terminals. The control inputs are used to control motor movement, and they are connected to the TI board. While the high level of the control signal is different for the TI board and DM542 driver, the 3-5 V logic level signal converter (LLC) needs to be used. The DIR+ and PUL+ inputs are connected to the signal high level (+5V), the DIR- input is connected to a digital output pin that controls the motor movement's direction. The PUL- input is connected to the Pulse Width Modulation (PWM) source, and the frequency of the pulses is moderate to the motor speed. The simplified electric scheme of the motor driver connection to the TI board and the motor itself is depicted in figure 4.8.

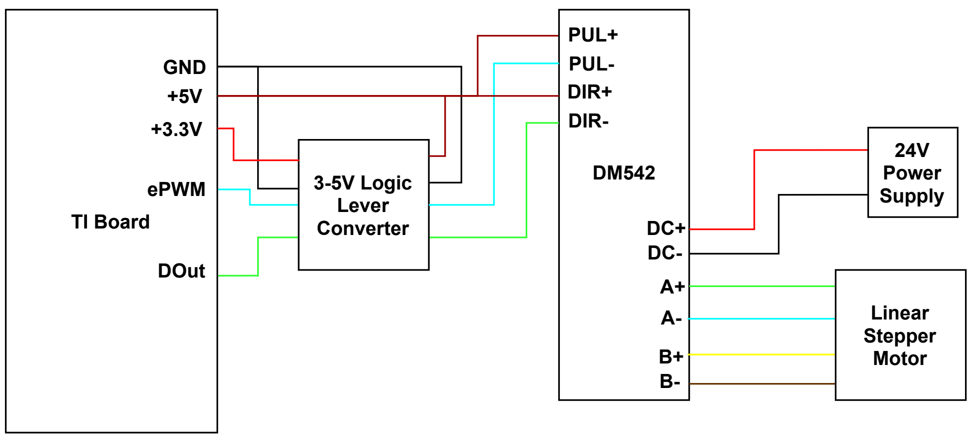

Figure 4.8: Scheme of the electric motor and driver connection.

4.2.3 Pressure Sensor

The pressure sensor needs to be used to allow precise control of the generated pressure. The selected pressure sensor is the *AiM 0-100 bar M10*[1], see figure 4.9. This pressure sensor was selected mainly because of its easy mechanical and electrical installation. Moreover, this sensor is designed and certified for the automotive; therefore, its pressure measurement should be reliable and robust. As the name suggests, the pressure range which can be measured by this sensor is from 0 Bar to 100 Bar, which is more than sufficient for our application. The selected sensor can be easily mounted into the conventional brake 3-way junction block; therefore, the installation is straightforward. The sensor's electrical connection is provided by 3-wire-connector, where the first wire is dedicated to the output signal, which corresponds to the measured pressure. The second wire is connected to the ground, and the last wire is connected to the supply voltage. The supply voltage range is 8-16 V. The output signal is the voltage corresponding to the measured pressure, the range of the output signal is 500-4500 mV, where 500 mV corresponds to 0 Bar and 4500 mV corresponds to 100 Bar; therefore, there is a linear dependency between the measured pressure and the output voltage.

Figure 4.9: Selected pressure sensor. Adopted from [Aim].

4.2.4 Linear Potentiometer

The linear potentiometer is used for measuring the absolute lever position. The main purpose of this sensor is to detect loss of the motor's steps and detect any malfunction of the pressure sensor or the hydraulic lines (e.g., leakage or lack of fluid). More about the use of this sensor and the functional safety of the BBW unit can be found in the following chapter 5. The selected sensor is the *Miniature Spring Return Linear Motion Position Sensor*, see figure 4.10a. The maximal stroke measurable by the sensor is 35.6 mm. The sensor will be mounted between the master piston and the stepper motor and

[1]The pressure sensor can be also found under the code X05PSA00100B10.

mechanically connected to the lever, see figure 4.14 in the following section 4.3. The sensor is electrically connected in a 3-wire configuration. The electrical connection of the sensor and BBW unit is depicted in the next section 4.3 in figure 4.12.

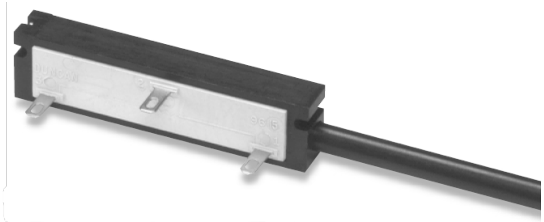

(a) : Selected linear potentiometer. Adopted from [RSC].

(b) : Selected limit switch. Adopted from [GMEa].

Figure 4.10: Selected sensorics.

4.2.5 Limit Switch

The relative position of the stepper motor rod can be obtained by computing the number of the motor's steps, more about it in chapter 5. However, this position is relative, not absolute. To get the absolute position, either the absolute position sensor needs to be added into the design, or the homing procedure needs to be implemented. For the implementation of the homing procedure, limit switches are needed. Moreover, the limit switches can safely stop the stepper motor from moving when the end positions of the motor rod range are reached. This is crucial to avoid losing steps. More about the homing procedure and limit switch usage can be found in chapter 5.

Two limit switches are used to safely stop the motor on the ends of its range, each on one end of the motor stroke range. The microswitches from the Zippo company were selected as the limit switches; see figure 4.10b. Both switches are mounted on the beam on the front side of the cube, and both are activated by the lever. The selected switches have one input pin and two output pins; normally open (NO) and normally closed (NC). Both switches are connected to the universal printed circuit board (PCB), which is connected to the TI board; refer to the overall electrical scheme in section 4.3, figure 4.12. Because the TI board's internal pull-down resistor cannot be activated from Simulink, the PCB is used to custom implement the pull-down resistors. Using the pull-down resistors is crucial to avoid accidental switching of floating signal levels.

4.2.6 DCDC Step-down Converter

The DCDC step-down converter is used for powering the TI board, while the voltage available in the vehicle is either 12V or 24V, and the TI board needs

5V. The output voltage of the selected step-down converter is tunable by the trimmer, and the input voltage needs to be in the range 1.25-32 V. The maximal value of the current is 5 A, which is more than sufficient for powering the TI board and other sensorics. Moreover, the converter is equipped with a tunable current limiter. The used DCDC step-down converter is depicted in figure 4.11.

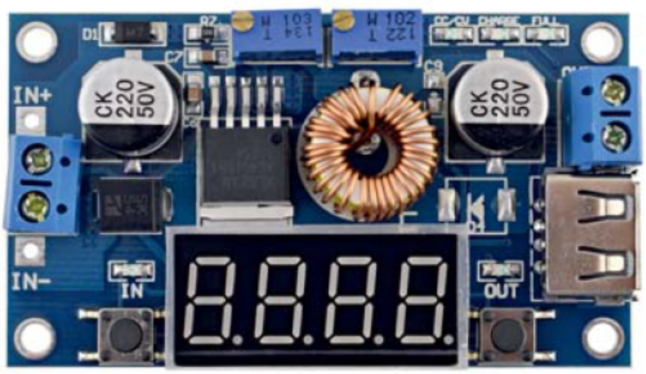

Figure 4.11: Selected DCDC step-down converter. Adopted from [GMEb].

4.2.7 Electrical Connection

The proposed Brake-by-Wire unit is connected to both 12V and 24V circuits. The 24V circuit is used to power the stepper motor, and the 12V circuit is used to power the control electronics and sensorics. For the needs of the TI board, private 3.3V and 5V circuits are implemented inside the electronic casing box. These low-level voltages are obtained from the 12V source using the step-down converter described above. The overall electrical scheme can be seen in the following section 4.3 in figure 4.12.

4.2.8 CAN

The CAN bus is used as the main communication bus. The CAN bus provides the connection of the proposed Brake-by-Wire and other units installed in the vehicle, such as the VCU or the Pedal unit. The shielded twisted wire is used as the CAN wire. The conventional CANON 9 connectors are used to allow an easy connection. More about the implemented CAN protocol can be found in chapter 5. Finally, the single wire connecting the digital output of the BBW unit to the digital input of the VCU is introduced. The purpose of this connection is to inform the VCU that the CAN connection between the VCU and the BBW unit has been lost. This is crucial because the BBW unit is a safety-critical system; therefore, every malfunction must be detected as quickly as possible.

4.3 Constructed Brake-by-Wire Unit

Finally, the overall electrical scheme of the control electronics and sensorics connection described above can be seen in figure 4.12. The list of used pins for connecting the control electronics with sensors and the motor driver can be seen in table 4.1. A casing box was designed to protect the control electronics from dirt, dust, and water and make it more compact. The casing box was created using the FreeCAD software and printed on the 3D printer. The 3D visualization of the designed box is depicted in figures 4.13a and 4.13b; the photo of the printed case can be seen in figure 4.15. The box lid was carved from transparent plexiglass; therefore, the control electronics can be easily visually inspected without disassembling the lid.

device	pin name	function	pin connected to
pressure sensor	pin 1	analog output	ADCA1
	pin 2	ground	gnd
	pin 3	supply voltage	+12V
potentiometer	pin 1	supply voltage	+3.3V
	pin 2	analog output	ADCB4
	pin 3	ground	gnd
limit switch 1	COM	common pin	+3.3V
	NO	normally open port	P104 via PCB pull-down
	NC	normally closed port	P18 via PCB pull-down
limit switch 2	COM	common pin	+3.3V
	NO	normally open port	P111 via PCB pull-down
	NC	normally closed port	P22 via PCB pull-down
motor driver	PUL+	step pulse high	+5V
	PUL-	step pulse low	P0 PWMA1 via LLC
	DIR+	direction high	+5V
	DIR-	direction low	P32 via LLC
	DC+	motor supply +	24V
	DC-	motor supply -	gnd
	A+	motor phase 1	pin 6
	A-	motor phase 1	pin 4
	B+	motor phase 2	pin 1
	B-	motor phase 2	pin 3
TI board	P16	count steps	P0
	CAN H	CAN high	CAN bus
	CAN L	CAN low	CAN bus
	GND	ground	CAN bus
	P123	backup connection	VCU
	USB	power supply	DCDC USB

Table 4.1: List of used pins for connecting control electronics and sensorics.

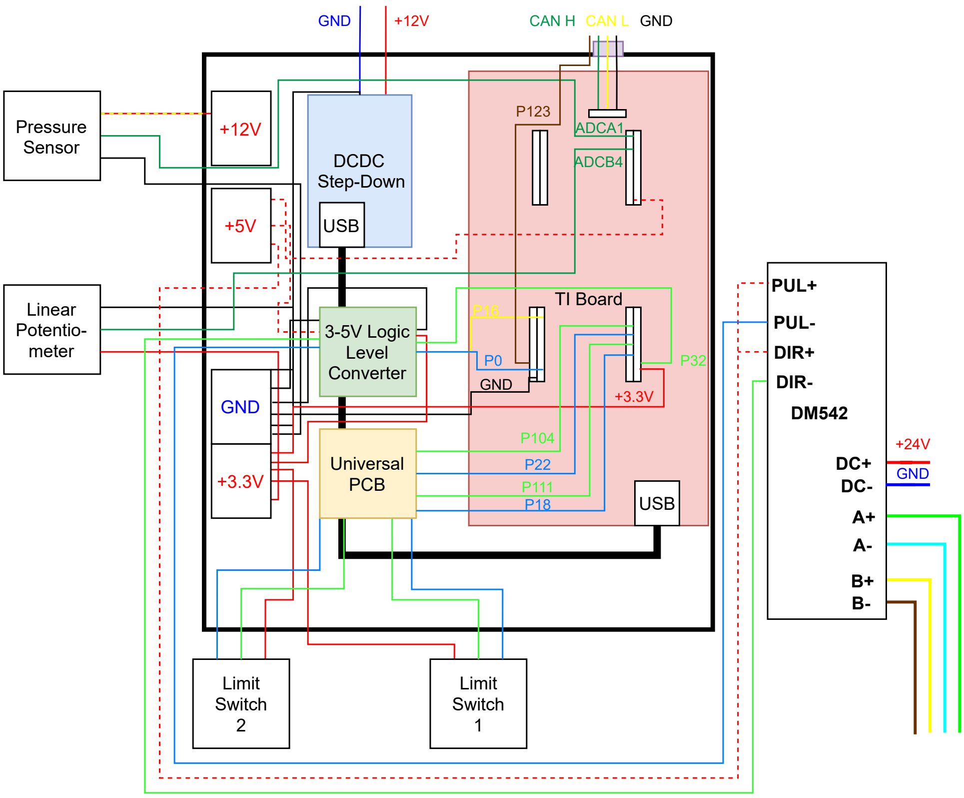

Figure 4.12: The overall electrical scheme of the designed Brake-by-Wire unit.

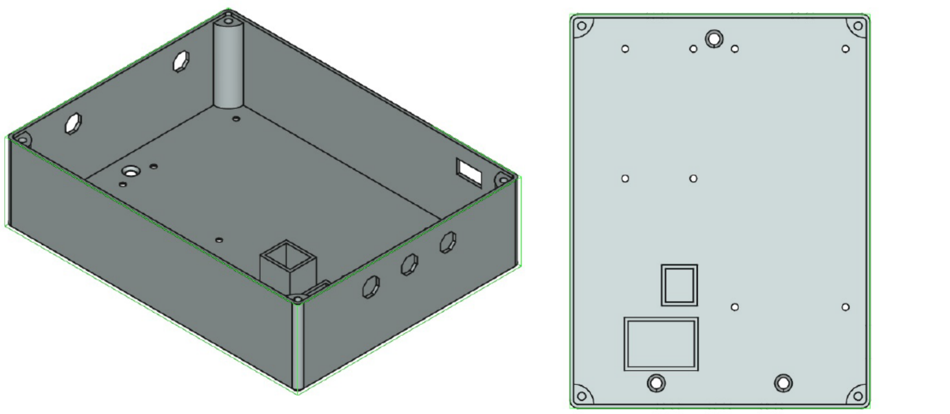

(a) : 3D visualization of the proposed electronic casing box.

(b) : Top view of the designed casing box.

Figure 4.13: 3D visualization of the designed electronic casing box.

4.3.1 Brake-by-Wire Unit Test Setup

To test the baseline functionality of the proposed BBW unit, the unit needs to be connected to the brake caliper so the brake pressure can be built. The Opel

Astra front brake caliper by ATE was purchased for testing purposes, while it has the same piston diameter as the brake caliper used in the prototype vehicle. The BBW unit and the brake caliper are connected by a conventional brake line. Instead of the brake disc and the brake pads, the brake piston compressor by Geko is used. The block scheme of the designed BBW unit with a connected brake caliper can be seen in figure 4.14. The photos of the constructed Brake-by-Wire unit are depicted in figures 4.16 - 4.19.

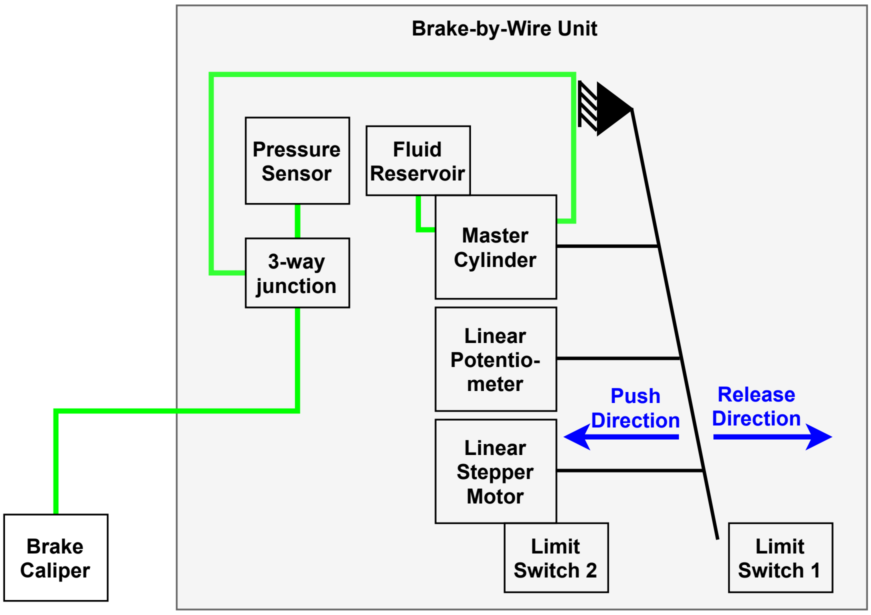

Figure 4.14: Block scheme of the proposed BBW unit.

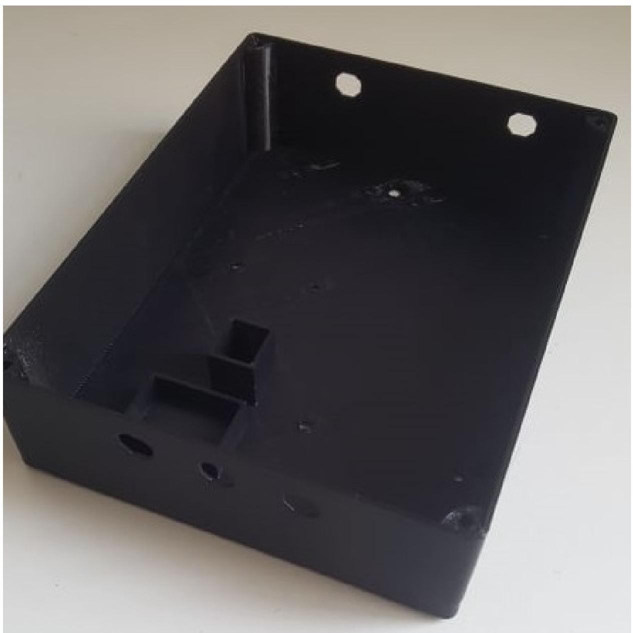

Figure 4.15: 3D printed eletronics casing box.

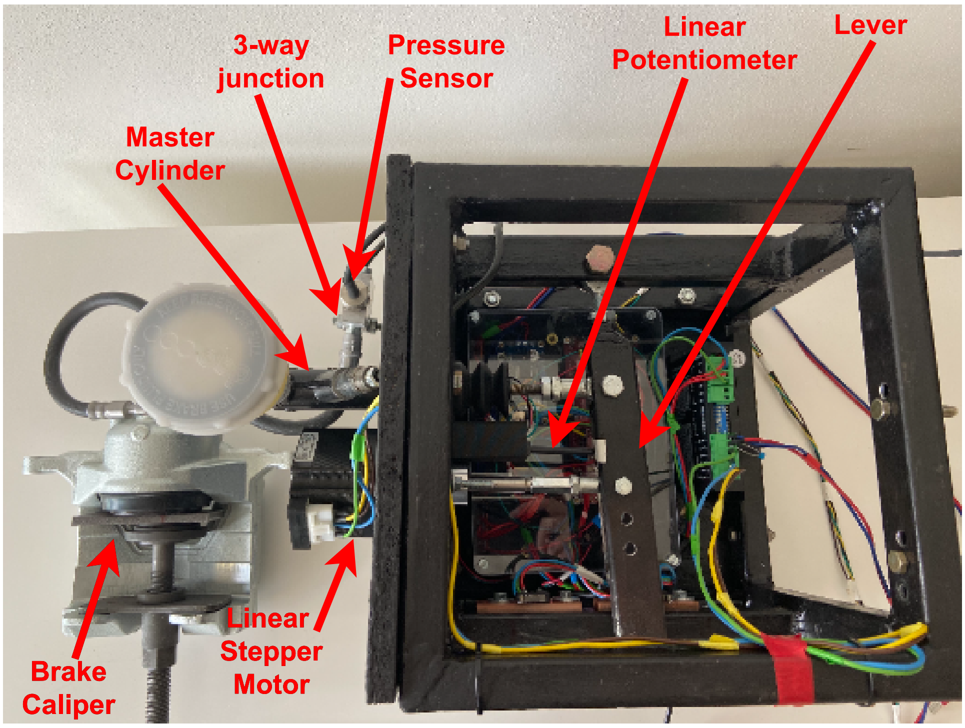

Figure 4.16: Top view of the constructed BBW unit.

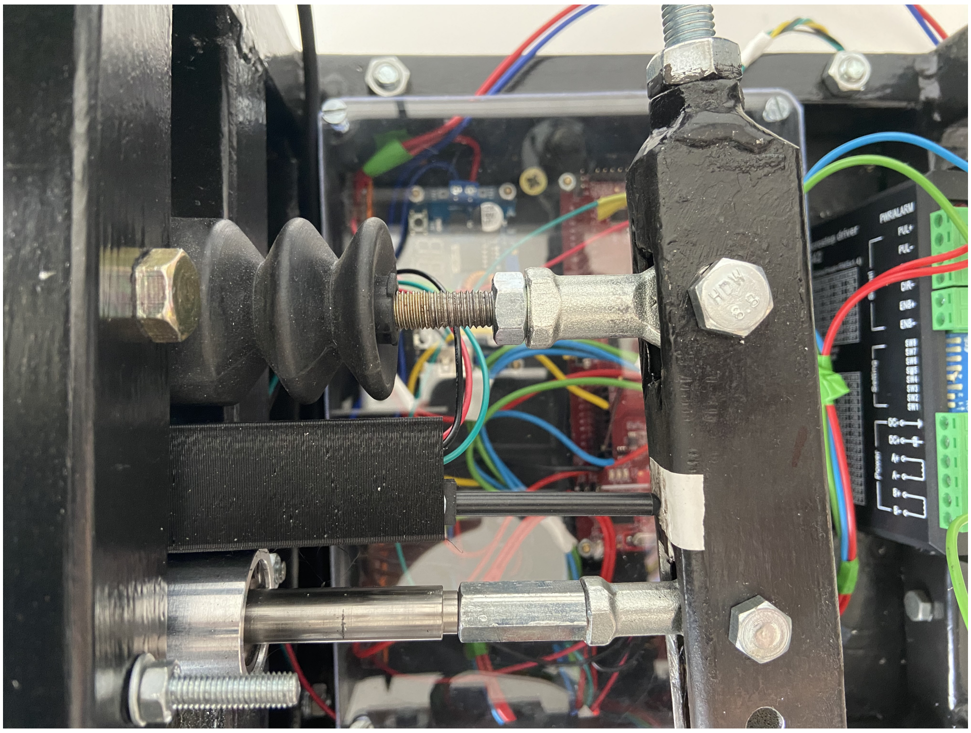

Figure 4.17: Detailed top view of the constructed BBW unit.

Figure 4.18: Side view of the constructed BBW unit.

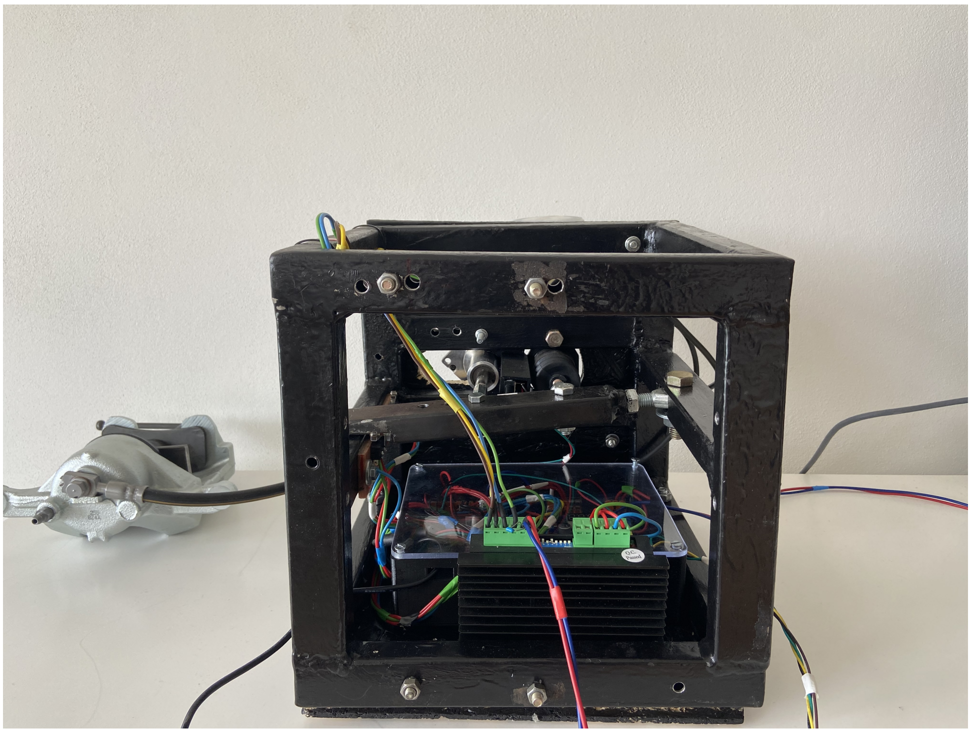

Figure 4.19: Front view of the constructed BBW unit.

Chapter 5

Software Implementation of the Brake-by-Wire Unit

In this chapter, the developed software and designed low-level control laws will be described. Firstly, the TI board setting and used software libraries will be listed. Secondly, the reading and preprocessing of the data obtained from the sensors described in chapter 4 will be discussed. Then, control laws for the motor position and brake pressure control will be developed. Next, the Brake-by-Wire unit's control logic and the elementary functional safety will be designed and described. Finally, the CAN messages for communication with the vehicle control unit and remaining vehicle units will be implemented. The validation and testing of the proposed hardware and software implementation of the Brake-by-Wire unit can be found at the end of this chapter.

5.1 Board Settings

The developed software solutions are implemented in the Matlab and Simulink environment, version 2021b. For interaction with the board periphery, the *Embedded Coder Support Package for Texas Instruments C2000 Processors* toolbox is used. This toolbox allows quite an easy setting of the board and periphery parameters. In addition, the developed software solutions use the standard Simulink libraries such as the *Stateflow*, *Vehicle Network Toolbox* or *Embedded Coder*. As mentioned in the previous chapter, the model-based approach is used for software development. As a numerical solver, the *discrete fixed-step* solver with step size of 0.001 s is used. To prevent looping or freezing the board, a built-in watchdog is used. Finally, the developed Simulink code is translated into C language using the built-in code generation toolbox. For more detailed installation and programming instructions of the TI board and its libraries in the Simulink environment, please refer to git repository [HVVJ].

5.2 Sensor Reading

5.2.1 Pressure Sensor

The selected pressure sensor has an analog output, therefore, it has to be connected to the ADC pin of the TI board. The pressure range of the selected sensor is from 0 Bar to 100 Bar. The electrical range of the sensor is from 0.5 V to 4.5 V and the dependency of the measured pressure on the measured voltage is linear. The pressure corresponding to the voltage can be computed using the equation

$$p_{meas} = \frac{V_{meas} - range_{min}}{range_{max} - range_{min}} \cdot range_{pressure}, \tag{5.1}$$

where the V_{meas} is the voltage value measured by the ADC in volts, the $range_{min}$ is the minimal value of the sensor electrical output, the $range_{max}$ is the maximal value of the sensor electrical output and $range_{pressure}$ is the pressure range of the sensor. Substituting the numerical values obtained from the datasheet into equation 5.1, the following equation emerges

$$p_{meas} = \frac{V_{meas} - 0.5}{4.5 - 0.5} \cdot 100. \tag{5.2}$$

However, the range of the TI board's ADC pin is only 0-3 V; thus, it is not possible to measure values greater than 3 V. Therefore, pressures greater than 62.5 Bar cannot be measured (substitute 3V into the equation 5.2 for V_{meas}). To solve this issue and allow the reading of the whole range of the pressure sensor, a simple voltage divider or an operational amplifier with the gain of $\frac{2}{3}$ can be used. In our case, neither of these options is needed because, due to the mechanical design of the BBW unit, the maximal desired value of the generated brake pressure should never overcome the value of 52 Bar, which is still in the measurable range.

Because the raw values measured by the ADC input pin are quite noisy, the raw signal is filtered using the median filter with the window length of 5 samples to filter out signal peaks. The filtered signal is converted to a voltage value. Because the 12 bit ADC converter is used and the range of the ADC input is 0-3 V, the formula for conversion of raw values to voltage values is the following

$$V_{meas} = \frac{3}{2^{12} - 1} ADC_{filtered}, \tag{5.3}$$

where $ADC_{filtered}$ is the filtered value measured by the ADC. Finally, applied brake torque is computed using the equation

$$T_{brake,meas} = 2\mu_{pad} p_{meas} S_{cp} r_{disc,eff}, \tag{5.4}$$

where μ_{pad} is the friction coefficient between the brake disc and pad, S_{cp} is the area of the caliper piston, and $r_{disc,eff}$ is the effective radius of the brake disc.

Finally, the basic range check, which checks whether the measured values are in a feasible range, is implemented. The block scheme of the described pressure reading and preprocessing is depicted in figure 5.1.

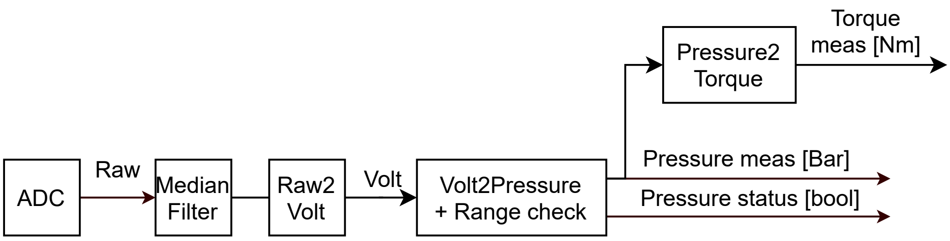

Figure 5.1: Pressure sensor reading and preprocessing scheme.

5.2.2 Limit Switches

The Brake-by-Wire unit is equipped with two limit switches, each of them placed at each of the ends of the lever range, see figure 4.14 in chapter 4. Each switch has two output pins, normally open and normally closed, which are connected to the digital inputs of the TI board. The TI board reads the values of those digital inputs and decides whether the limit switch is pushed or released. Both switches are used for detecting that the linear motor is at one of the ends of its stroke. Moreover, the limit switch number 1, refer to figure 4.14, is used for the homing procedure described in section 5.4. Finally, simple validity checks of the limit switch values are implemented in order to detect the situations such as both limit switches being pressed simultaneously or both NO and NC pins of one switch having either low or high values at the same time.

5.2.3 Linear Potentiometer

The linear potentiometer is used for measuring the position of the lever. The selected sensor is connected to 3.3 V power supply so that the analog output signal can be easily measured by the built-in ADC pin of the TI board. The measured raw signal is filtered using the median filter with a window length of 5 samples at first. Then, the filtered signal is converted to a voltage value using the equation 5.3. Finally, the measured linear position is computed using the formula

$$pos = \frac{V_{meas} - range_{min}}{range_{max} - range_{min}} \cdot range_{potentiometer}, \tag{5.5}$$

where V_{meas} is the voltage value measured by the ADC in volts, the $range_{max}$ is the maximal value of the sensor electrical output, and it is equal to 3 V, the $range_{potentiometer}$ is the measurable range of the used sensor, which is equal to 35.6 mm, and the $range_{min}$ is the minimal value of the sensor electrical output. The value of the $range_{min}$ should correspond to the zero position of the lever. Therefore, to obtain the precise value of the $range_{min}$, the value of the $range_{min}$ is computed during the homing procedure, where the zero position of the lever is ensured. Moreover, every time the limit switch 1 is pushed, meaning the lever is in the zero position, the value of $range_{min}$ is recomputed. Furthermore, a simple validity check of the measured position is implemented to ensure that the measured value is always in a feasible range. Finally, the measured linear position of the lever is converted to the linear position of the motor rod by multiplying it with the scaling factor 1.16. The scaling factor is derived from the mounting distance between the stepper motor and the linear potentiometer. The block scheme of the linear potentiometer data reading and preprocessing is depicted in figure 5.2.

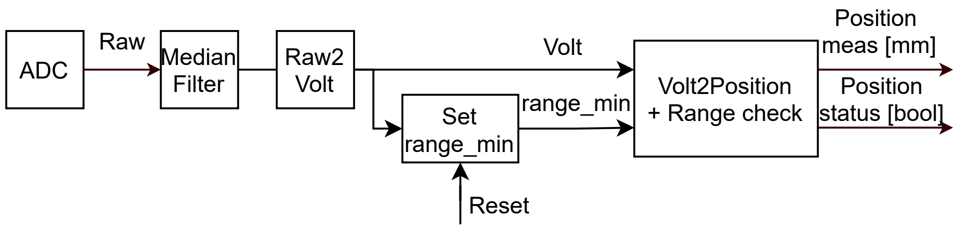

Figure 5.2: Block scheme of the linear potentiometer sensor data reading and preprocessing.

5.3 Designed Control Laws

5.3.1 Stepper Motor Control

The number of generated pulses and the motor direction need to be controlled to control the stepper motor. The direction of the motor can be easily set using the digital output pin. For pulse generation, the ePWM pin can be used. The ePWM block generates the PWM signal with a given frequency and duty cycle. The duty cycle of the PWM signal is either 50 % or 0 % depending on whether the motor should move or not. The frequency of the PWM pulses corresponds to the motor speed; therefore, it needs to be set dynamically. The motor's maximal and minimal linear speed need to be set to the computed PWM frequency range. The maximal linear speed is $v_{max} = 100\,\mathrm{mms^{-1}}$ according to the datasheet and the minimal linear speed is set to $v_{min} = 3\,\mathrm{mms^{-1}}$. Firstly, the time that the motor needs to complete one stroke can be computed using the equation

$$t = \frac{stroke_{tot}}{v}, \tag{5.6}$$

where $stroke_{tot}$ is the total stroke of the linear motor which is equal to 38.1 mm and v is the motor linear speed. Substituting the minimal and the maximal speed into the equation 5.6, the following minimal and maximal times are computed

$$t_{max} = 0.381\,\text{s} \quad (5.7)$$
$$t_{min} = 12.7\,\text{s}, \quad (5.8)$$

where t_{max} corresponds to the v_{max} and t_{min} corresponds to the v_{min}. Then, the number of steps needed for the total stroke can be calculated using the equation

$$steps_{total} = \frac{steps_{rev} \cdot stroke_{tot}}{stroke_{rev}}, \quad (5.9)$$

where $steps_{rev}$ is the number of steps per revolution, which is equal to 200, and $stroke_{rev}$ is the motor stroke per revolution, which is equal to 6 mm. Finally, the minimal and the maximal frequency of the PWM, can be obtained from the equation

$$f = \frac{steps_{total}}{t}. \quad (5.10)$$

Substituting t_{min} and t_{max} values into the equation 5.10, the following values are obtained

$$f_{max} = 3333.33\,\text{Hz} \quad (5.11)$$
$$f_{min} = 100\,\text{Hz}. \quad (5.12)$$

In Simulink, the desired frequency of the PWM signal is specified using a timer period (TP) register, which takes the number of clock cycles as an input. The following formula can be used to convert the computed frequencies to the timer period

$$TP = \frac{1}{2 \cdot prescaler} \frac{f_{clock}}{f}, \quad (5.13)$$

where f is the PWM signal frequency, f_{clock} is the CPU clock frequency, which is equal to 200 MHz, and the $prescaler$ value is equal to 16. The computed timer period corresponding to the maximal and the minimal PWM frequency are the following

$$TP_{max} = 1875 \quad (5.14)$$
$$TP_{min} = 65\,000, \quad (5.15)$$

where TP_{max} corresponds to f_{max} and TP_{min} corresponds to f_{min}. Finally, to avoid step changes of the PWM input signal and thus to avoid sudden changes of motor speed, the rate limiter block is used to limit the maximal acceleration and deceleration of the motor.

Steps Counting

To allow the feedforward control of the stepper motor, the number of steps, thus the number of generated PWM pulses, needs to be known. Because there is no simple way to count the generated pulses in the Simulink, the eCAP pin will be used. The eCAP pin is connected directly to the pin generating the PWM signal for the motor driver and captures the generated pulses. Each time the pulse is captured, the external interrupt is raised, and the step counter is either increased or decreased by one, depending on the direction of the motor movement.

The block scheme of the implemented stepper motor control can be seen in figure 5.3.

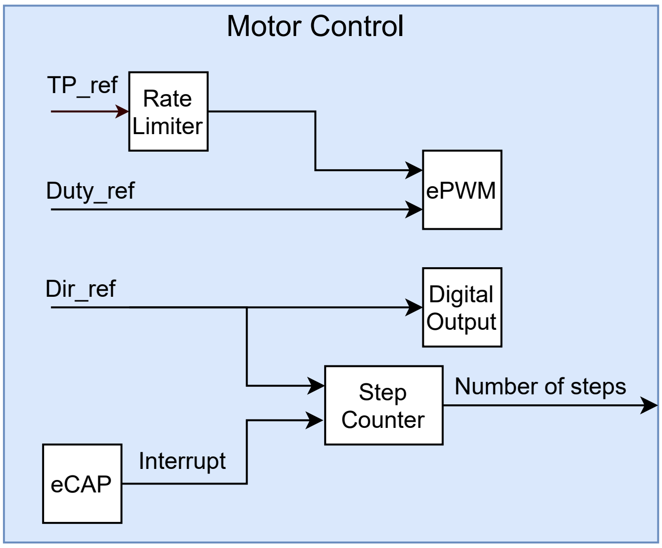

Figure 5.3: Block scheme of the stepper motor control.

5.3.2 Position Control

The stepper motor position control law consists of a simple feedback loop, and its block scheme can be seen in figure 5.4. The position control law was designed mainly for testing purposes and as a backup solution for when the pressure sensor malfunction occurs. For a more detailed description of the proposed functional safety of the BBW unit, please refer to section 5.4.

Firstly, the position reference is converted to the number of steps using the equation

$$steps = \frac{steps_{rev}}{stroke_{rev}}, \tag{5.16}$$

where $steps_{rev}$ is the number of steps per single revolution and $stroke_{rev}$ is the length of the stroke per single revolution. Then the regulation error is computed. The sign of the regulation error is used for setting the motor direction, and the magnitude of the regulation error is used for setting the frequency of the PWM. Because the maximal motor speed is dependent on the motor load, and without the pressure sensor, there is no information about the motor load, the motor speed needs to be set to such a value that is feasible for every motor load possible. Therefore, a constant frequency value of the PWM is set for the push direction of the motor; the definition of the push and release directions can be found in figure 4.14 in chapter 4. On the other hand, when the motor moves in the release direction, no load force is acting against it, and the maximal actuation speed can be increased. Moreover, to prevent the oscillation of the motor around the reference point, the motor is stopped when the absolute value of the regulation error is smaller than the selected threshold. The pseudocode of the algorithm of the *Set PWM* block described above can be seen in algorithm 1.

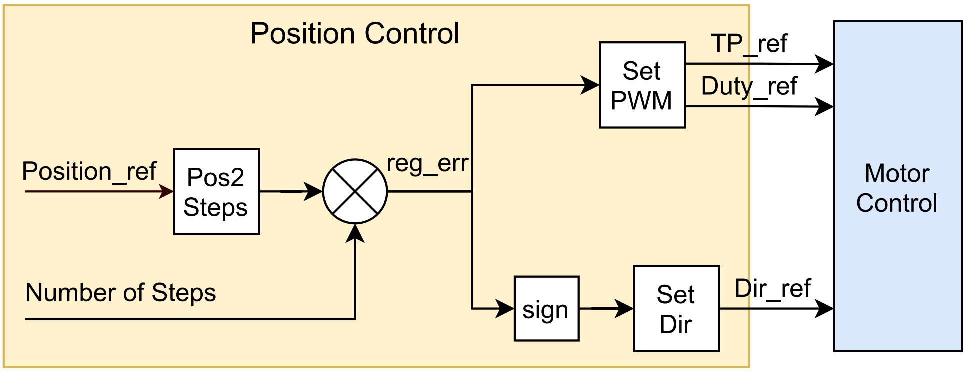

Figure 5.4: Block scheme of the developed position control law.

Algorithm 1 Set PWM value for position control

Require: reg_{err}
  if $|reg_{err}| < 10$ **then** ▷ Stop motor
    $TP_{ref} = 65000;$
    $Duty_{ref} = 0;$
  else
    if $reg_{err} < -50$ **then** ▷ Release direction
      $TP_{ref} = 5000;$
    else ▷ Push direction
      $TP_{ref} = 14000;$
    end if
    $Duty_{ref} = 50;$
  end if

5.3.3 Pressure Control

The pressure control law is the main control law of the designed BBW unit. It controls the generation of the desired brake pressure. The developed control law is depicted in figure 5.5. The designed feedback law takes the measured pressure and pressure reference as inputs. The sign of the computed regulation error is used to set the motor direction, and the magnitude of the regulation error is used for controlling the motor movement. To ensure the fastest actuation speed possible, the PWM frequency is set dynamically according to the measured pressure, corresponding to the momentary motor load. For storing the reference TP_{lt} values, a lookup table is used. The lookup table stores the discretized values of the pressure-TP curve, which was computed using the velocity-force curve obtained from the motor supplier; please refer to figure 3.9. The values of the momentary maximal speed are decreased by 20 % to make the designed controller more robust. Therefore, the computed pressure-TP curve is scaled by a factor 1.2. The computed and scaled pressure-TP curve is displayed in figure 5.6.

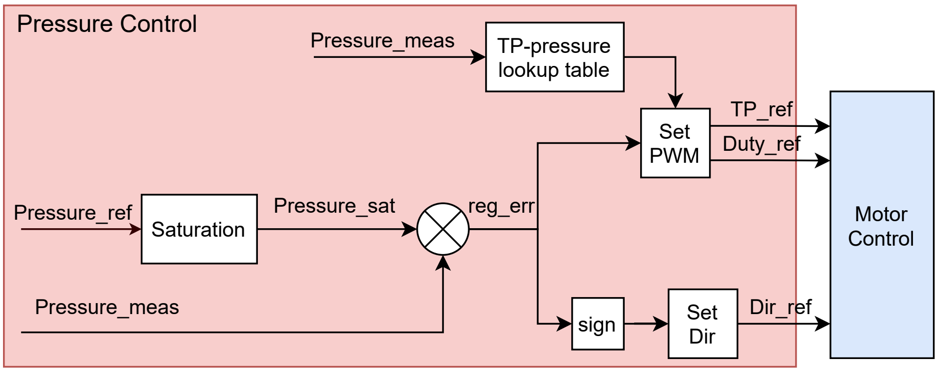

Figure 5.5: Block scheme of the developed pressure control law.

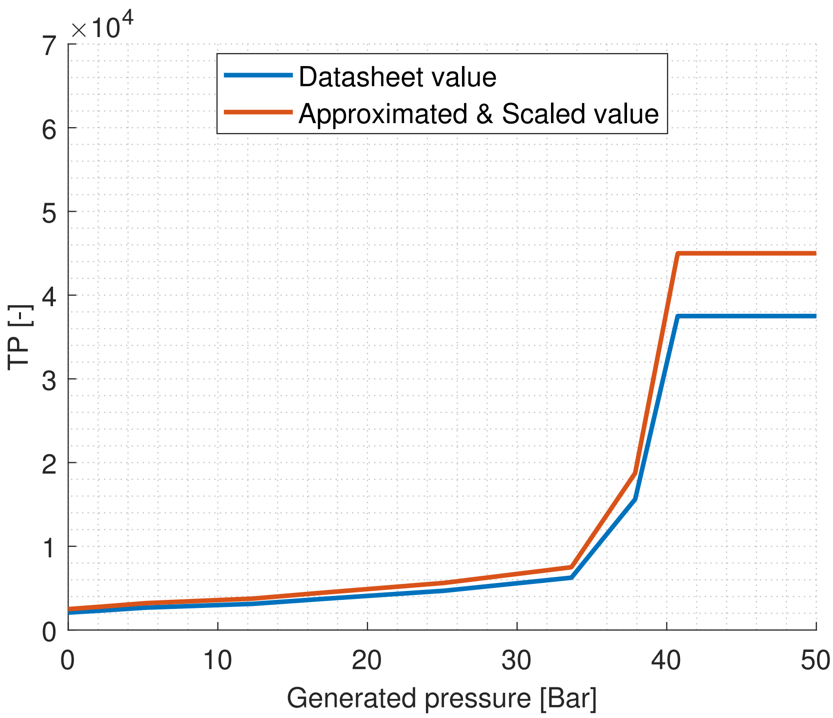

Figure 5.6: Computed pressure-TP curve for dynamical speed control.

The lookup table values TP_{lt} are used for moving in the push direction. The constant value is used to increase the actuation speed for moving in the release direction. Finally, to prevent overshoots and oscillations, the motor is stopped when the amplitude of the regulation error is smaller than the selected threshold.

5.4 Control Logic and Functional Safety

The Brake-by-Wire unit control logic is implemented using the *Stateflow* library. The Brake-by-Wire unit can be in one of the following four operational modes; *Homing*, *Pressure mode*, *Position mode* and *Brake bleeding procedure*, see figure 5.7. Moreover, the *Safe mode*, which stops the motor movement in case of a critical error, is added to the design. The operational mode of the BBW unit can be set either by the VCU via the CAN bus or by the BBW unit itself, according to its current error status.

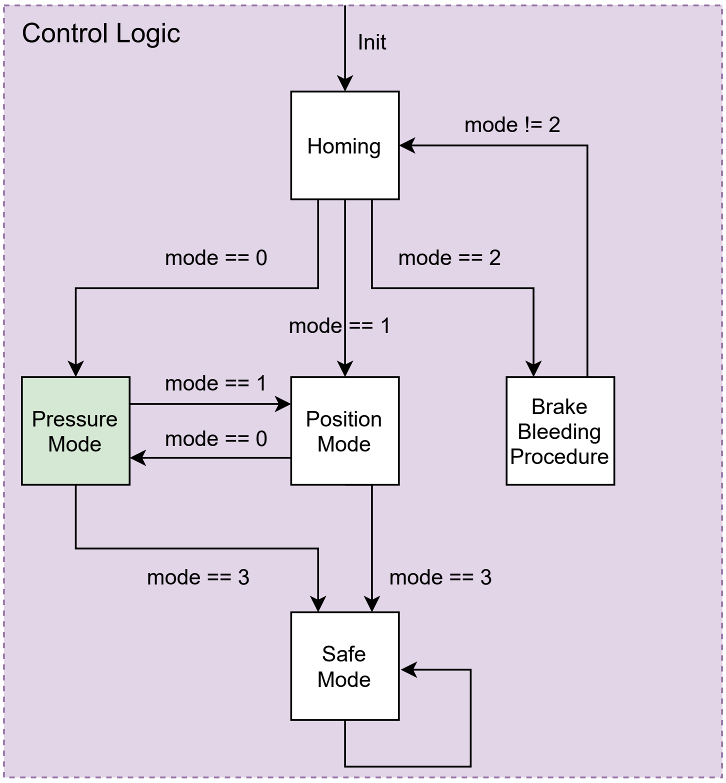

Figure 5.7: The block scheme of the designed control logic.

The homing mode is set as the initial mode. Therefore, whenever the BBW unit is turned on, it is always in the homing mode. The homing mode is responsible for the homing procedure, which is needed to set the stepper motor's and the lever mechanism's zero position. The implemented homing procedure slowly moves the motor in the release direction until the limit switch 1 is depressed. The depression of this limit switch means that the zero position of the lever is reached. Thus the number of measured steps is set to zero, and the $range_{min}$ value of the linear potentiometer is set to the currently measured position. When the homing is done, one of the three remaining operational modes can be selected.

The Brake bleeding procedure is a service mode intended for automatic brake bleeding when installing the Brake-by-Wire unit in the vehicle. This mode can be activated only manually from the vehicle control unit, and it can be entered only from the homing mode after the homing procedure is done. After installation of the BBW unit in the vehicle, this mode should never be entered under normal operational conditions.

The Pressure mode and the Position mode can be activated either by the VCU or the BBW unit itself. Both modes consist of the following three states; *Push only*, *Operation*, *Release only*. Values of the limit switches are used for the transition between these states. In the *Operation state*, both limit switches are released, and the movement of the motor is unrestricted. In the *Push only* state, the limit switch 1 is depressed; therefore, only the motor movement in the push direction is allowed in order to prevent mechanical damage of the whole mechanism or losing steps. Similarly, in *Release only* state, the limit switch 2 is depressed, and only the movement in the release direction is allowed. The same state machine is designed for both modes, *Pressure mode* and *Positional mode*. The only difference is in the used control law, as mentioned above. The scheme of the *Pressure mode* is depicted in figure 5.8.

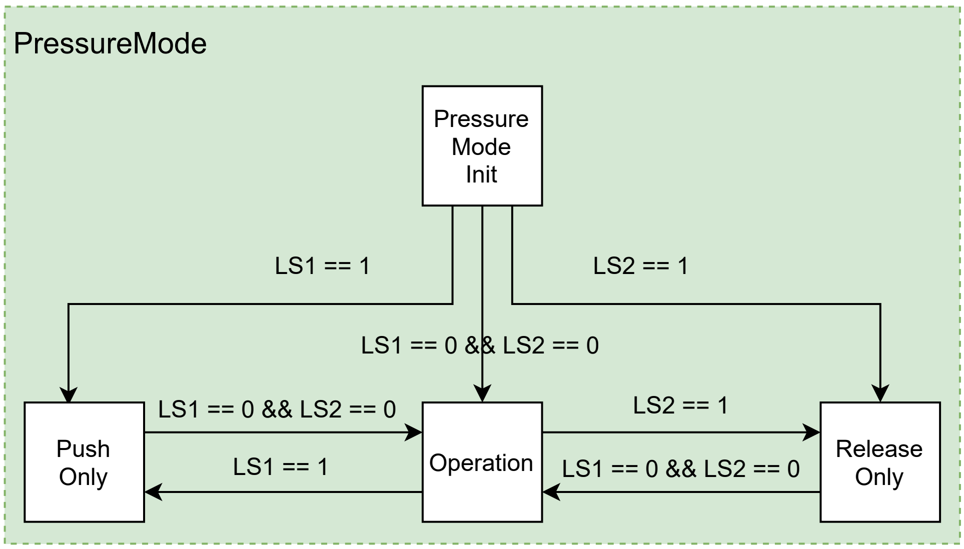

Figure 5.8: Block scheme of the *Pressure mode*.

Finally, the *Safe mode* is used for safely stopping the movement of the stepper motor in case of any critical malfunction. In this mode, the BBW unit is not able to deliver the desired brake torque anymore. Moreover, this mode is terminal; a hard reset of the BBW unit must be done to get the BBW unit back in the operational modes. Furthermore, when the *Safe mode* is reached, the VCU is informed, and it can adjust the control strategy on the vehicle level.

5.4.1 Error Function

The error function needs to be implemented to detect errors and allow automatic change of the BBW unit operational modes. This function takes the validity statuses of the measurements and the measurements themselves as the input. The output of the function is an error code and the control mode. The error code is the numerical value representing the detected error; the list of considered errors and their error codes can be found in table 5.1. The control mode is either the *Pressure mode*, the *Position mode* or *Safety mode*, depending on the severity of the detected error.

error code	control mode	error description
0	pressure control	no error detected
1	position control	pressure sensor error
2	pressure control	potentiometer error
3	pressure control	limit switch 1 error
4	pressure control	limit switch 2 error
5	pressure control	both limit switches pressed simultaneously
6	position control	high stroke and low pressure detected
7	position control	limit switch 2 pressed and low pressure detected
100	safety mode	otherwise

Table 5.1: Considered errors and their error codes.

5.5 CAN Interface

The designed BBW unit is responsible only for generating and monitoring the brake torque, more precisely, the brake pressure. The reference value of the brake torque is computed in the VCU according to the driver's demand, which corresponds to the brake pedal depression rate, and it is sent to the BBW unit via the CAN bus. Due to the fact that the BBW unit is a safety-critical system, the Pedal unit, the VCU, and the BBW unit need to be connected to the same CAN bus. This ensures that the driver can send a brake request to the BBW unit even in case of a malfunction of the VCU. Under normal operational conditions, the BBW unit communicates only with the VCU, and the messages from the Pedal unit are ignored. When the VCU stops responding, the BBW unit starts to receive the messages directly from the Pedal unit, so the ability to slow down or stop the vehicle is preserved. The scheme of the proposed CAN connection of the BBW unit with the Pedal unit and the VCU is depicted in figure 5.9. Finally, to increase the functional safety of the communication connection even more, the Pedal unit's and the BBW unit's digital outputs are connected to the VCU's digital inputs. This connection is used to inform the VCU about potential CAN bus malfunctions detected either by the BBW or the Pedal unit.

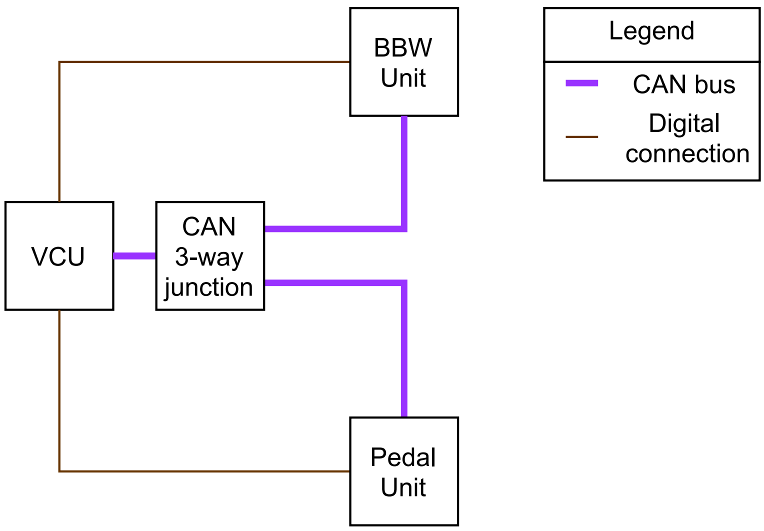

Figure 5.9: Simplified scheme of the BBW unit CAN communication.

5.5.1 Heartbeats

Heartbeat messages are used to detect that all nodes are connected to the CAN bus and work properly. Because no CAN protocol such as CANOpen is used, the custom implementation of the heartbeat messages needs to be done. The implemented heartbeat message is a standard CAN message transferring a single bit, which is set to one. The lowest number possible is used as the message identificator to maximize the message priority.

The Brake-by-Wire unit transmits a heartbeat message and receives heartbeat messages from the VCU and the Pedal unit. Moreover, each time the heartbeat message is received, the status LEDs on the TI board start blinking. Therefore, the functionality of the CAN communication can be easily visually checked. Furthermore, when no heartbeat message from the VCU is received, the high value is set to the digital output pin connecting the BBW unit to the VCU; therefore, the VCU is informed about the malfunction of the CAN bus. The frequency of the heartbeat messages is the same as the frequency of the normal messages, and it is set to 100 Hz.

5.5.2 Messages

All designed CAN messages were created using the *Vector CANdb++ Editor*, which can be freely downloaded from the Vector website. The implemented CAN matrix is attached in the file `CAN_matrix_Brake_by_wire.dbc` in appendix E. A brief description of the implemented messages follows. For a more detailed description of the implemented CAN messages, please refer to table C.1 in appendix C.

Received Messages

The BBW unit receives a single message from the VCU unit under normal operational conditions. This message contains the brake torque reference and the control mode reference. When the VCU is disconnected or stops responding, the BBW unit starts to receive the message from the Pedal unit. This message contains information about the brake pedal position and its validity; more about the Pedal unit can be found in chapter 7, section 7.3. The received brake pedal position is converted into the brake torque reference; more follows in section 5.6. Finally, the heartbeat messages from the VCU and the Pedal unit are received.

Transmitted Messages

The BBW unit transmits two messages dedicated to the VCU. The first message contains information about the generated brake torque, the generated pressure, or the motor position. The second message contains information about the BBW unit mode, error codes, sensor statuses, and more.

5.6 Designed Software Architecture

Now, when all partial system and control laws are implemented, the overall software solution for the Brake-by-Wire unit can be designed. The block scheme of the developed architecture is depicted in figure 5.10.

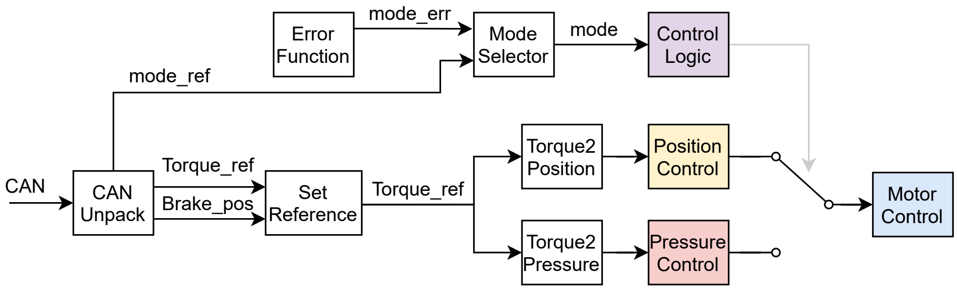

Figure 5.10: Developed control system architecture for the Brake-by-Wire unit.

At first, the BBW unit receives and evaluates the signals from the CAN bus. Under normal operational conditions, the brake torque reference obtained from the VCU is directly propagated to the output of the *Set Reference* block. When the VCU is not responding, the *Set Reference* block calculates the brake torque reference from the brake pedal position obtained from the Pedal unit using the equation

$$T_{ref} = 1200 \cdot Brk_{pos}, \tag{5.17}$$

where Brk_{pos} is the brake position normalized to interval 0-1, and the 1200 is the maximal value of brake torque that can be generated. When both the Pedal unit and the VCU are not responding, the *Set Reference* block generates the constant brake torque of 200 Nm on its output to prevent the vehicle from moving.

Next, the computed brake torque reference is transformed to the brake pressure reference using the equation

$$p_{ref} = \frac{T_{ref}}{2\mu_{pad} S_{cp} r_{eff}} \cdot 10^{-5}, \tag{5.18}$$

where T_{ref} is the brake torque reference, μ_{pad} is the friction coefficient between the brake disc and pads, S_{cp} is the area of the wheel caliper piston and 10^{-5} converts the computed pressure from Pascals to Bars. At the same time, the position reference is computed from the brake torque reference using the equation

$$pos_{ref} = 28 \cdot \frac{T_{ref}}{1200}, \tag{5.19}$$

where 1200 corresponds to the maximal brake torque value that can be generated and 28 corresponds to the maximal allowed stroke of the linear stepper motor.

Then, the control mode needs to be determined. The control mode can be set either by the VCU or by the error function, which has a higher priority. According to the selected control mode, the control logic state machine activates either the pressure control law or the position control law. Finally, the activated control law commands the motor controller, which controls the movement of the stepper motor.

5.7 Validation of Designed Solution

This section will finally examine the performance of the designed hardware and software implementation of the developed Brake-by-Wire unit.

5.7.1 Test 1 - Step Response

In the first test scenario, the step response of the designed Brake-by-Wire unit is examined. The reference signal and measured signal can be seen in figure 5.11. The rise time of the system can be easily measured from this test. The measured rise time is approximately 0.38 s, which is in contradiction with the design requirement for 0.1 s rise time. This behavior is mainly caused by the limited power and speed of the selected actuator, as discussed in chapter 3. To improve the rise time of the system, modifications of the developed Brake-by-Wire unit will be proposed; more about these modifications can be found in the following chapter 6.

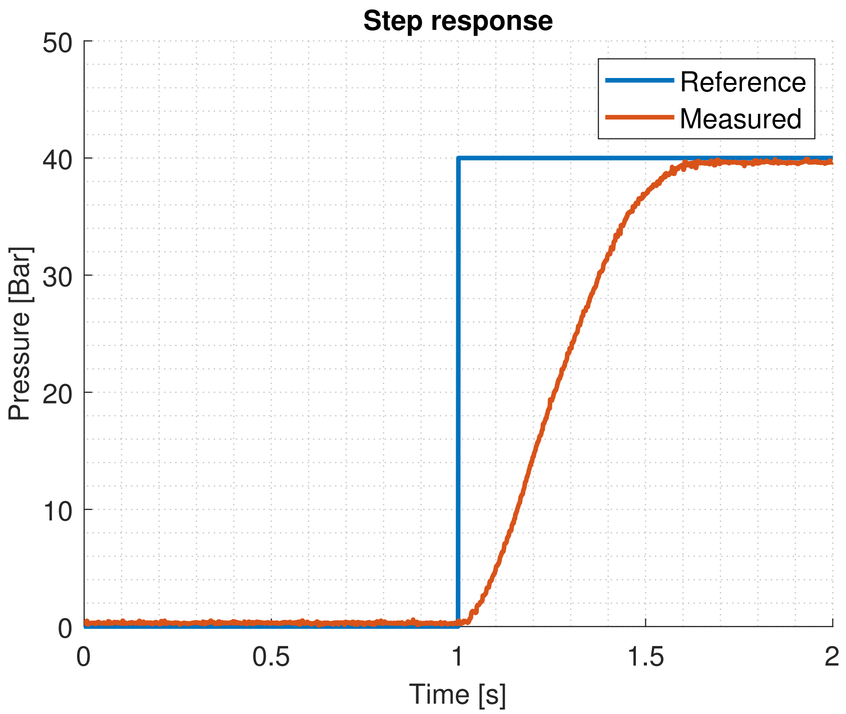

Figure 5.11: System step response.

5.7.2 Test 2 - Pressure Reference Tracking

In the second test scenario, the tracking of the pressure reference is inspected. The reference signal and measured signal are depicted in figure 5.12. As it can be seen, the designed system is able to track the pressure reference up to 40 Bar quite accurately. The maximal value of the generated pressure is limited to 45 Bar, but as it can be seen in figure 5.12, the generation of pressures greater than 40 Bar is slow, inaccurate and unreliable. Therefore, the maximal pressure value needs to be limited to the 40 Bar. This is in contradiction with the design requirement to generate pressures up to approximately 50 Bar, and it leads to the reduction of the maximal vehicle deceleration to approximately $8\,\mathrm{ms}^{-2}$, which is still acceptable. Moreover, this issue is also addressed in the following chapter 6.

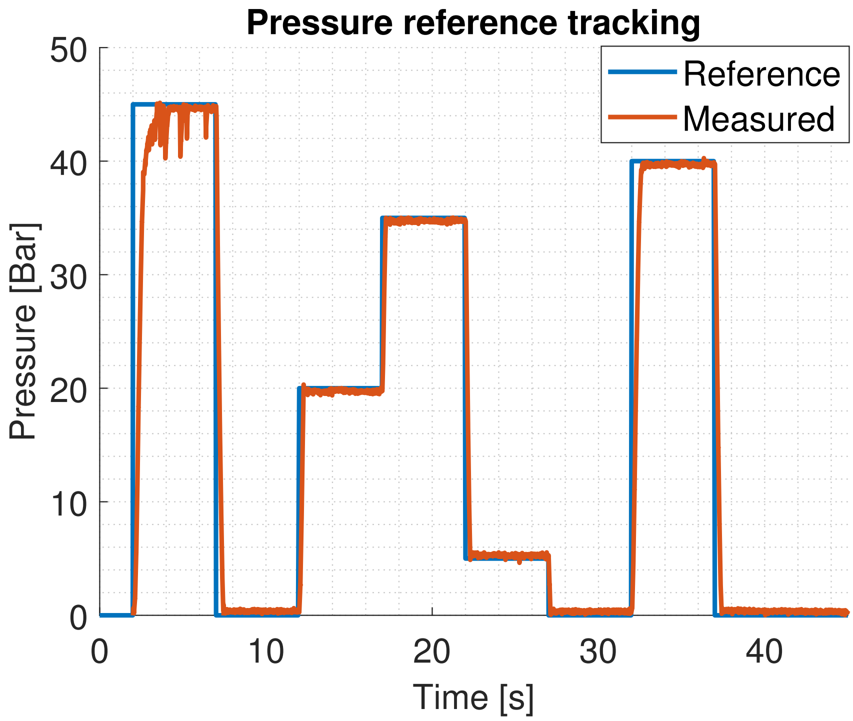

Figure 5.12: Pressure reference tracking.

5.7.3 Test 3 - Position Control

Finally, in the last test scenario, the position control law, which serves as the backup control law in case of the pressure sensor malfunctioning, is tested. For easy comparison with the pressure control law tested in the first and second test scenario, the pressure reference is used as well. The pressure reference is used for computation of the brake torque reference using the equation

$$T_{ref} = 2\mu_{pad} S_{cp} p_{ref} r_{eff} \cdot 10^5. \tag{5.20}$$

Then, the reference position is computed using the equation 5.19.

The computed reference position and the measured motor position are captured in the top subgraph of figure 5.13. The detail of the position tracking is depicted in the middle subgraph of the same figure. As it can be seen, the designed position control law is able to track the reference signal accurately. The rise time of the system is approximately 2 s, which is significantly higher compared to the pressure control mode. This is caused by the fact that the motor load force is unknown; therefore, the motor speed cannot be changed dynamically and needs to be set to a constant value, which is feasible for all load forces. However, the position control mode is intended as the backup mode for when the pressure control mode cannot be used. Therefore, there are no strict requirements on the actuation speed of the position control mode. Finally, in the bottom subgraph of figure 5.13, the comparison of the pressure reference and the generated pressure is displayed. It can be seen that the pressure reference cannot be tracked so precisely as in the pressure control mode. This is caused by the fact that the relation between the motor position and the generated pressure is nonlinear, but the equations used to compute the reference position from the reference pressure are linear. This behavior is expected, and there is no need to address it. The main purpose of the designed position control law is only to slow the vehicle down in case of emergency situations when the pressure control mode cannot be used for some reason. Also, there are no strict requirements on its performance or actuation speed.

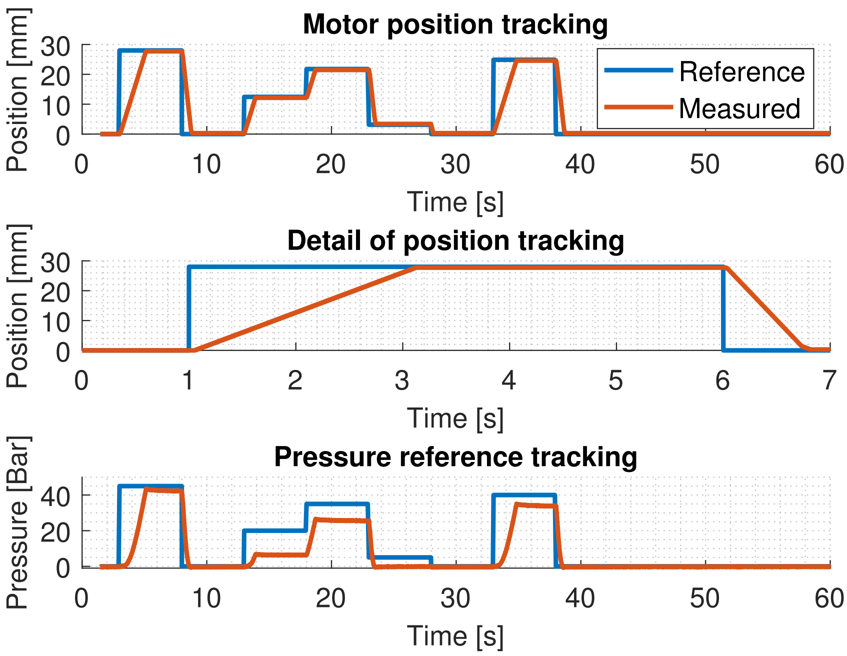

Figure 5.13: Motor position reference tracking.

5.7.4 Validation Summary

As it can be seen from the tests performed above, the designed and developed hardware and software solution is able to generate and hold the desired pressures. The maximal pressure value which can be generated is set to 40 Bar instead of the required 50 Bar. This leads to a decrease of the maximal value of the vehicle deceleration, but the designed solution is still able to generate sufficient brake pressure for slowing down the vehicle. Another issue of the designed solution is the relatively high rise time. The rise time of the developed system is approximately 0.4 s, which is four times greater than required. The slower actuation time will prolong the time and distance needed for slowing down or stopping the vehicle, and that can potentially cause dangerous situations.

Both of these issues were expected and are caused by the selected linear stepper motor. As discussed in chapter 3, the purchased actuator was a compromise between the actuator parameters, its price, and most importantly, its availability and delivery time. A design modification of the developed Brake-by-Wire solution will be done to address these issues. More about it can be found in the following chapter dedicated to the modification of the designed and developed Brake-by-Wire unit.

Chapter 6

Modifications of the Developed Brake-by-Wire Unit

Several changes of the designed and constructed Brake-by-Wire unit need to be made to improve the response time and increase the maximal value of the generated pressure. The modifications should be done in such a way that only a minimal change of the designed Brake-by-Wire construction is needed. Due to the fact that two identical linear stepper motors, described in chapter 3, were already purchased, the addition of the second motor into the design seems to be the easiest and fastest way of performance improvement. Theoretically, the addition of the second motor should double the actuation speed and force of the designed Brake-by-Wire actuator. Therefore, the actuation speed and the maximal magnitude of generated pressure should increase significantly.

This chapter will briefly describe the mechanical and hardware modification of the already developed Brake-by-Wire unit. Then, the necessary software modification will be done. Finally, the validation of the proposed modifications and its comparison to the originally developed solution can be found at the end of this chapter in section 6.4.

6.1 Mechanical Modifications

To allow easy integration of the second stepper motor and the most straightforward control of both motors, the second stepper motor will be mounted on the right side of the Brake-by-Wire cube, opposite the first stepper motor, and it will be connected to the lever at the same place as the first stepper motor, see figure 6.1. This construction ensures that the magnitude of the motor stroke of both motors is the same; only the direction of the motor movement is reversed. The proposed construction design dramatically simplifies the control of both motors because the same PWM signal can be used for controlling both motors. Therefore, the movement of both motors is synchronized, and it is ensured that the motors will never move against each other. More about the modified control laws can be found in section 6.3.

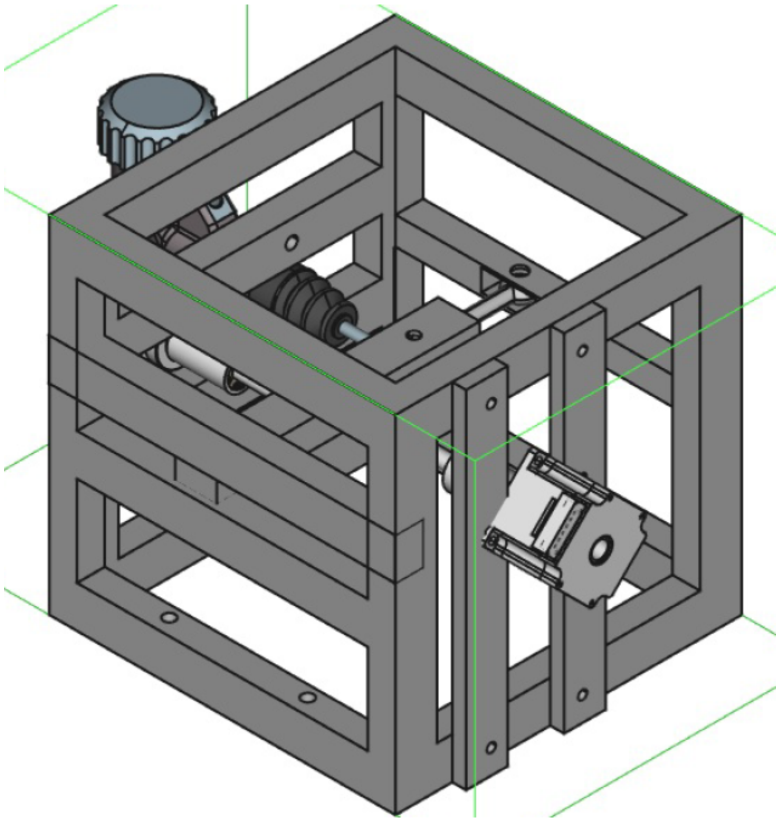

Figure 6.1: 3D model of modified mechanical construction of the Brake-by-Wire unit. The stepper motor model is adopted from [Nana]. The master cylinder model is adopted from [Hod18].

Four additional holes are drilled into the right side of the cube. These holes are used for mounting two iron strips that hold the second motor, see figure 6.1. The motor rod is connected to the lever by a uniball bearing. This uniball bearing is fitted on top of the uniball bearing connecting the first motor and lever. Therefore, the same screw is used for connecting both uniball bearings with the lever. The main advantage of this connection is that the strokes of both motors are the same and that no modification of the lever mechanism needs to be done. However, because the uniball bearings are placed on each other, the non-zero parasite moment around the y-axis of the lever is generated, see figure 6.4. Therefore, the lever mechanism has a tendency to rotate around the y-axis. To prevent this rotation and to fix the lever in the correct position, an additional beam is added to the front side of the cube, see figure 6.1. The top view and side view of the modified mechanical construction is depicted in figures 6.3 and 6.2. The block scheme of the modified Brake-by-Wire unit can be seen in figure 6.5. Finally, the photo of the modified Brake-by-Wire unit can be seen in figures 6.6 and 6.7.

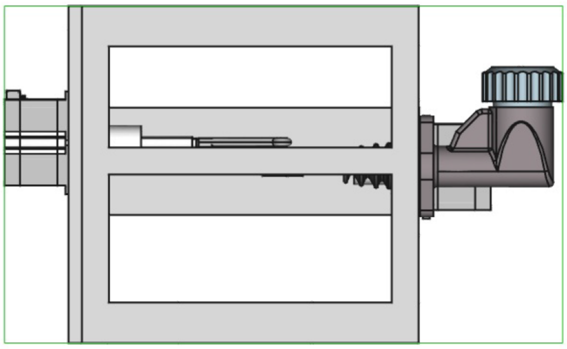

Figure 6.2: Side view of the modified mechanical construction of the Brake-by-Wire unit. The stepper motor model is adopted from [Nana]. The master cylinder model is adopted from [Hod18].

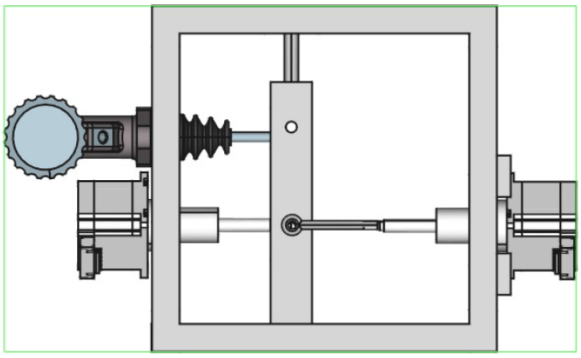

Figure 6.3: Top view of the modified mechanical construction of the Brake-by-Wire unit. The stepper motor model is adopted from [Nana]. The master cylinder model is adopted from [Hod18].

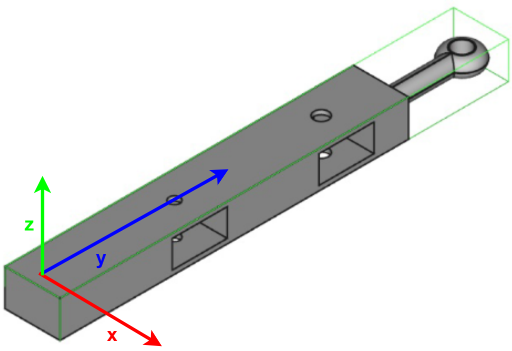

Figure 6.4: Coordinate system of the lever mechanism.

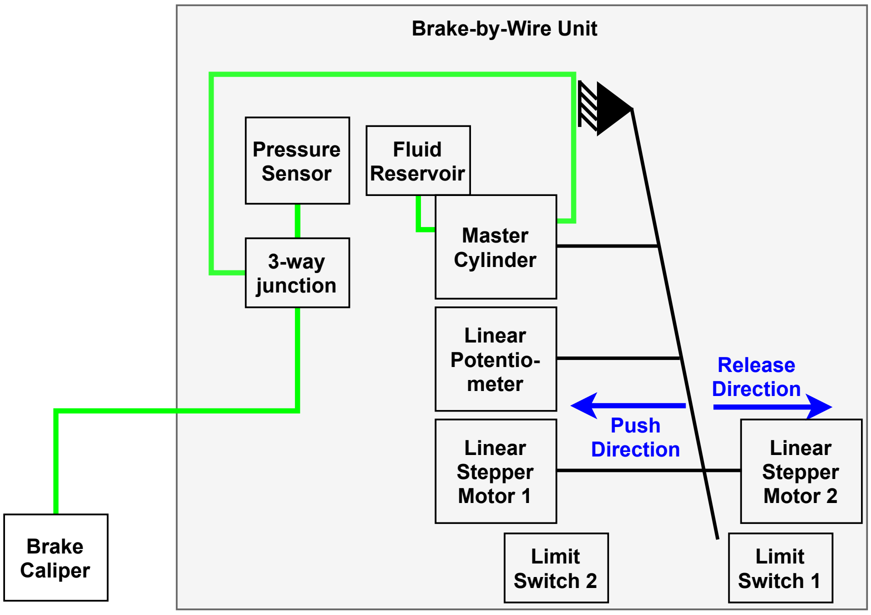

Figure 6.5: Block scheme of the modified Brake-by-Wire unit.

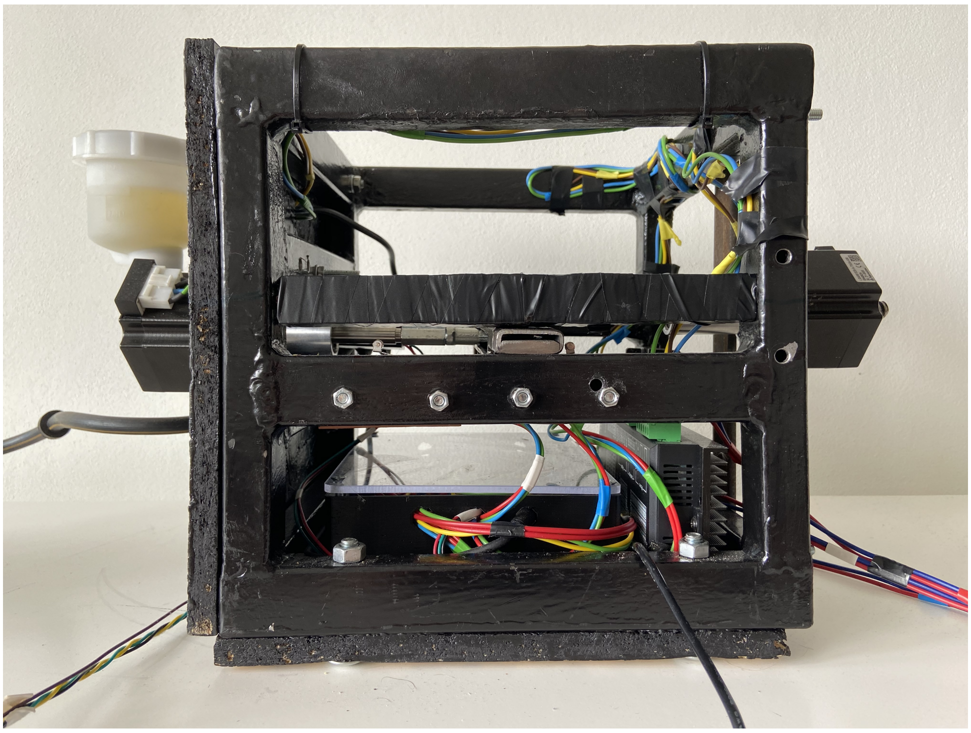

Figure 6.6: Front view of the modified Brake-by-Wire unit.

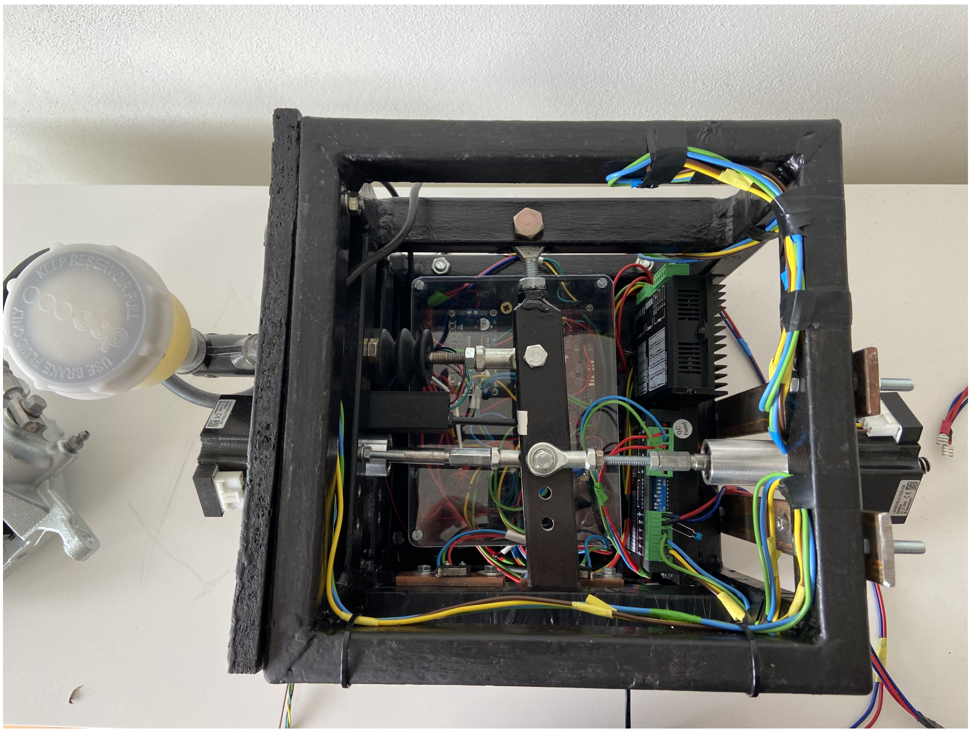

Figure 6.7: Top view of the modified Brake-by-Wire unit

6.2 Hardware Modifications

The hardware modification is relatively straightforward. An additional motor driver needs to be added to the design to control the additional second stepper motor.

device	pin name	function	pin connected to
motor driver 2	PUL+	step pulse high	+5V
	PUL-	step pulse low	P2 PWMA2 via LLC
	DIR+	direction high	+5V
	DIR-	direction low	P4 via LLC
	DC+	motor supply +	24V
	DC-	motor supply -	gnd
	A+	motor phase 1	pin 6
	A-	motor phase 1	pin 4
	B+	motor phase 2	pin 1
	B-	motor phase 2	pin 3

Table 6.1: List of used pins for connecting the second motor driver.

The electrical wiring of the second motor is the same as the wiring of the first one, which is depicted in chapter 4 in figure 4.8. The PUL+ and the

DIR+ pins of the motor driver are connected to 5 V. The PUL- pin of the motor driver is connected to the TI's pin that generates the PWM signal. The DIR- pin of the motor driver is connected to the digital output pin of the TI board. The pinout of the added second motor driver is captured in table 6.1 above, and the modified electrical scheme of the Brake-by-Wire unit is depicted in figure 6.8.

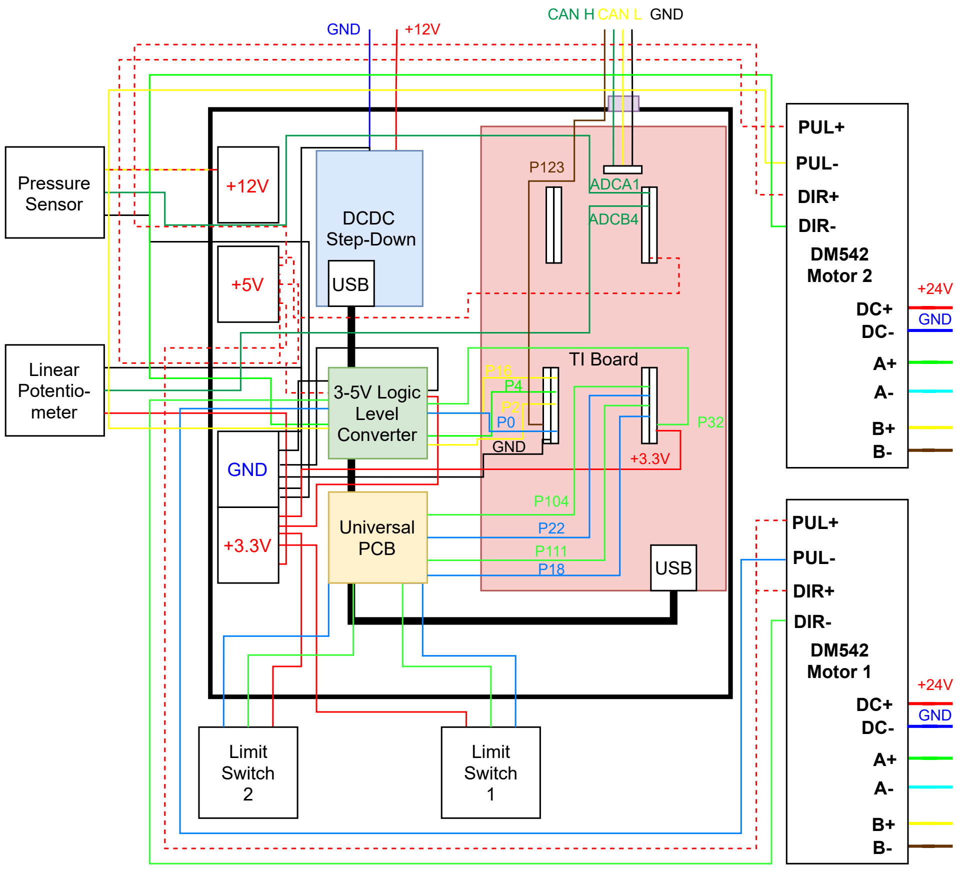

Figure 6.8: The overall electrical scheme of the designed Brake-by-Wire unit.

6.3 Software Modifications

The software modification of the Brake-by-Wire unit is also straightforward because only the modification of the motor control law needs to be done. The modified motor control law has to be able to control both stepper motors synchronously. Therefore, both generated PWM signals need to be the same. This can be easily ensured by using the same TP_{ref} and $Duty_{ref}$ signals as inputs for both ePWM blocks that are responsible for PWM generation. The directions of motor movement have to be always opposite; thus, the negation of the Dir_{ref} signal is used as the direction reference for the second motor. The modified control scheme of the stepper motors is depicted in figure 6.9.

As mentioned at the beginning of this chapter, the addition of the second motor should double the maximal available force and speed. This means that the modified Brake-by-Wire unit should be able to generate pressures up to 80 Bar. However, as discussed in chapter 5, the maximal pressure value which can be measured is limited up to 62.5 Bar due to the limited input range of the used ADC pin. Still, the maximal required pressure to safely stop the vehicle is approximately 50 Bar. Therefore, the maximal pressure value can be safely limited up to 60 Bar. Moreover, if the need for generating greater pressures emerges sometime in the future, an operational amplifier or voltage divider can be used to address this issue.

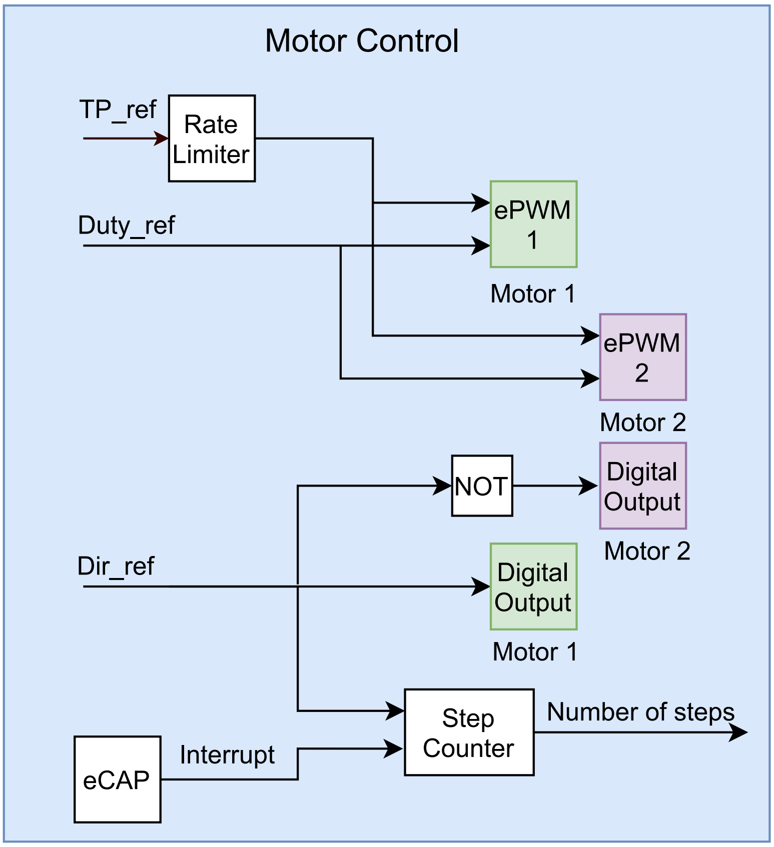

Figure 6.9: Block scheme of the modified stepper motor control.

Then, the pressure-TP curve needs to be recomputed to increase the actuation speed of the Brake-by-Wire unit, and the reference values TP_{lt} stored in the lookup table need to be updated. The updated pressure-TP value is depicted in figure 6.10.

Finally, the equation 5.17 needs to be modified to allow the generation of brake pressures up to 60 Bar. The updated and modified equation 5.17 is the following

$$T_{ref} = 1630 \cdot Brk_{pos}, \tag{6.1}$$

where 1630 is the maximal value of the brake torque that can be generated by the modified system.

Lastly, the equation 5.19 is updated to the following form

$$pos_{ref} = 28 \cdot \frac{T_{ref}}{1630}. \tag{6.2}$$

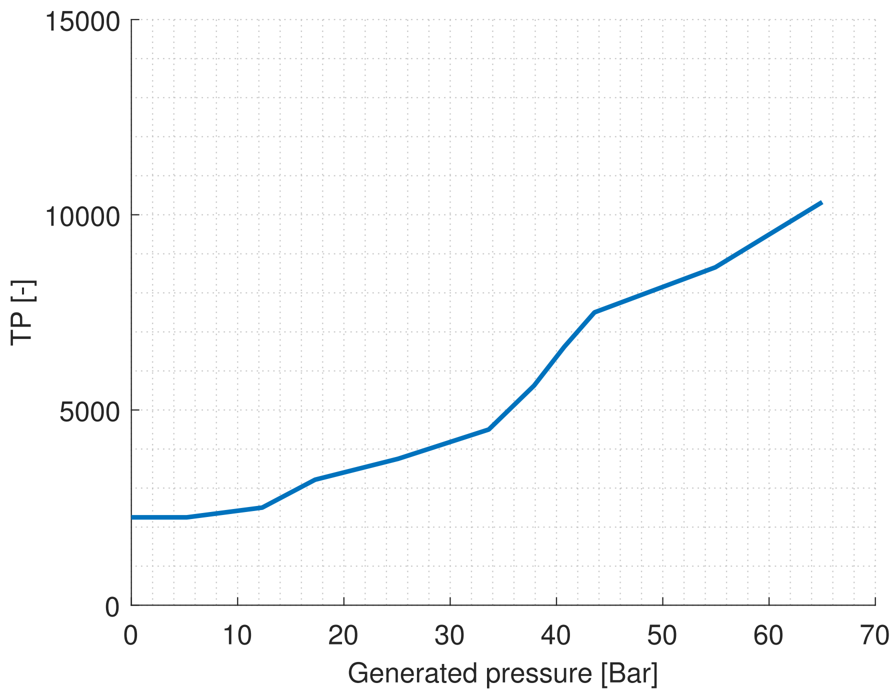

Figure 6.10: Computed pressure-TP curve for the dynamical setting of the motor speed.

6.4 Validation of the Modified Solution

In this section, validation of the modified Brake-by-Wire system will be done. The same test scenarios will be used to allow easy comparison with the original system.

6.4.1 Test 1 - Step Response

Step responses of the original and modified systems are depicted in figure 6.11. As it can be seen, the settling time and the rise time of the modified system are significantly shorter. The measured rise time of the modified system is approximately 0.22 s, which is nearly two times better than the rise time of the original system.

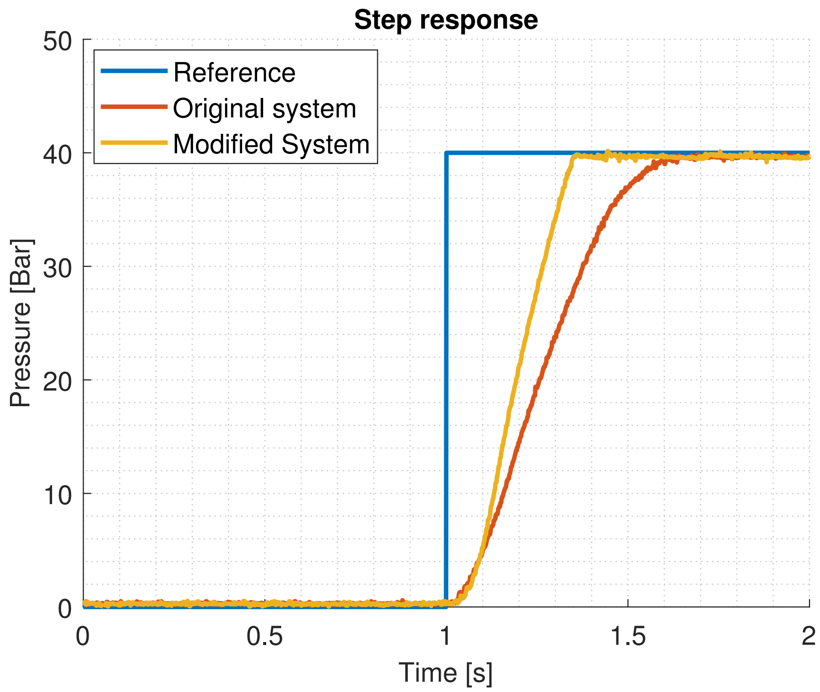

Figure 6.11: Comparison of step responses of the original and modified system.

6.4.2 Test 2 - Pressure Reference Tracking

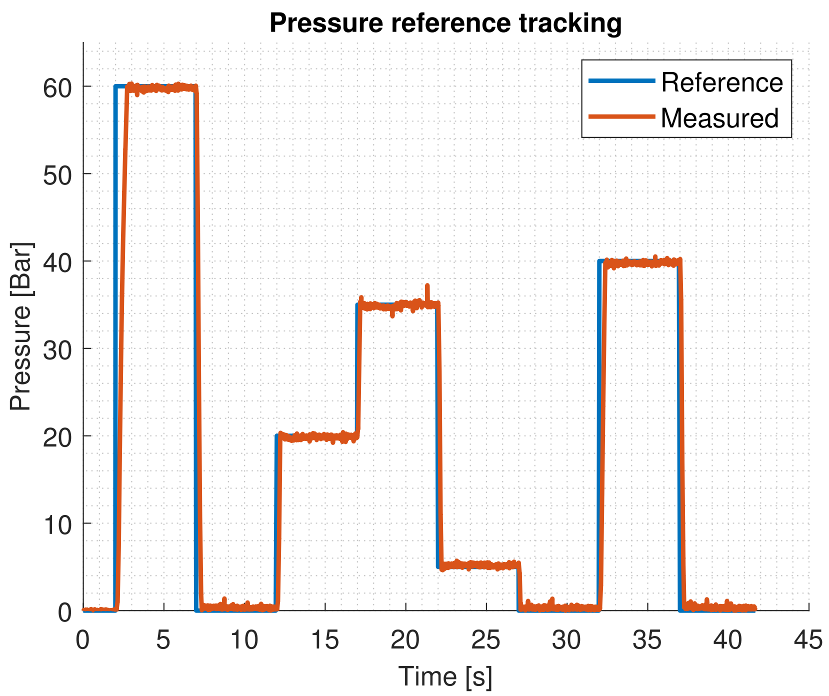

Figure 6.12: Pressure reference tracking.

The reference signal and the measured signal are depicted in figure 6.12. As it can be seen, the modified system is able to accurately and precisely track the pressure reference up to 60 Bar. The maximal value of the generated pressure is limited by the pressure sensor reading, as discussed in the previous section. Still, the modified system fulfills the design requirement to generate pressure up to 50 Bar.

6.4.3 Test 3 - Brake Pedal Reference Tracking

In the third test scenario, the tracking of the pressure reference generated by the depression of the brake pedal is examined. The brake pedal position is read by the Pedal unit, more about the design and implementation of the Pedal unit can be found in the following chapter 7. Then, the measured pedal position is transmitted to the Brake-by-Wire unit via CAN bus. The Brake-by-Wire unit recomputes the brake pedal position to the reference torque using the equation 6.1. Then, the computed brake torque is transformed to the brake pressure using the equation 5.18. The generated reference pressure and the measured generated pressure can be seen in figure 6.13.

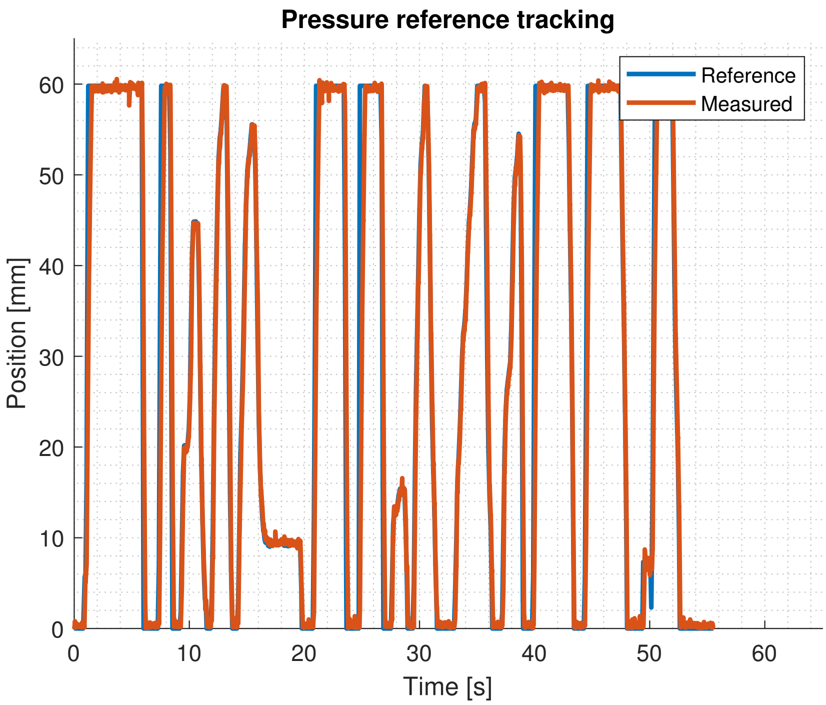

Figure 6.13: Tracking of the pressure reference generated by the Pedal unit.

As shown in the figure above, the designed Brake-by-Wire system can track the reference signal generated by the Pedal unit fast and precisely. This test scenario shows that the designed Brake-by-Wire unit can accurately track the reference signal commanded by the driver. Therefore, the developed solution should be applicable in the real vehicle.

6.4.4 Validation Summary

As it can be seen from the performed tests, the modified Brake-by-Wire unit improves the performance of the originally designed unit. The maximal value of the generated pressure is increased from 40 Bar to 60 Bar. Therefore, the design requirement on the pressure magnitude from chapter 3 is fulfilled. The rise time of the modified system is decreased from the original 0.38 s to 0.22 s, which is a significant increase in the actuation speed. Finally, the third tested scenario shows that the developed Brake-by-Wire solution can interact with the developed Pedal unit described in the following chapter. It can also control the pressure generation fast and precisely according to the brake pedal position, which is controlled by the driver.

Chapter 7

Braking System Strategies on Vehicle Level

In this chapter, the development and validation of the vehicle stability control systems will be described. Unfortunately, the prototype vehicle is still not constructed at this moment. Therefore, testing of the developed Brake-by-Wire unit and proposed stability control algorithms in the real prototype vehicle is not possible. Because of that, the Virtual vehicle unit is developed. The implemented Virtual vehicle unit is used for hardware-in-the-loop (HIL) testing of the constructed Brake-by-Wire unit and the developed stability control algorithms. The implemented Virtual vehicle unit is briefly described in section 7.1. The proposed vehicle stability control laws are briefly introduced in section 7.2. The developed driver interface is described in section 7.3. Finally, the hardware-in-the-loop test setup is described in section 7.4 and the test results are discussed.

7.1 Virtual Vehicle Unit

The hardware-in-the-loop simulation is a commonly used tool for testing developed solutions and algorithms in the automotive industry. The hardware-in-the-loop is a real-time simulation that connects the real systems with the simulation models. The HIL simulation of the designed solutions is more time- and cost-effective compared to testing on the real vehicle, and it is easily reproducible. Moreover, a simulation of scenarios that can be dangerous or damaging to the real vehicle can be easily performed. In our case, the HIL simulation provides the virtual vehicle for validation of the developed brake system solution. The HIL system used in this thesis includes the designed Brake-by-Wire unit in the loop, while the vehicle dynamics and vehicle stability control laws are implemented and simulated in the proposed Virtual vehicle unit.

The Virtual vehicle unit has three main functions. Firstly, it simulates the longitudinal and lateral dynamics of the vehicle and creates the simulation driving data for proposed high-level stability control algorithms. Secondly, it is used to implement and deploy the developed high-level control algorithms. Thirdly, it emulates the functionality and communication interface of the vehicle control unit (VCU) so that the functionality of the VCU and the Virtual vehicle unit is the same from the Brake-by-Wire unit's point of view. A brief description of the hardware and software implementation of the Virtual vehicle unit follows.

7.1.1 Hardware Implementation of the Virtual Vehicle Unit

First of all, the hardware platform for deploying the implemented virtual vehicle model needs to be determined. The TI board is selected as the hardware platform for the Virtual vehicle unit because it offers sufficient computational power, and it can be easily connected to the Brake-by-Wire unit using the built-in CAN interface. Moreover, the TI board offers a real-time simulation of the implemented models, a necessary feature for the HIL testing. Finally, the TI board is programmable in the Simulink environment; therefore, deploying the existing vehicle model and stability control laws implemented in Simulink is quite straightforward. The photo of the proposed Virtual vehicle unit can be seen in figure 7.1. A 3D printed casing box is designed to protect the TI board from dirt and dust and make the designed Virtual vehicle unit more compact, see figure 7.1.

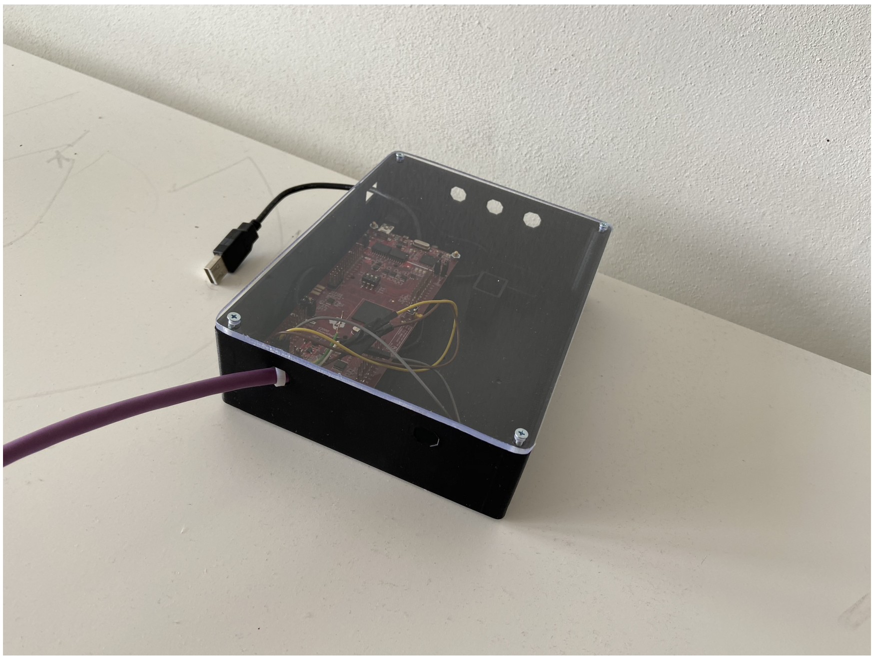

Figure 7.1: Photo of developed Virtual vehicle unit.

7.1.2 Software Implementation of the Virtual Vehicle Unit

The software implementation of the Virtual vehicle unit can be divided into the following three main parts; twin-track vehicle model, high-level control algorithms, and communication interface, see figure 7.2. The description of the implementation of the proposed high-level control law is omitted in this section, while it is discussed in great detail in the following section 7.2. The twin-track model from [Cib19] is adopted as the vehicle model. This is the same model which has been used for developing the stability control algorithms in my bachelor's thesis; for a more detailed description of the original model, please refer to [Cib19] and [Ves20]. The original twin-track model has 16 states and 16 inputs. The block scheme of the adopted twin-track model is depicted in figure 7.3. For the purposes of the Virtual vehicle unit, the original model has to be slightly modified. Because only discrete-time simulations can be deployed on the TI board, the time domain of the adopted vehicle model needs to be changed from continuous to discrete. This means that all blocks such as continuous integrators, transfer functions, and filters need to be replaced by their discrete-time alternatives. Moreover, the used model solver needs to be changed from the *Euler* to the *discrete fixed-step* solver with a step size of 0.001 s.

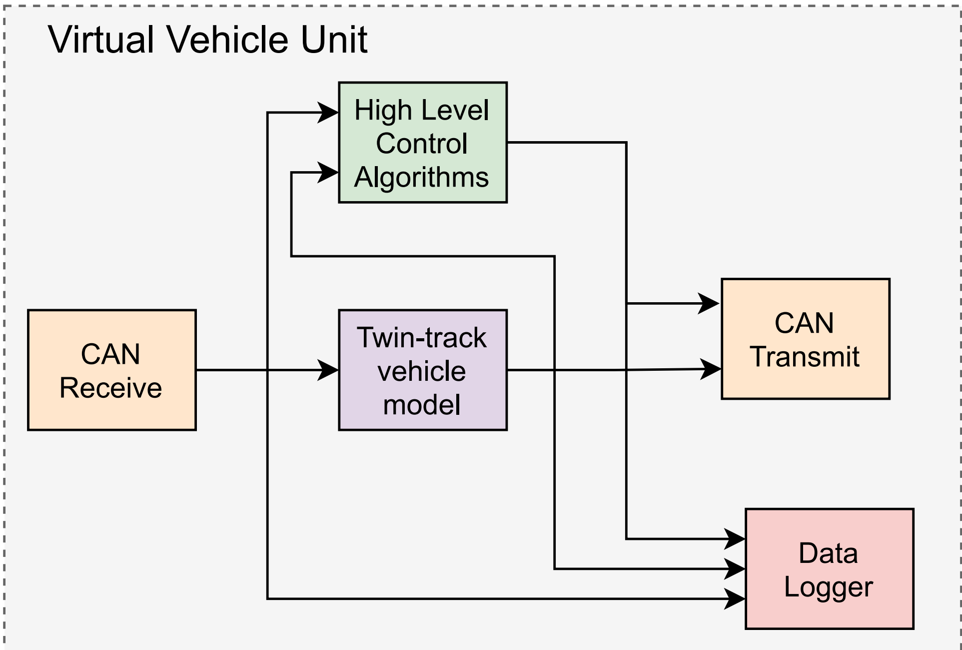

Figure 7.2: Block scheme of the proposed Virtual vehicle unit.

The CAN communication interface is used to easily connect the Virtual vehicle unit with the Brake-by-Wire and Pedal unit. The Virtual vehicle unit can receive and transmit the CAN messages from both the Pedal and the Brake-by-Wire unit. Therefore, it provides the same functionality as the VCU from the Pedal and Brake-by-Wire unit's point of view. Because of that, there is no difference between the VCU and the Virtual vehicle unit from the point of view of the CAN communication interface. Therefore, these two terms are interchangeable in this case. The description of the implemented CAN interface can be found in chapter 5, where the CAN messages dedicated to communication between the Brake-by-Wire unit and the VCU are described. The CAN messages dedicated to communication between the Virtual vehicle unit, and the Pedal unit are briefly described in the following section 7.3.

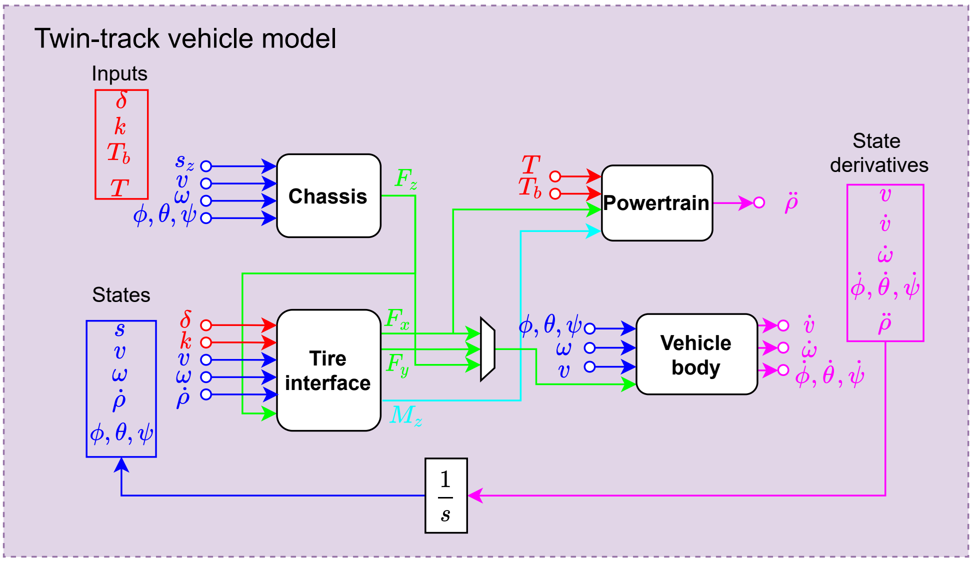

Figure 7.3: Scheme of the vehicle twin-track model used in the Virtual vehicle unit. Adopted from [Ves20].

7.2 Vehicle Stability Control Law

As shown and described in the previous chapters, the constructed Brake-by-Wire unit is able to generate and track the arbitrary reference brake torque value commanded by the VCU. Still, the designed Brake-by-Wire unit itself cannot maintain the lateral and longitudinal stability of the vehicle or prevent the wheels from locking. Therefore, to ensure the vehicle's longitudinal and lateral stability, the high-level stability control law needs to be implemented in the VCU. The stability control law generates the reference brake torque for each wheel in order to ensure the maximal stability and maneuverability of the vehicle under various road and driving conditions. The proposed high-level stability control system is adopted from my former work [Ves20]. For a more detailed description, derivation, and simulation validation of the designed stability control law, please refer to [Ves20]. A brief description of the adopted control system follows.

7.2.1 Inner Control Law

The proposed control system consists of an inner and outer control loop. The inner control loop implements the feedback control of the angular wheel speeds. The wheel speed control law takes the reference and measured angular wheel speed of each wheel as an input. Then, in the ω *Controller* block, the reference brake torque on each wheel is computed using the PI controller. Finally, the computed reference brake torque is divided between the traction motors and friction-based hydraulic brakes. The anti-windup filter is implemented to solve the windup phenomenon introduced by the integral term of the PI controller. Therefore, the input for the total brake torque applied on the wheel, denoted as T_{meas_i}, is added to the inner control loop. The block scheme of the inner control loop is depicted in figure 7.4.

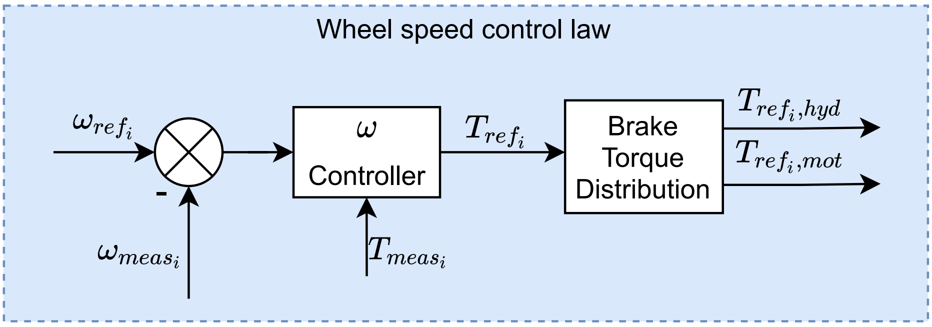

Figure 7.4: Inner control law of developed stability control system.

7.2.2 Outer Control Law

The outer control loop implements the feedback controller controlling the longitudinal acceleration of the vehicle body. The body acceleration control law takes the reference and measured longitudinal vehicle acceleration, and reference and measured yaw rate derivation as an input. Then, using the *Body2Wheel* transformation block, the longitudinal acceleration is transformed from the body coordinate system to the wheel coordinate system. Next, the regulation error is computed, and the *Ax Controller* block computes the reference slip ratios for each wheel denoted as λ_{ref_i}. The reference angular wheel speed of each wheel is computed in the $\lambda 2\omega$ block using the equation

$$\omega_{ref_i} = \frac{v_{x_i}(1 + \lambda_{ref_i})}{r_i}, \tag{7.1}$$

where v_{x_i} is the longitudinal speed of the i^{th} wheel center in the i^{th} wheel coordinate system, and the r_i is the effective radius of the i^{th} wheel. Finally, the computed reference angular wheel speed is used as the input for the inner control loop described above. The scheme of the implemented outer control loop can be seen in figure 7.5.

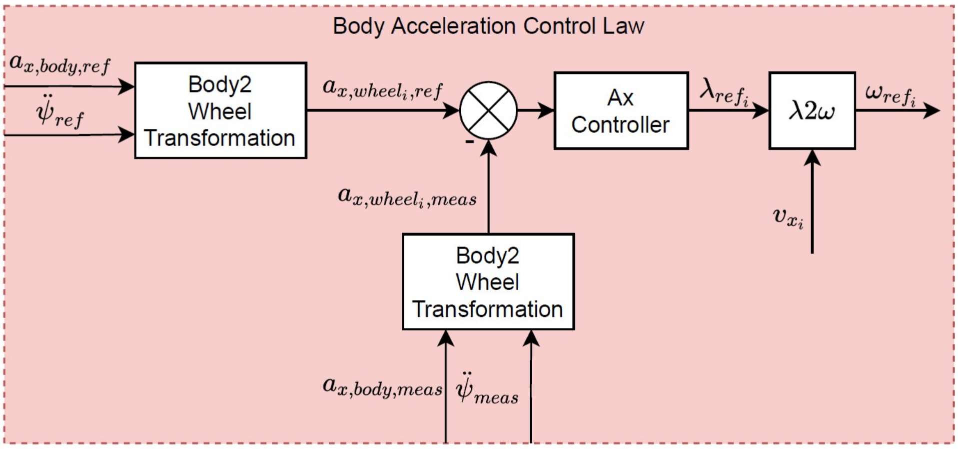

Figure 7.5: Outer control law of developed stability control system.

7.2.3 Stability Control Law

The original stability control law and the simulation test setup developed and implemented in my bachelor's thesis are depicted in figure 7.6. For more information about the proposed control law, please refer to [Ves20]. The modification of the original control law and test setup for purposes of the HIL simulation can be found in the following section 7.4.

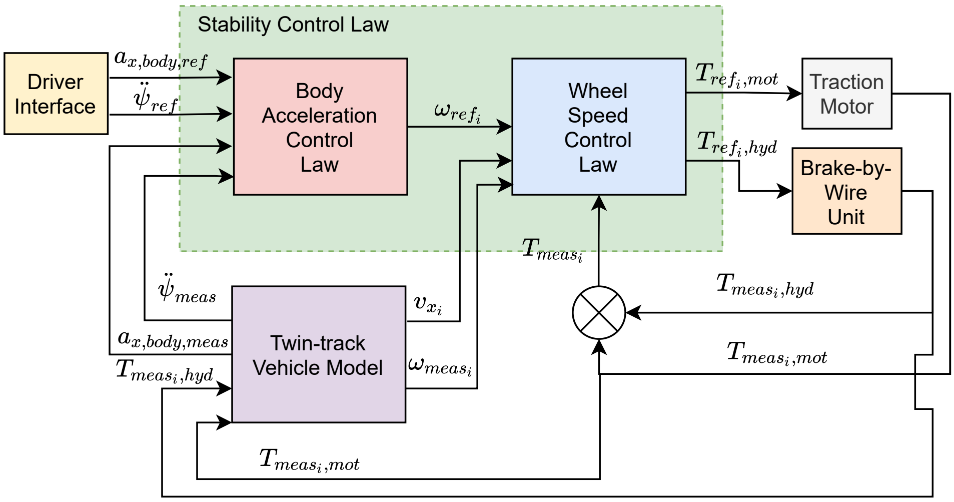

Figure 7.6: The original stability control law and test setup.

7.3 Pedal Unit

The Pedal unit is the part of the driver's interface that allows an easy, natural, and intuitive control of the developed brake system. The name Pedal unit is slightly misleading because the developed Pedal unit contains the brake pedal only, while the throttle pedal is not necessary for controlling and testing the developed brake solution. Nevertheless, the Pedal unit was developed in such a way that both hardware and software changes needed for the addition of the throttle pedal are straightforward and minimal. Firstly, the selected hardware and the hardware implementation of the proposed Pedal unit will be briefly described. Then, the software and the communication interface of the Pedal unit will be implemented.

7.3.1 Hardware Implementation of the Pedal Unit

The proposed Pedal unit consists of two main parts; the control electronics box and the brake pedal itself. The brake pedal is connected to the control electronics box using a 6-wire connector. For testing purposes, both the brake pedal and the control electronics box are mounted on a chipboard construction; thus, the brake pedal can be conveniently operated by foot, see figures 7.10 and 7.11.

Brake Pedal

The throttle pedal from Opel Agila was selected as the brake pedal. The throttle pedal was selected instead of a brake pedal because the majority of today's vehicles are equipped with electric throttle control; thus, the throttle pedal is equipped with integrated position sensors. The selected pedal has two integrated potentiometer position sensors with an analog output. The electrical connection of the pedal is provided by a 6-wire connector; two of them are connected to the supply voltage, two of them are connected to the ground, and the remaining two are connected to the potentiometer outputs.

Control Electronics Box

The control electronics box of the Pedal unit should implement the following two services; reading and preprocessing the analog signals generated by the brake pedal and transmission of the measured pedal position via CAN bus. The TI board was selected as the main computational unit of the Pedal unit because it satisfies both requirements. The DCDC step-down converter, described in chapter 4, is used for powering the TI board. The electrical scheme of the designed Pedal unit is depicted in figure 7.7. A casing box was created to protect the control electronics from water, dust, and dirt and facilitate the installation of the Pedal unit in the vehicle. The casing box was printed on the 3D printer, and the box lid was carved from transparent plexiglass. The 3D model and visualization of the casing box are depicted in figure 7.8. The photo of the designed Pedal unit can be seen in figures 7.10 and 7.11.

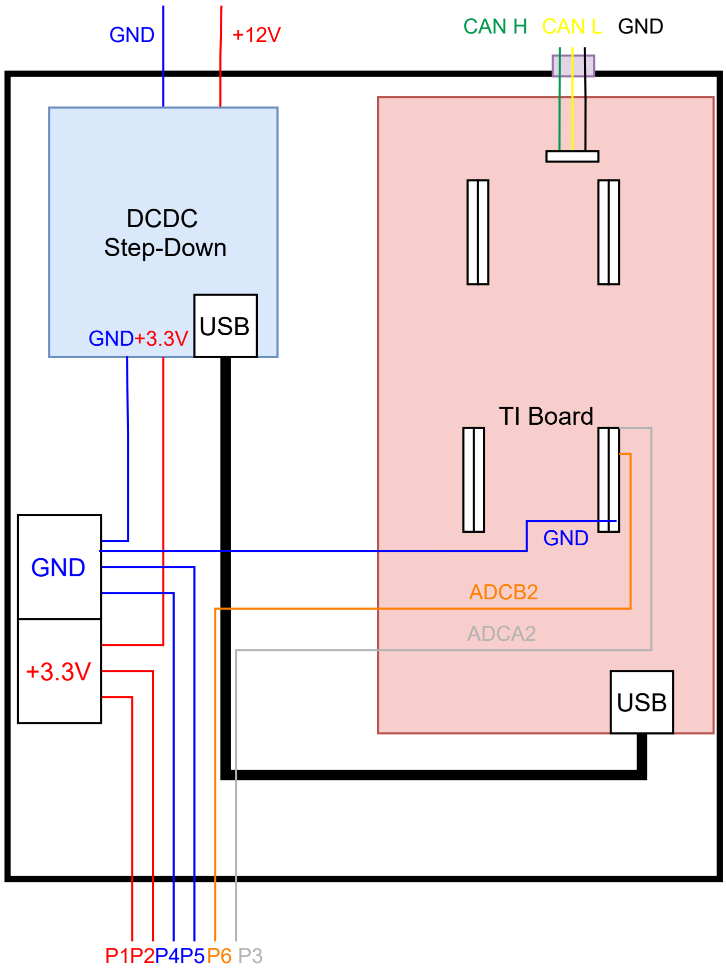

Figure 7.7: The electrical scheme of the designed Pedal unit.

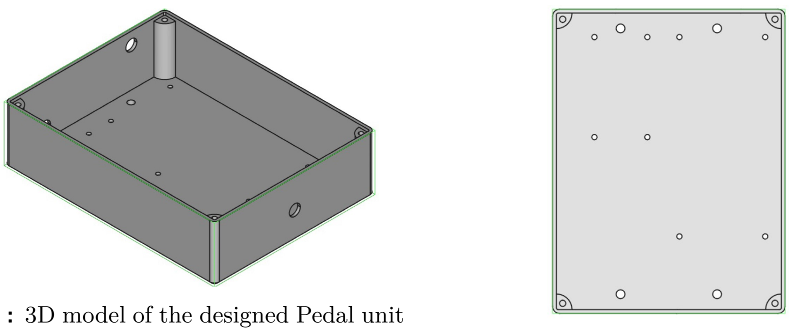

(a) : 3D model of the designed Pedal unit casing box.

(b) : Top view of the designed casing box.

Figure 7.8: 3D visualization of the designed electronics casing box for the Pedal unit.

7.3.2 Software Implementation of the Pedal Unit

Pedal Position Reading

As mentioned above, the selected pedal is equipped with two potentiometers reading the pedal position. The analog outputs of those potentiometers are connected to the ADC pins of the TI board. First of all, the values measured by the ADC are filtered using a discrete low pass filter. Then, the measured raw values are converted to the pedal position using the equation

$$pos_i = \frac{ADC_{i_{meas}} - range_{i_{min}}}{range_{i_{max}} - range_{i_{min}}}, \tag{7.2}$$

where $ADC_{i_{meas}}$ is filtered raw value measured by the i^{th} ADC, $range_{i_{min}}$ is the minimal value of the i^{th} potentiometer electrical output, and $range_{i_{max}}$ is the maximal value of the i^{th} potentiometer electrical output. The values of $range_{i_{min}}$ and $range_{i_{max}}$ for both potentiometers were measured experimentally. The pos_i computed from equation 7.2 is in interval 0-1, where 0 corresponds to the fully released pedal, and 1 corresponds to the fully depressed pedal. Next, the pedal position and its validity are computed using algorithm 2. Moreover, a blue status LED is used to allow an easy visual inspection of the Pedal unit's functionality. This LED starts blinking when the brake pedal is depressed, and the frequency of the blinking is moderate to the rate of the brake pedal depression. Finally, the computed pedal position is published in the CAN bus. The block scheme of the software implementation of the Pedal unit is depicted in figure 7.9.

Algorithm 2 PedalPositionCalculation

```
Require: pos_1, pos_2
  thr = 0.05                                  ▷ Sensor drift threshold
  pos = 0                                     ▷ Brake position
  status = 0                                  ▷ Validity of computed brake position
  if |pos_1 − pos_2| < thr then
      pos = (pos_1 + pos_2) / 2
      status = 0
  else
      pos = 0
      status = 1
  end if
```

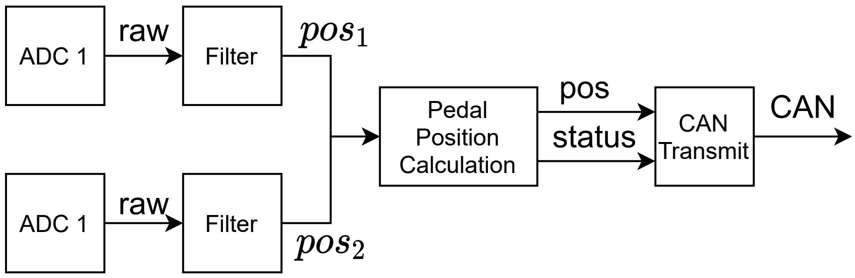

Figure 7.9: Block scheme of the software implementation of the developed Pedal unit.

CAN Interface

As discussed in the previous chapter, for safety reasons, the Pedal unit should be connected to the same CAN bus as the Brake-by-Wire unit and the VCU. Moreover, the Pedal unit is connected with the digital input pin of the VCU; thus, it can inform the VCU about any CAN bus malfunctions. The frequency of the CAN messages is set to 100 Hz. The Pedal unit receives heartbeat messages from the VCU. In case the heartbeat message is correctly received, the red status LED of the TI board starts blinking; thus, the CAN bus functionality can be easily visually inspected. In case the heartbeat message is not received for a period longer than 0.01 s, the status LED stops blinking, and the value of the Pedal unit's digital output connected to the VCU is set to a high value. The Pedal unit transmits two messages. The first one is the heartbeat message, and the second message contains information about the measured pedal position and its validity. A more detailed description of the implemented CAN messages can be seen in appendix C in table C.1.

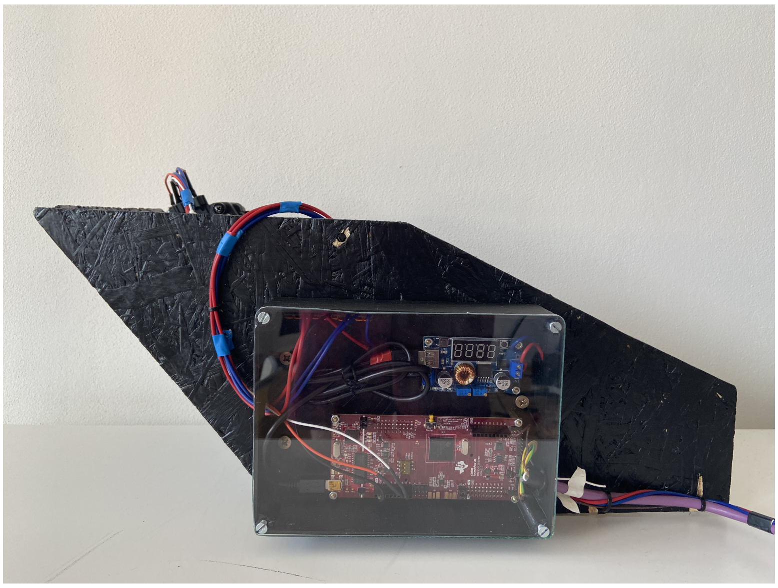

Figure 7.10: Side view of the constructed Pedal unit.

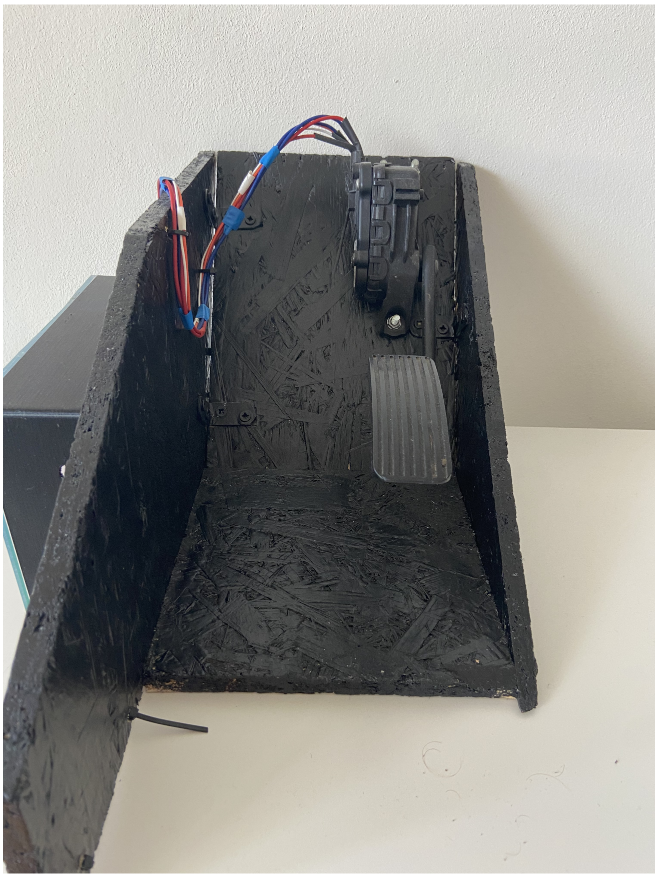

Figure 7.11: Top view of the constructed Pedal unit.

7.4 Test Setup

Now, when the Virtual vehicle unit and Pedal unit are implemented, the HIL simulation setup can be designed. The proposed test setup consists of the Pedal unit, the Virtual vehicle unit, and the Brake-by-Wire unit; all of them are connected to the same CAN bus. The pedal unit is used as a driver interface for generating the reference acceleration signal. The Brake-by-Wire unit is in the loop and generates brake torques commanded by the Virtual vehicle unit. In the Virtual vehicle unit, the twin-track model of the vehicle is running, and the vehicle stability control law is deployed. The block scheme of the HIL test setup is depicted in figure 7.14. The photo of the real HIL setup can be seen in figures 7.15 and 7.16.

7.4.1 Modifications of the Adopted Stability Control Law

For purposes of the HIL simulation, the originally designed control law depicted in figure 7.6 needs to be modified in the following way. First of all, the brake torque distribution block in the inner control loop is removed because the HIL test setup is not equipped with the traction motor; thus, all the brake torque will be generated by the brakes. Moreover, the designed HIL simulation setup contains only one Brake-by-Wire unit. Therefore, the reference torque needs to be generated only for one wheel. The block schemes of the modified inner and outer control laws are depicted in figures 7.12 and 7.13.

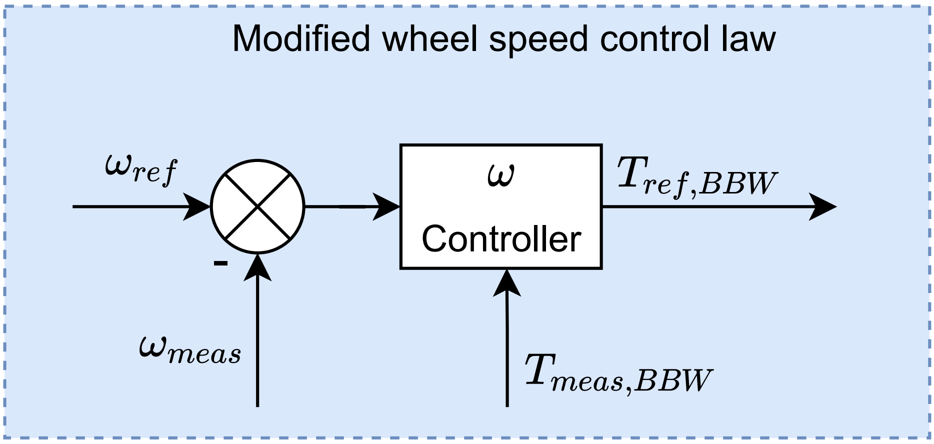

Figure 7.12: Modified inner control loop.

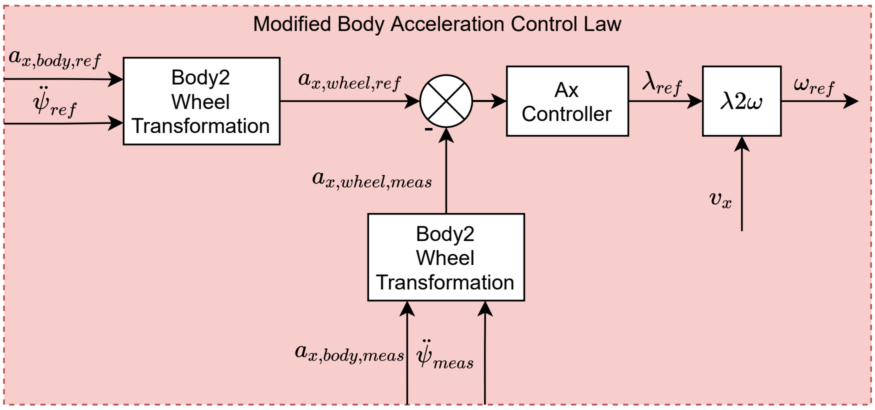

Figure 7.13: Modified outer control loop.

The brake torque generated by the Brake-by-Wire unit is applied to all four wheels to generate sufficient brake force. Moreover, to ensure lateral stability of the vehicle, the same road-wheel friction coefficient is set for all four wheels, and the vehicle is moving straightforwardly in all performed tests. Therefore, the yaw rate derivation reference $\ddot{\psi}_{ref}$ is equal to zero in all performed tests. This means that the compensation of the vehicle lateral instability induced either by cornering or a different road-wheel friction coefficient for each wheel cannot be tested using the proposed HIL setup. To enable testing of the vehicle's lateral stability, at least one more Brake-by-Wire unit needs to be added to the HIL simulation setup. Therefore, only the longitudinal vehicle stability can be tested on the proposed HIL setup.

Finally, the *Position2Acceleration* block and *Cruise control* block are added to the Virtual vehicle unit design. The *Position2Acceleration* transforms the received brake pedal position to the reference acceleration value using the equation

$$a_{x,body,ref} = -10 \cdot Pedal_{pos}, \tag{7.3}$$

where $Pedal_{pos}$ is the received brake pedal position. Moreover, this block detects when the brake pedal is fully released and activates the cruise control system to maintain the vehicle's speed. The *Cruise control* block implements simple feedback control law controlling the vehicle's longitudinal speed. The *Cruise control* block is activated only when the brake pedal is fully released. When the brake pedal is depressed, *Cruise control* system is deactivated, and the stability control law described above takes over the longitudinal dynamics of the vehicle. The modified scheme of the developed Virtual vehicle unit is depicted in figure 7.14. The photo of the real HIL simulation setup is depicted in figures 7.15 and 7.16. Finally, the performed HIL simulations are described, and the test results are discussed and evaluated.

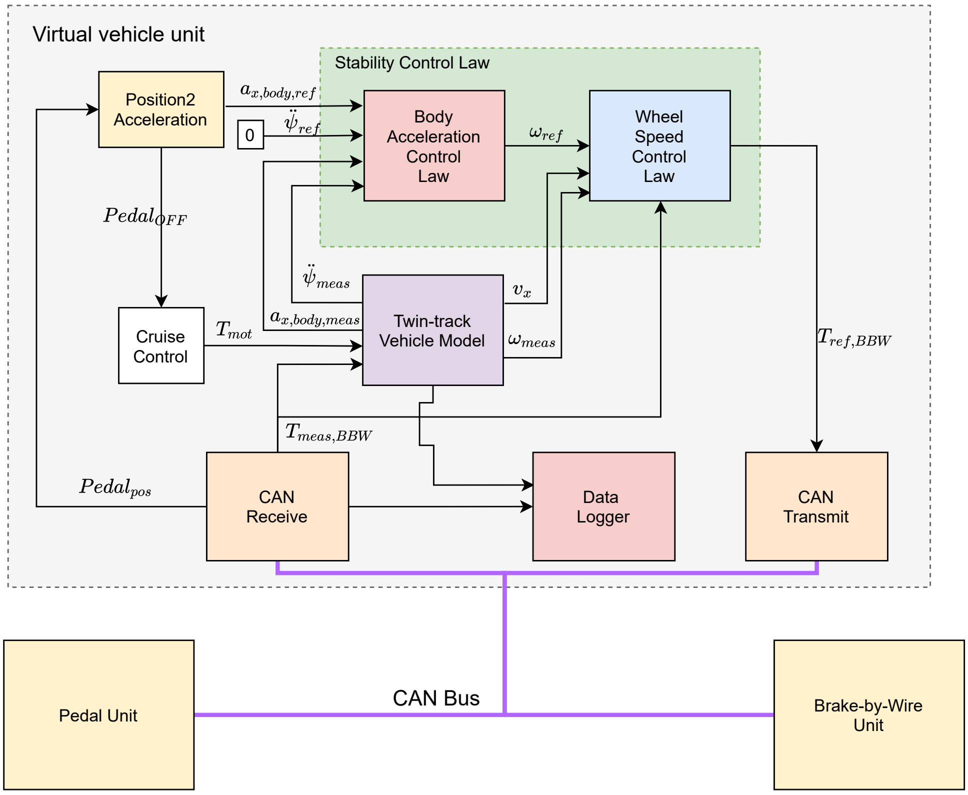

Figure 7.14: Block scheme of the developed HIL setup.

Figure 7.15: Photo of the hardware-in-the-loop simulation setup.

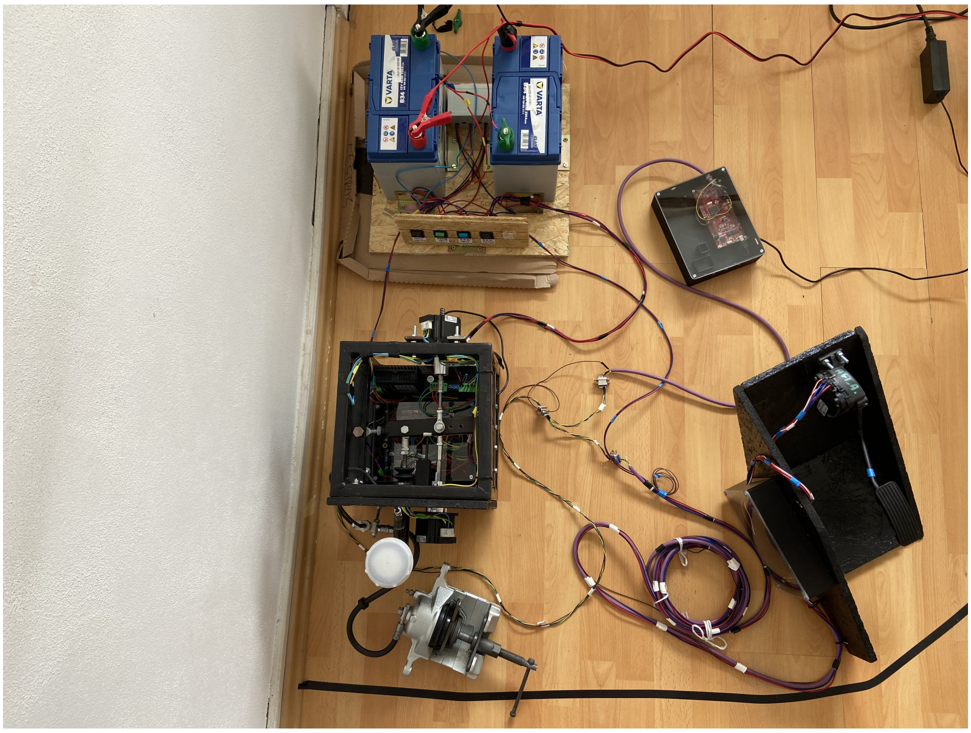

Figure 7.16: Top view of the hardware-in-the-loop simulation setup.

7.4.2 Test 1 - Step Response

In the first test scenario, the step response of the designed high-level vehicle stability control law is examined. In this test, the vehicle is moving straight-forwardly, the road-wheel friction coefficient is set to 1 for all wheels, and the initial speed of the vehicle is set to 100 km/h. The reference longitudinal acceleration and measured acceleration are depicted in the top subgraph of figure 7.17. The reference and generated brake torque can be seen in the middle subgraph. Finally, in the bottom subgraph, the vehicle's longitudinal speed and the wheels' longitudinal speed are displayed. As it can be seen, the designed vehicle stability control law and the Brake-by-Wire unit track the reference acceleration accurately. From the top subgraph, the rise time of the system can be easily obtained; the measured rise time is approximately 0.4 s, which is sufficient. In the bottom subgraph, it can be seen that wheel speed corresponds to the vehicle speed. Therefore, the wheel lock is prevented, and the vehicle's longitudinal stability is ensured.

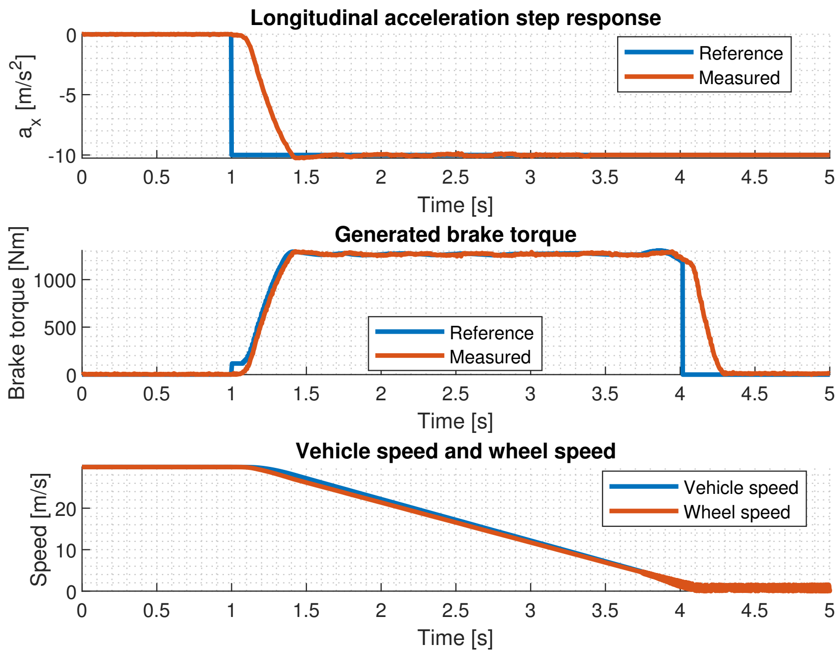

Figure 7.17: Test 1 - Step response.

7.4.3 Test 2 - Reference Tracking

In the second test scenario, the tracking of the reference acceleration signal is tested. The vehicle is moving straightforwardly, the road-wheel friction coefficient is set to 1 for all wheels, and the initial vehicle speed is set to 100 km/h. The reference and measured vehicle acceleration are captured in the top subgraph in figure 7.18. As it can be seen, the designed brake system solution can precisely track various acceleration signals. In the middle subgraph, the computed reference torque and the torque generated by the Brake-by-Wire unit can be seen. Finally, the time evolution of the vehicle and wheel longitudinal speed is captured in the bottom subgraph. Again, it can be seen that the wheel speed corresponds to the vehicle speed all the time; therefore, longitudinal stability is ensured.

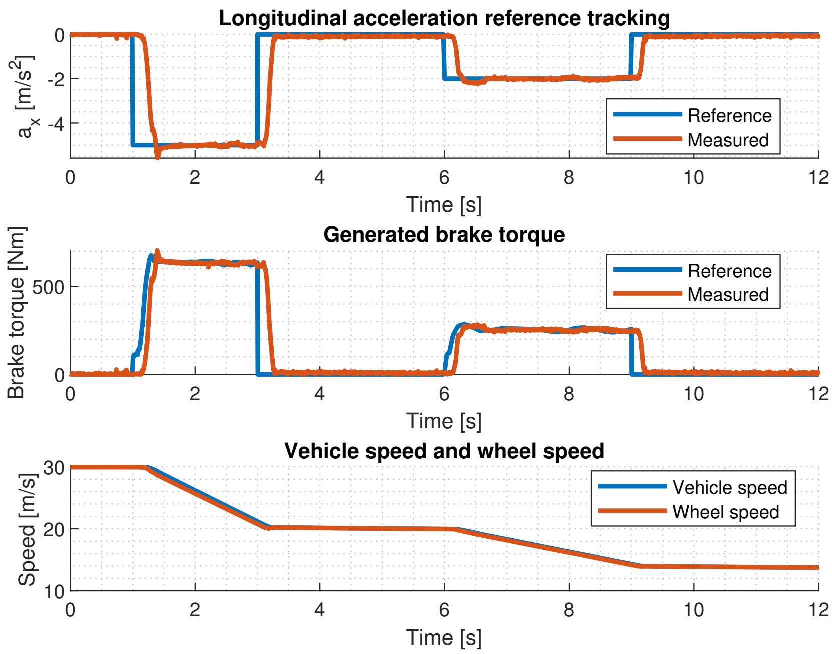

Figure 7.18: Test 2 - Acceleration reference tracking.

7.4.4 Test 3 - Brake Pedal Reference Tracking

In this test scenario, the reference acceleration tracking is examined as well. However, in this test, the reference acceleration is generated by the Pedal unit by brake pedal depression. In this test scenario, the vehicle is moving straightforwardly, and the road-wheel friction coefficient is set to 1. The initial vehicle speed is set to 100 km/h. Moreover, when the brake pedal is fully released, the cruise control system is activated, and the vehicle maintains the speed of 100 km/h. In the top subgraph of figure 7.19, the reference acceleration generated by the Pedal unit and the real vehicle longitudinal acceleration are depicted. As it can be seen, the developed brake solution is capable of tracking all various acceleration references.

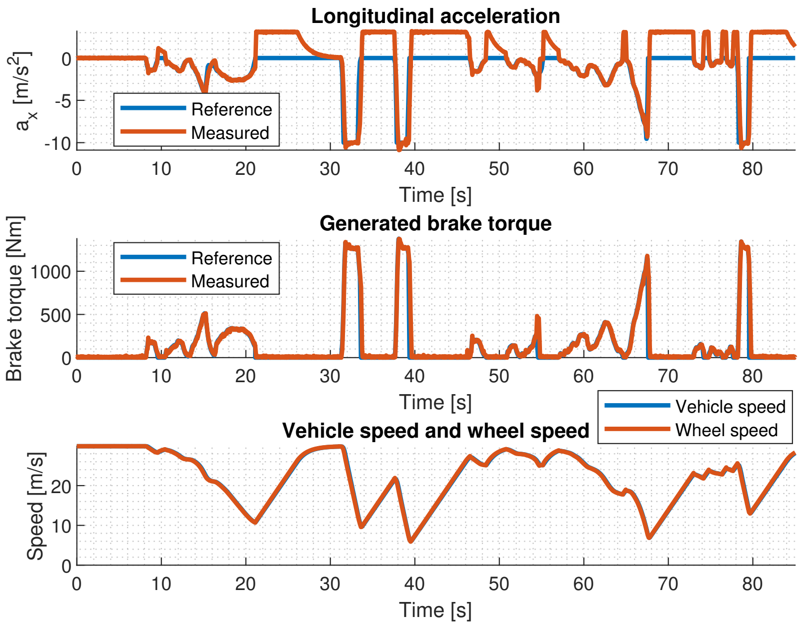

Figure 7.19: Test 3 - Brake pedal reference acceleration tracking.

7.4.5 Test 4 - μ Step

In the fourth test scenario, the reference tracking under various road conditions is examined. The reference acceleration is generated by the Pedal unit in the same manner as in the previous test scenario. The initial vehicle speed is set to 100 km/h, and the initial value of the road-wheel friction coefficient μ is set to 1. To simulate various road conditions, the value of the μ coefficient is changed during the simulation; see the bottom subgraph in figure 7.20. The value of $\mu = 1$ corresponds to a dry asphalt road, the value of $\mu = 0.6$ corresponds to a slightly wet road, the $\mu = 0.4$ corresponds to a wet asphalt road, and finally, the $\mu = 0.2$ corresponds to a snowy road. As it can be seen in the top subgraph, the developed brake solution is able to generate maximal deceleration without wheel locking for both $\mu = 1$ and $\mu = 0.6$. For $\mu = 0.4$ and $\mu = 0.2$, the value of the maximal deceleration is limited. However,the designed control system is able to prevent the wheel lock, thus ensuring the vehicle's longitudinal stability and delivering the maximal vehicle deceleration possible, regardless of the brake pedal position. The detailed view of the vehicle acceleration, wheel and vehicle speeds, and generated brake torque for $\mu = 0.2$ is captured in figure 7.21.

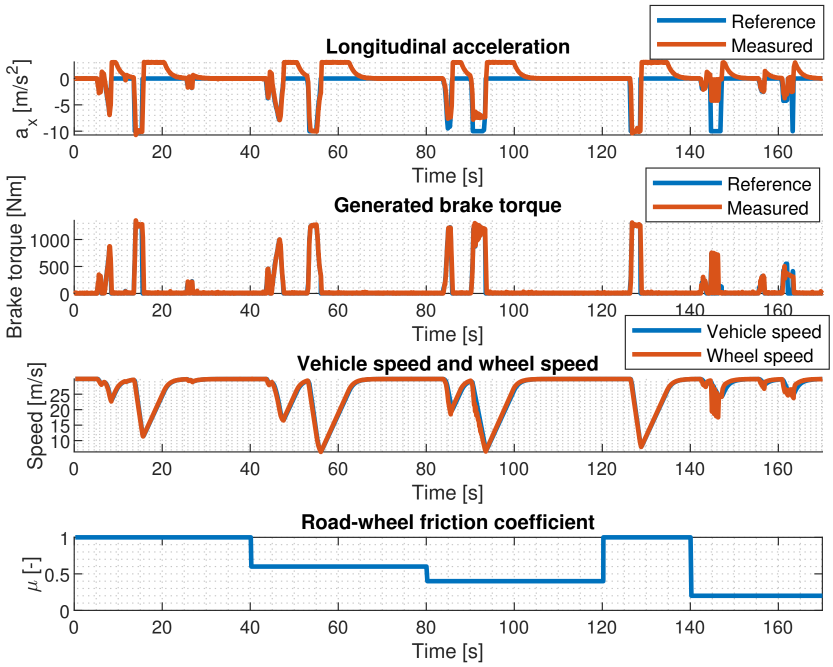

Figure 7.20: Test 4 - reference signal tracking for various road condtions.

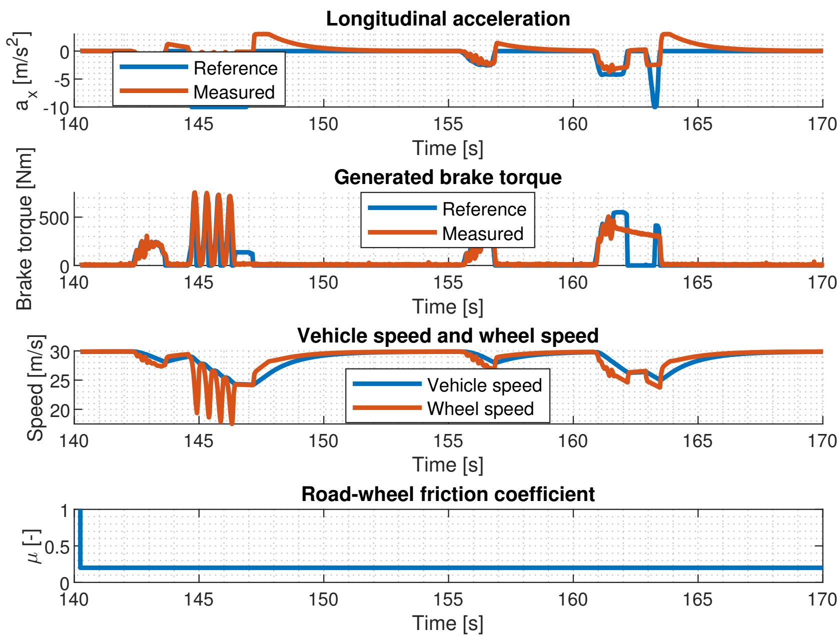

Figure 7.21: Test 4 - detailed view of signal tracking for $\mu = 0.2$.

7.4.6 Test 5 - μ Step Without the High-level Control Law

Finally, in the last test scenario, the behavior of the vehicle when the developed high-level stability control law is turned off is tested. In this test, the vehicle is moving straightforwardly, the initial vehicle speed is set to 100 km/h, and the initial value of μ is set to 1 for each wheel. To simulate various road conditions, the value of μ is dynamically changed in the same way as in test number 4. In this case, the driver directly generates the reference brake torque. Then, the reference brake torque is computed from the pedal position using the equation

$$T_{brake,ref} = 1630 \cdot Pedal_{pos}. \tag{7.4}$$

As it can be seen, for values of $\mu = 1$ and $\mu = 0.6$, the driver is able to safely slow down or even stop the vehicle without the wheels locking. However, in the case of $\mu = 0.4$, the brake pedal needs to be operated significantly more carefully in order to prevent the wheel lock. Finally, for $\mu = 0.2$, it is nearly impossible to maintain the vehicle stability and slow down the vehicle without locking the wheels. The value of the reference brake torque and generated brake torque, vehicle and wheel speeds and vehicle acceleration can be seen in figure 7.22. The detailed view of the vehicle acceleration, wheel and vehicle speeds and brake torque for $\mu = 0.2$ can be seen in figure 7.23.

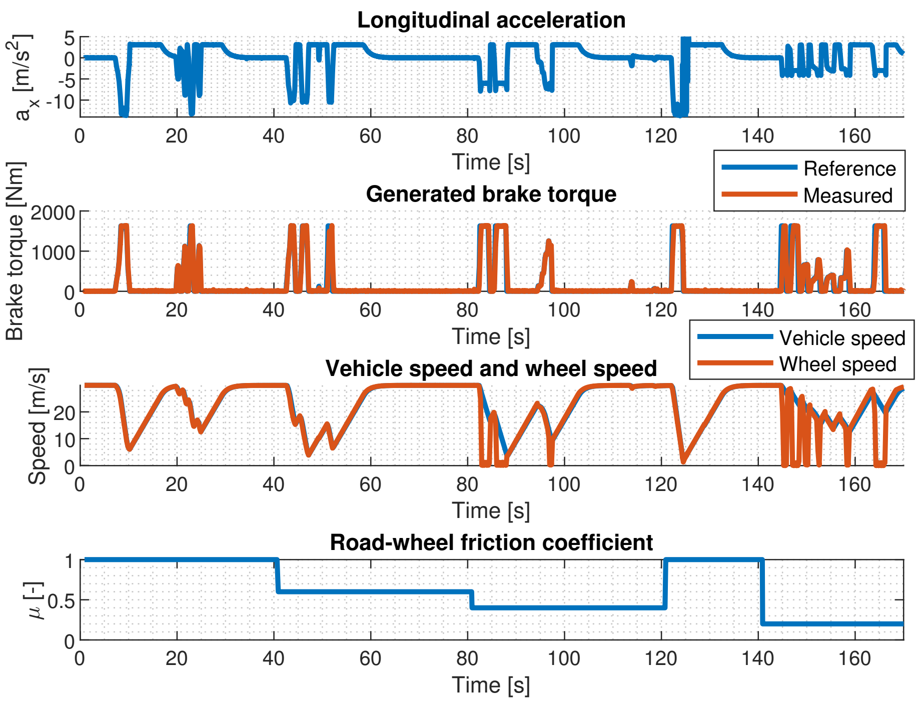

Figure 7.22: Test 5 - longitudinal stability control law turned off

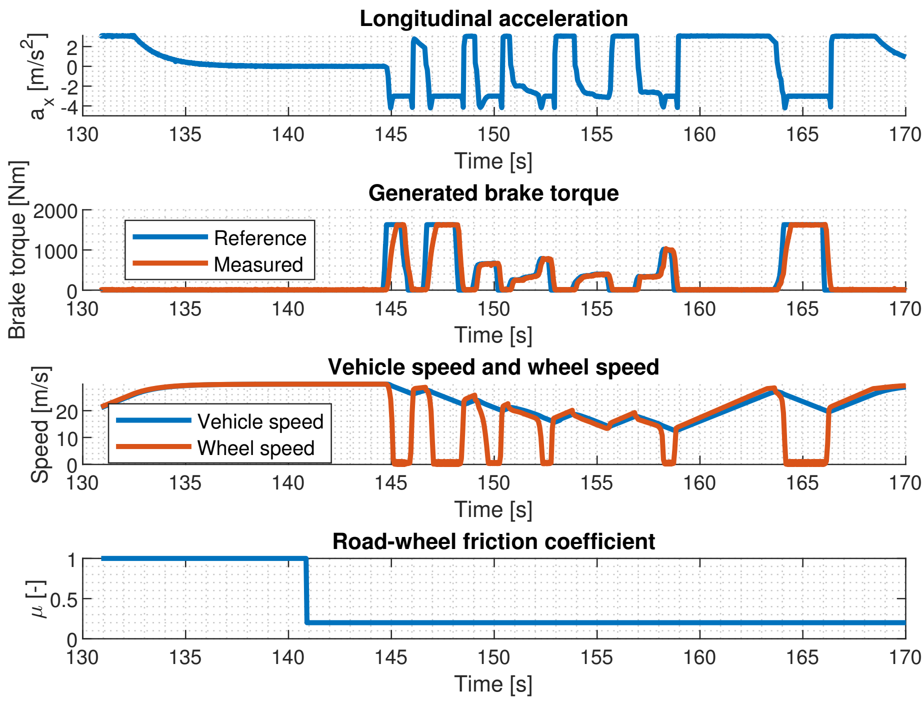

Figure 7.23: Test 5 - detailed view.

7.4.7 Validation Summary

The developed brake system solution consisting of the constructed Brake-by-Wire unit and designed high-level vehicle stability control law was validated on the proposed HIL simulation setup. All performed tests showed that the implemented brake solution is capable of safely slowing down and stopping the vehicle while maintaining longitudinal vehicle stability under various and adverse road conditions such as wet or snowy roads.

Chapter 8

Conclusion

This work is dedicated to mechanical design and hardware and software implementation of the innovative Brake-by-Wire solution applicable to the real vehicle. Firstly, the current state-of-the-art solutions developed both by academic researchers and industrial manufacturers are studied in order to get a comprehensive overview of currently available brake system solutions. Secondly, several possible brake solutions suitable for the needs of the SDS prototype vehicle have been considered, and the most suitable one has been selected. The decentralized hydraulic-based brake system actuated by the electro-hydraulic unit, formed by the master cylinder operated by the linear stepper motor, was selected as the best brake solution for the SDS project.

The custom mechanical construction of the Brake-by-Wire unit was designed. The designed construction is used for mounting the linear stepper motors, the master cylinder, and control electronics. Moreover, the custom lever transmission mechanism was designed to connect the selected master cylinder and linear stepper motors. Then, the necessary sensorics and control electronics were selected. Finally, the 3D casing box for control electronics was designed and printed on the 3D printer to protect the control electronics from harsh environment. The software implementation of the developed Brake-by-Wire unit consists of two control laws. The main control law, called the pressure control law, is designed to allow easy generation and control of the brake pressure. Moreover, the second control law, named the position control law, was designed in order to increase the functional safety of the proposed Brake-by-Wire unit in case of pressure sensor malfunction. To increase the functional safety of the Brake-by-Wire unit, the error detection and fault tolerance mechanisms were implemented in the unit's control logic. Finally, the CAN communication interface connecting the Brake-by-Wire unit with the remaining vehicle units was implemented.

Several tests were made to validate the functionality of the designed Brake-by-Wire system. The performed tests showed that the Brake-by-Wire unit is able to generate various reference pressures and can track the reference pressure signal precisely. However, performed tests also showed that the maximal magnitude of the brake pressure and the actuation speed is lower than had been required. Therefore, the second linear stepper motor was added to the design to increase the maximal magnitude of pressure and increase the actuation time. The same validation tests of the modified Brake-by-Wire unit were performed and compared with the original results. The performed tests showed that the addition of the second motor to the design increased the pressure magnitude up to 62 Bar and significantly increased the actuation speed.

In the last chapter, the brake system control strategies on the vehicle level were designed. The high-level control laws designed in my previous work were adopted and tested on the real hardware. Due to the fact that the testing on the prototype vehicle was not possible at this moment, the hardware-in-the-loop simulation was developed as a workaround. The hardware-in-the-loop simulator consists of the developed Brake-by-Wire unit, the Virtual vehicle unit, and the Pedal unit. The Virtual vehicle unit was developed to simulate the longitudinal and lateral dynamics of the vehicle under various road and driving conditions. The twin-track model was used as the simulation vehicle model. Moreover, the Virtual vehicle unit was used to deploy the proposed high-level vehicle stability control algorithms. Finally, the Pedal unit was developed as the driver interface dedicated to brake system actuation. The performed hardware-in-the-loop simulation showed that the proposed brake system solution is capable of delivering sufficient brake torque and ensures the vehicle's longitudinal stability and wheel lock prevention under various adverse road and driving conditions.

8.1 Future Work

Finally, the ideas for future improvement of the designed brake system solution are listed below.

- Implementation of the second Brake-by-Wire unit; so that the lateral stabilization of the vehicle can be tested as well.
- To perform tests on the real prototype vehicle.
- Implementation of the control laws and logic for traction motors and implementation of the battery management system; so that the already implemented brake torque distribution between friction-based brakes and traction motor can be tested.

Appendix A

Bibliography

[AEEGE17] E.M. Attia, N.M. Elsodany, H.A. El-Gamal, and M.A. Elgohary, *Theoretical and experimental study of magneto-rheological fluid disc brake*, Alexandria Engineering Journal **56** (2017), no. 2, 189–200, [Online], Accessed: 2022-04-21.

[AG19] AUDI AG, *2.1 vehicle and component specifications*, 2019, [Online], Accessed: 2022-04-23, `http://www.evc1000.eu/en/the-project/documents/deliverables/public_deliverables`, p. 42.

[Aim] *Aim brake pressure sensor m10 0-100 bar*, [Online], Accessed: 2022-05-02, `https://www.aimshop.com/products/aim-brake-pressure-sensor-m10-0-100-bar-motocross`.

[Air] *Fly-by-wire*, [Online], Accessed: 2022-04-22, `https://www.airbus.com/en/who-we-are/our-history/commercial-aircraft-history/fly-by-wire-1980-1987`.

[Ber09] Mark Bernacki, *Design and development of and extended range electric by-wire/wireless hybrid vehicle with a near wheel motor drivetrain*, 2009, Ontario. Master thesis. University of Ontrario Institute of Technology.

[Cib19] Vít Cibulka, *MPC based control algorithms for vehicle control*, Master thesis, Czech Technical University, Prague, 2019.

[Dex] *Electric/hydraulic brake actuator 1000 psi*, [Online], Accessed: 2022-04-29, `https://www.dexteraxle.com/product/2324/132/electric-hydraulic-brake-actuator-1000-psi`.

[Dix] *What is coefficient of friction?*, [Online], Accessed: 2022-04-27, `https://www.dixcel.co.jp/en/subcontent/literature/literature03.html`.

[DM] *Driver dm542 pro krokové motory 3a 50v*, [Online], Accessed: 2022-04-29, `https://www.laskakit.cz/driver-dm542-pro-krokove-motory-3a-50v/#relatedFiles`.

[EHK10] *Předpis evropské hospodářské komise organizace spojených národů (ehk/osn) č. 13-h – jednotná ustanovení pro schvalování osobních automobilů z hlediska brzdění*, 2010, [Online], Accessed: 2022-04-27, `https://esipa.cz/sbirka/sbsrv.dll/sb?DR=SB&CP=42010X0831(02)`.

[Gmb14] Robert Bosch GmbH, *Bosch automotive handbook*, 9th edition ed., Wiley, Germany, 2014.

[GMEa] *Mikrospínač na panel, 1pól, (on)-on, páčka s rolnou sm-05s-05b0-z*, [Online], Accessed: 2022-05-02, `https://www.gme.cz/mikrospinac-zippy-sm-05s-05b0-z`.

[GMEb] *Modul dc/dc měnič step-down 1,25 - 32v/5a, usb, led displej*, [Online], Accessed: 2022-05-02, `https://www.gme.cz/modul-dc-dc-step-down-1-25-32v-5a-usb-led-displej`.

[Han] Tomáš Haniš, *Smart driving solutions*, [Online], Accessed: 2022-04-29, `https://sds.fel.cvut.cz/`.

[Hod18] Bruce Hodder, *Brake master cylinder, 3/4" bore, chirco #cpr721578*, 2018, [Online], Accessed: 2022-04-29, `https://grabcad.com/library/brake-master-cylinder-3-4-bore-chirco-cpr721578-1`.

[HRHG06] Lok Man Ho, Richard Roberts, Henry Hartmann, and Bernd Gombert, *The electronic wedge brake - ewb*, SAE TECHNICAL PAPER SERIES (2006), no. 24th Annual Brake Colloquium & Exhibition, 12, [Online], Accessed: 2022-04-29.

[HSPG02] H. Hartmann, M. Schautt, A. Pascucci, and B. Gombert, *The mechatronic wedge brake,*, SAE Technical Paper 2002-01-2582 **2002** (2002), no. 2002-01-2582, 8, [Online], Accessed: 2022-04-29.

[Hu22] Donghai Hu, *Design and control of hybrid brake-by-wire system for autonomous vehicle*, 1 ed., Springer, Singapore, 2022.

[HVVJ] Tomáš Haniš, David Vošahlík, Tomáš Veselý, and Jiří Jirák, *Sds car*, [Online], Accessed: 2022-05-18, `https://gitlab.fel.cvut.cz/hanistom/lukaev/-/tree/master/wheel_computer`.

[Hyd] *Hydraulic trailer brake actuator*, [Online], Accessed: 2022-04-29, `https://www.hydrastarusa.com/products/hydrastar/`.

[Jer18] Benjamin Jerew, *How electronic throttle control (etc) works*, 2018, [Online], Accessed: 2020-04-22, https://www.liveabout.com/how-electronic-throttle-control-works-4158200.

[Li19] Wenfei Li, *Investigation of advanced brake-by-wire systems for electric vehicles*, 2019, Dissertation, University of Wollongong.

[Maj15] Jan Majzner, *Návrh brzdové soustavy osobního automobilu*, 2015, Ostrava. Bachelor thesis. Technical University Ostrava.

[Meu18] Guillaume Meurisse, *Investigation of a new e-caliper concept with a mechanical backup system*, 2018, Stockholm. Master thesis. KTH Royal Institute of Technology.

[Mot20] *Disc brake pad friction codes explained*, 2020, [Online], Accessed: 2022-04-27, https://www.motortrend.com/how-to/disc-brake-pad-friction-codes-explained/.

[Nana] *Lga561s20-a-tsga-038 – captive linear actuator – nema 23*, [Online], Accessed: 2022-04-29, https://en.nanotec.com/products/10084-lga561s20-a-tsga-038.

[Nanb] *Linear actuators with stepper motors*, [Online], Accessed: 2022-04-29, https://en.nanotec.com/products/157-linear-actuator-stepper-motor.

[Pec18] Radek Pecák, *Abs slaví čtyřicátiny. začalo to u letadel, povinné je však teprve 12 lel*, 2018, [Online], Accessed: 2022-04-22, https://www.autorevue.cz/abs-slavi-ctyricatiny-zacalo-to-u-letadel-povinne-je-vsak-teprve-12-let.

[Pol] *Glideforce md122006-p medium-duty linear actuator with feedback: 100kgf, 6" stroke (5.9" usable), 0.58"/s, 12v*, [Online], Accessed: 2022-04-29, https://www.pololu.com/product/3614.

[Pro19] Martin Procházka, *Návrh brzdného mechanismu zkušebního zařízení*, 2019, Praha. Bachelor thesis. Czech Technical University in Prague.

[RSC] *Lineární převodník lineární měření ip40 sensata / bei sensors*, [Online], Accessed: 2022-05-02, https://cz.rs-online.com/web/p/snimace-rizeni-pohybu/9234139.

[SFE15] Michael Struth, Georg Schulze Forsthövel, and Lutz Eckstein, *Functional potential by crosslinking domains – optimized recuperation for the speede research vehicle*, 24th Aachen Colloquium Automobile and Engine Technology 2015 (Aachen), 2015, p. 16.

[SL15] Chang-Woo Song and Seung-Yop Lee, *Design of a solenoid actuator with a magnetic plunger for miniaturized segment robots*, Applied sciences **2015** (2015), 13.

[ST10] Sergio M. Savaresi and Mara Tanelli, *Active braking control systems design for vehicles*, 1 ed., Springer Verlag, New York, 2010.

[Tes07] *The magic of tesla roadster regenerative braking*, 2007, [Online], Accessed: 2022-04-23, `https://www.tesla.com/blog/magic-tesla-roadster-regenerative-braking`.

[TI] *Launchxl-f28379d*, [Online], Accessed: 2022-04-29, `https://www.ti.com/tool/LAUNCHXL-F28379D`.

[Ves20] Tomáš Veselý, *Abs system modelling and control strategies development*, 2020, Praha. Bachelor thesis. Czech Technical University in Prague.

[vHNK14] B.A.P. van Duifhuizen, P.D. Hobo, H. Nijmeijer, and A. Khajepour, *Modeling, design and control of an individual wheel actuated brake system*, D&C, Eindhoven University of Technology, 2014 (English), Traineeship report. - DC 2014.052.

[Wil] *Gs compact remote master cylinder*, [Online], Accessed: 2022-04-29, `https://www.wilwood.com/MasterCylinders/MasterCylinderProd?itemno=260-15088`.

Appendix B

Linear Stepper Motor Datasheet

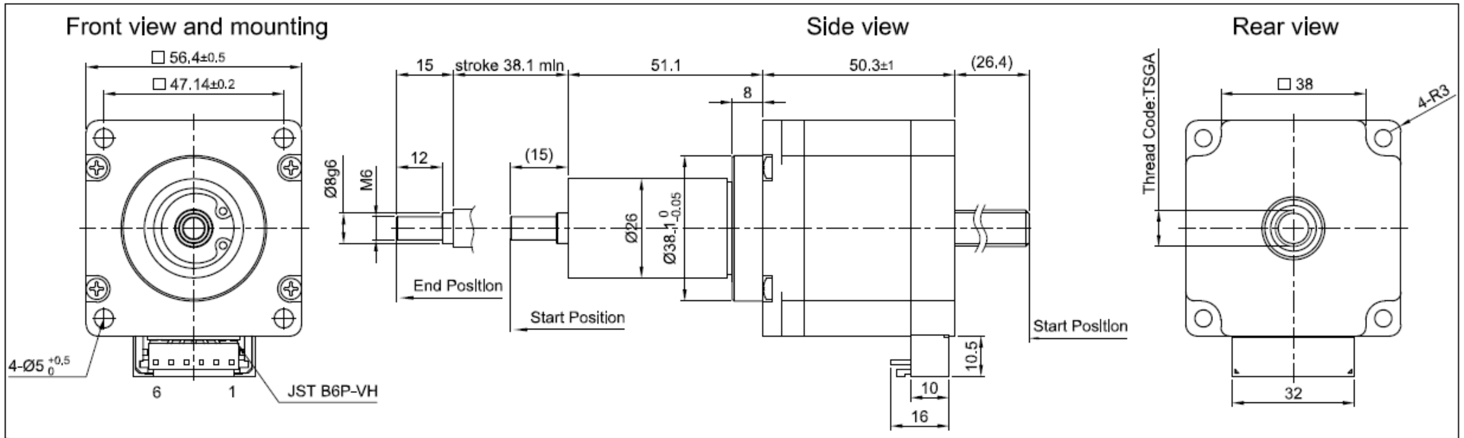

SPECIFICATION / CONNECTION	BIPOLAR
AMPS/PHASE	2.0
RESISTANCE/PHASE (Ohms)@25°C	1.5±15%
INDUCTANCE/PHASE (mH) @1KHz	4.3±20%
THREAD DIAMETER (mm) [in]	10 [0.394]
THREAD LEAD(mm) [in]	6 [0.236]
THRUST (N)	476.7
RESOLUTION (mm/STEP)	0.03
MAX. SPEED (mm/sec.) AT 24V	100
WEIGHT (Kg) [lb]	0.75 [1.65]
TEMPERATURE RISE: MAX.80°C (MOTOR STANDSTILL; FOR 2 PHASE ENERGIZED)	
AMBIENT TEMPERATURE −10°~ 50°C [14°F ~ 122°F]	
INSULATION RESISTANCE 100 MOhm (UNDER NORMAL TEMPERATURE AND HUMIDITY)	
INSULATION CLASS B 130° [266°F]	
DIELECTRIC STRENGTH 500VAC FOR 1 MIN. (BETWEEN THE MOTOR COILS AND THE MOTOR CASE)	
AMBIENT HUMIDITY MAX. 85% (NO CONDENSATION)	

Please regard the application note at www.nanotec.com for further informations.

MOTOR

CONNECTOR PIN NO.	WINDING
1	A
3	A\
4	B
6	B\

FULL STEP 2 PHASE−Ex.,
WHEN FACING MOUNTING END (X)

STEP	A	B	A\	B\
1	+	+	−	−
2	−	+	+	−
3	−	−	+	+
4	+	−	−	+

CW ↓ CCW ↑

WIRING DIAGRAM

(A) (A\) (B) (B\)

REV	DESCRIPTION	DATE	DRN
A	−	18.08.21	X T

Nanotec® PLUG & DRIVE

Surface specification DIN ISO 1302 | General tolerances DIN ISO 2768-cH | Work piece edge DIN ISO 13715

	SIGNATURE	DATE
APVD	P.R.	23.04.20
CHKD	GYQ	23.04.20
DRN	X T	23.04.20

LINEAR ACTUATOR

DWG.NO LGA561S20-A-TSGA-038

Appendix C

CAN Communication Interface

Sender	Message name	Receiver	ID	Content
BBW Unit	Heartbeat BBW Unit	VCU	1	1. Heartbeat BBW Unit
	BBW Message 1	VCU	257	1. Number of steps 2. Position potentiometer 3. Measured pressure 4. Measured torque
	BBW Message 2	VCU	258	1. BBW mode 2. Motor direction 3. Duty cycle 4. Frequency 5. Limit switch 1 6. Limit switch 1 status 7. Limit switch 2 8. Limit switch 2 status 9. Reset 10. Error code 11. Pressure status 12. Potentiometer status
VCU	Heartbeat VCU	BBW Unit Pedal Unit	2	1. Heartbeat VCU
	VCU Message 1	BBW Unit	153	1. Brake torque reference 2. BBW mode reference
Pedal Unit	Heartbeat Pedal Unit	VCU BBW Unit	0	1. Heartbeat Pedal Unit
	Pedal Unit Message 1	VCU BBW Unit	256	1. Brake position 2. Position validity

Table C.1: Description of the implemented CAN messages.

Appendix D

Parameters of Used Vehicle Model

Name	Value	Unit	Description
m	1500	kg	Mass of vehicle body
g	9.81	m/s^{-2}	Gravitational constant
J_{xx}	200	$kg \cdot m^2$	Moment of inertia in x-axis
J_{yy}	1300	$kg \cdot m^2$	Moment of inertia in y-axis
J_{zz}	1400	$kg \cdot m^2$	Moment of inertia in z-axis
S_z	0.25	m	Vertical distance between CG and spring anchor
wheelbase	2.745	m	wheelbase
c_w	0.18	$-$	Drag coefficient
ρ	1.22	$kg{\cdot}m^{-3}$	Air density
A	2	m^2	Area exposed to aerodynamic forces
J_ω	1	$kg \cdot m^2$	Wheel moment of inertia
r	0.33	m	Wheel radius
$c_{a,1,3}$	30000	N/kg	Front spring stiffness
$c_{a,2,4}$	40000	N/kg	Rear spring stiffness
$d_{a,1,3}$	8000	$N \cdot s/m$	Front damping coefficient
$d_{a,2,4}$	8000	$N \cdot s/m$	Rear damping coefficient

Table D.1: Vehicle body parameters. Adopted from [Cib19].

Appendix E

Attachment

The following files are attached to the thesis.

`PedalUnit/`	all codes for implemented Pedal unit
`BrakeByWireUNit/`	all codes for implemented Brake-by-Wire unit
`HIL/`	twin-track model and developed HIL simuation setup
`Documentation/`	datasheet of the used hardware
`3DModels/`	3D CAD models
`brake_actuator.m`	script for computing brake system parameters
`CAN_matrix_Brake_by_wire.dbc`	CAN communication implementation